Two Themes in Perceptual Ecology: Visual Attention and Awareness

Thesis by

F. Christopher Kolb

In Partial Fulfillment of the Requirements

for the Degree of

Doctor of Philosophy

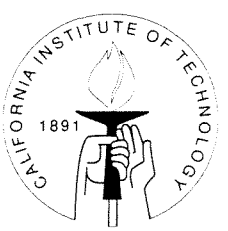

California Institute of Technology

Pasadena, California

1996

(Submitted June 4, 1996)

© 1996

F. Christopher Kolb

All Rights Reserved

Acknowledgements

I am deeply indebted to my thesis advisor, Pietro Perona and Sloan Center advisor, Richard A. Andersen for their encouragement, and generous and invaluable criticisms of my work. They were both a great help in enabling me to appreciate the geography and depth of the issues involved.

John Allman's seminal paper *Stimulus specific responses from beyond the classical receptive field* is the most pervasive influence; my understanding of it and my approach to the questions it raises were shaped in discussions with Allan C. Dobbins and Zhaoping Li.

More recently, the results of stimulating discussions with Jochen Braun - my chief collaborator - and Christof Koch have made their way into every chapter. Achim (Jochen) has, in addition, read the manuscript and made many very helpful suggestions, besides doing what he could to force clarifications. I have also benefited much from talks with David J. Heeger and Roger B. H. Tootel.

I am extremely grateful for all the advice and technical support I have received from my colleagues Michael C. Burl, Stefano Soatto, and - most notably - Markus Weber.

For generous support while writing this thesis I am very grateful to the Alfred P. Sloan Foundation and the National Science Foundation, Division of Integrative Biology and Neuroscience and Center for Neuromorphic Systems Engineering as part of the Engineering Research Center Program.

Finally I want to acknowledge my greatest debt of all, to Arianne Faber Kolb, who has given me the time and space in which to study, persevered with the tedium of having a part-time husband and been a permanent source of love and support.

Abstract

The nature of *consciousness* poses the central problem for both neuroscience and philosophy of mind: how is the brain constructed to enable the mind, a collection of perceptual, emotional, and intentional functions that evolve around a fleeting stream of *subjective* (sensory) experience? This thesis is about how to approach mental processes, such as *mindfulness* (attention) and *minding* (awareness), for the primary human sense, vision, with reductionist tools. Neurobiological studies of consciousness have proven elusive in the past for the neural structures, by which visual attention and awareness operate, are difficult to observe. Although cellular studies of visual attention have come a long way to explain a specific instance of conscious awareness, where certain aspects of the world stand out in consciousness at the expense of others, there is no indication that cognitive neuroscience may soon stride the "anatomical path" to self-understanding.

The difficulty lies in anatomically isolating one component of consciousness from the other in sensory interactions that are the product of complex neural mechanisms. It is here we make our prevalent contribution by experimentally unfolding the ecological range of sensory interactions that (potentially) reveal the cortical specificity of visual attention and awareness. Each chapter of this thesis delivers possible neural mechanisms and/or sites that pertain to component operations of visual awareness: "seeing" without looking (Chapter 2, perception outside the focus of attention), "looking" without seeing (Chapter 3, unconscious visual perception), "reading" without seeing the letters (Chapter 4, visual interpretation devoid cognition), "sensing" which eye sees (Chapter 5, unmasking the visual origin of eye), "learning" what the other eye sees (Chapter 6, dichoptic collaboration in "filling-in").

This thesis provides a conceptual framework that draws together results from visual neuroscience and psychophysics. It describes new approaches to determine the neural correlates and events responsible for imparting sense-data to the level of abstract thought and planned action. The central theme, however, is the discovery of "blindsight" in normals (Chapters 3 and 4). Visual behavior in the absence of visual awareness (blindsight) has been established unequivocally in patients with lesions in area V1, but remains controversial for normal observers ("subliminal perception"). We describe two visual displays that induce blindsight in normal observers, using an *objective* measure to distinguish conscious and unconscious performance. Both displays are designed to stimulate area V1 strongly and extrastriate areas poorly. In each display, one quadrant differs from the other three, and this "odd" quadrant is consciously perceived in one form of the display (C-form) but not another (NC-form) (100-200ms presentation time).

The first display consists of paired dots moving on orthogonal trajectories (different directions in odd and other quadrants), either within 0.2° of each pair (NC-form) or separated by several deg (C-form), so that the two forms differentially stimulate units in area MT but not area V1 (Qian & Andersen, 1994). The second display dichoptically presents arrays of oriented Gabor-elements (different orientations in odd and other quadrants), producing either binocular rivalry (NC-form) or fusion (C-form), so the two forms differentially stimulate binocular but not monocular units. To *objectively* demonstrate unconscious performance, we randomly interleave two forms of each display in a block of trials. Observers perform a forced-choice task (locating the odd quadrant), and rate their confidence in the choice of quadrant (scale of 1 to 10). Performance is comparable (and far above chance) for C- and NC-forms, but performance and confidence are correlated only for C-forms and essentially uncorrelated for NC-forms, confirming that performance in NC-forms is not accompanied by visual awareness. We surmise that performance may be based on stimulation of area

V1 while conscious experience may result from stimulation of extrastriate areas.

Contents

List of Figures

Chapter 1 Introduction

Nothing ever becomes real till
it is experienced.
John Keats (1795-1821)

My experience is what
I agree to attend to.
William James (1842-1910)

1.1 Perception outside the focus of attention

The thesis opens with an account of what the capacity for objective visual perception might amount to. A candidate ecological constraint upon visual behavior is *selective visual attention.* Visual attention is one of several mechanisms that modulate neural information processing in the human and non-human primate brain (Heilman *et al.*, 1990; Posner & Petersen, 1990; Colby, 1991; Kinchla, 1992; Posner & Driver, 1992). Visual attention allows us to separate currently (*i.e.* behaviorally) relevant from irrelevant visual information, enabling us to concentrate on a mere fraction of the total information (Helmholtz, 1850; James, 1890; Broadbent, 1958; Neisser, 1967; Treisman, 1969). In ignorance of the underlying neural mechanisms, visual attention has been described as a "limited capacity", a "spotlight", a "biased competition", and as something that is "guided by a saliency map" (Koch & Ullman, 1985; Robinson & Petersen, 1992; Desimone, 1992; Desimone & Duncan, 1995). These, at best metaphorical, descriptions hint at the two main facts known about attention: first, visual attention can select only a limited amount of information at any one time

and second, the attentional selection is stimulus-driven ("bottom-up") unless volition intervenes ("top-down") (Helmholtz, 1866; Schneider & Shiffrin, 1977; Haenny *et al.*, 1988; Corbetta *et al.*, 1990; Yantis & Jonides, 1990; Yantis, 1994; Mack *et al.*, 1992; Rock *et al.*, 1992).

A psychophysical technique that is useful in understanding how visual attention accomplishes perceptual selection is *visual search* (Neisser, 1976; Schneider & Shiffrin, 1977; Sperling & Melchner, 1978; Treisman & Gelade, 1980; Nakayama & Silverman, 1986; Treisman, 1988; Duncan & Humphreys, 1989; Cave & Wolfe, 1990). In visual search, several items are presented simultaneously and the observer is asked to detect a particular item ("target") among those present ("distractors"). Depending on the types of items involved, the deployment of visual attention follows different strategies: in some cases, visual attention scans the display item by item until the target is found, and in others, visual attention shifts directly to the item sought, evidently because this item has already been located with the help of *parallel, preattentive mechanisms* (Treisman & Gelade, 1980; Julesz, 1981).

A stimulus that readily attracts attention is called *visually salient.* James (1890) spoke of "*instinctive* stimuli which, by reason of their nature rather than their force, appeal to our congenital impulses and have a directly exciting quality". Thus to be salient, a stimulus need not be "forceful", *e.g.*, in terms of size or contrast. The observation that there are congenitally salient stimuli is particularly apparent in the perception of visual texture. The idea that abrupt changes in visual texture ("texture gradients") are visually salient as a result of parallel, preattentive processing, specifically as a result of short-range inhibition between certain simple stimulus features ("textons") is abundantly supported by experimental evidence (Julesz, 1981, 1991; Sagi & Julesz, 1987; Sagi, 1990; Malik & Perona, 1990; Nothdurft, 1991; Bravo & Nakayama, 1991).

A closer look at the mechanisms of bottom-up selection reveals that, when the

target of a visual search is less salient than the distractors, search times increase steeply with the number of distractors, implying sequential scanning by visual attention. However, when the target is more salient than the distractors, search times are relatively independent of the number of distractors ("search asymmetry") (Treisman, 1985; Treisman & Souther, 1985; Treisman & Gormican, 1988). Hence a question of central importance is: how does the search asymmetry, the difference in visual behavior pertaining to the search for the most salient and the least salient target in a visual display, relate to the issue of visual attention? Nonetheless, visual attention is thought to control access to levels of processing that directly influence behavior (Neisser, 1967; Kahneman, 1973).

In a series of psychophysical experiments Braun and Julesz (1996 a, b) investigated the role of attention in the two types of visual search. In their experiments, observers were asked to carry out a letter discrimination and a search task concurrently. To discriminate the letters, observers had to direct visual attention ("active attention") at the center of the display and leave unattended the periphery that contained target and distractors. In the concurrent task situation, visual search for the least salient item was severely impaired while visual search for the most salient item was only moderately affected. Hence they concluded that both active visual attention (top-down) and saliency (bottom-up) could independently contribute to the makeup of conscious visual experience.

Stimulus intensity, in the form of size, brightness, speed of movement, and so on, is an important factor contributing to visual saliency. However, absolute intensity does not automatically imply saliency, as is immediately evident when other, even more intense stimuli are presented at the same time (Treisman & Souther, 1985; Treisman & Gormican, 1988; Schiller & Lee, 1991; Braun, 1994). Apparently, only relative stimulus intensity can guarantee visual saliency, suggesting that the underlying neural mechanisms are of a competitive nature (Koch & Ullman, 1985). Therefore, a stimulus

feature that penetrates to the level of consciousness by being the most salient feature ("competition for saliency") should do so by virtue of eliciting peak activation in the cortical map that represents that particular type of stimulus feature (*e.g.*, orientation, color, motion, etc.) (Koch & Ullman, 1985; Treisman, 1988; Nakayama, 1991; Duncan & Humphreys, 1992; Desimone & Duncan, 1995) (see Figure 1.1).

The focus of Chapter 2 is the ecological nature of saliency-based vision. We demonstrate for a variety of dynamic visual textures, that it is the underlying competitive nature of the neural mechanisms involved in texture segmentation that govern perception outside the focus of attention, rather than a special (statistical) property of the texture itself (Rubenstein & Sagi, 1990). For the case of motion-defined textures whose visual neuronal correlates are known, at least in the macaque and rhesus monkey, we go on to determine the cortical constraints on stimulus competition for saliency. A necessary and sufficient condition for stimuli to win the competition for saliency is to elicit (differential) responses at extrastriate visual areas (*e.g.*, middle temporal visual area) - differential striate cortical activation by itself appears to be insufficient.

1.2 Psychophysics of perceptual tasks without visual awareness

Clinical evidence suggestive of residual yet non-phenomenal vision in man and monkey following striate cortical destruction raises the problem of the neural mechanisms for visual awareness in healthy people and animals. A startling amount of visually evoked behavior can be demonstrated in "cortically" blind (scotoma) patients. Prominent among the residual visual abilities of these patients is the capacity to detect and localize stimuli shown within the field defect by either eye movements or by visually guided reaching (Popper *et al.*, 1973; Weiskrantz *et al.*, 1974; Perenin & Jeannerod, 1975;

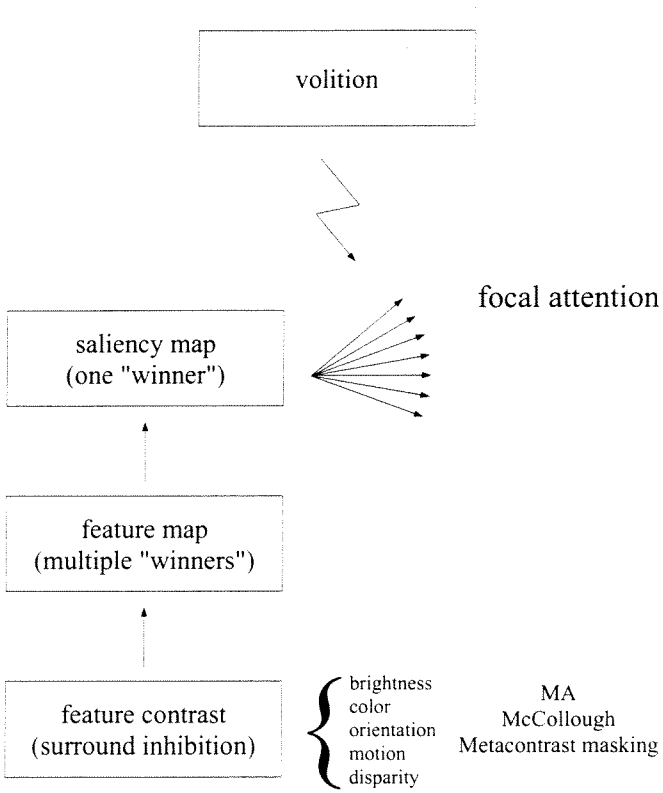

Figure 1.1: Visual attention is often conceptualized as modulation of neural activity in multiple *feature maps* and one *saliency map* (Koch & Ullman, 1985). Local image features such as brightness, color, orientation, motion, and disparity are represented in functionally separate feature maps. Within each such map, neighboring locations are thought to inhibit each other (*lateral inhibition*). Because of *surround inhibition*, the response to a local stimulus is stronger the fewer features it has in common with neighboring features. For example, provided a texture is sufficiently dense, surround inhibition attenuates uniform regions much more than discontinuous or singular regions, thus creating a *feature contrast* and rendering the latter visually salient. To provide unambiguous guidance to attention, the activity of different feature maps (multiple winners) is thought to be pooled in one saliency map (one winner). Therefore, stimuli that produce a peak of activity in the saliency map attract focal attention - unless *volition* intervenes. In addition, high-level volitional effects may directly enter into the saliency map (Koch, personal communication). Attentional modulation of neuronal responses has now been observed in most visual areas, including area V1 (Desimone & Duncan, 1995). Attention is also known to modulate low-level adaptation effects, such as the motion aftereffect (MA) (Chaudhuri, 1990), the McCollough effect (Dodwell & Humphrey, 1990), and metacontrast masking (Ramachandran & Cobb, 1995).

Mohler & Wurtz, 1977; Feinberg *et al.*, 1978; Zihl, 1980; Weiskrantz, 1986). Collectively termed "blindsight" (Weiskrantz *et al.*, 1974), the remaining visual functions are summarized as the capacity to detect and localize visual stimuli in the absence of an ability to identify them (Humphrey, 1972).

Chapter 3 presents an attempt to mimic human perception without visual awareness as a result of striate cortical lesions. The chapter describes two different psychophysical displays which seem to induce blindsight in normal observers. Observers report no phenomenal awareness of a target but are nevertheless able to reliably locate it within the display. The apparent dissociation between awareness and performance is not a threshold phenomenon but occurs over a wide range of performance. Recent single-unit recordings from alert non-human primates viewing similar displays allows us to consider possible neural correlates of this effect. In both of our displays, inhibitory interactions should attenuate responses (at least in certain subpopulations of neurons) in extrastriate but not striate visual cortex. Therefore, lack of phenomenal awareness may result from an attenuated or altered extrastriate response, while continued performance may be based on a largely normal striate response. This would support the recent hypothesis by Crick and Koch (1995) that phenomenal awareness correlates with activity in extrastriate, but not striate visual cortex.

Crick and Koch (1995) argue that in the case of striate cortex, lack of (direct) prefrontal connectivity causes lack of visual awareness. It is indeed likely that the frontal cortex (prefrontal and motor areas) with its access to stored sensory information and with its projections to limbic structures is crucially involved in manipulating and integrating low-level representations into high-level cognitive and psychological representations (*e.g.* consciousness). Goldman-Rakic (1984) discovered that adult monkeys with prefrontal lesions perform as poorly as human infants on Piaget's AB Stage IV Object Performance Test, a traditional task used to assess cognitive development in infants. This particular test requires that the subject realize that an object

exists in time and space when absent from view. Throughout the chapter, we purport to show that a visual stimulus registered in striate but not extrastriate cortex can guide behavior without entering higher cognitive states, such as consciousness.

The use of "anatomically targeted" psychophysical stimuli permits us to *functionally anaesthetize* extrastriate cortical areas (*e.g.*, area MT), consequently blocking the transmission from striate to extrastriate cortical areas. Hence our situation resembles clinical blindsight in that extrastriate input is greatly reduced and much of the remaining input is derived from subcortical sources (Stoerig & Cowey, 1993). And because of the lack of visual awareness and the preserved functionality of the superior colliculus and the pretectum, it has often been assumed that blindsight reflects predominantly subcortical processing (Campion *et al.*, 1983). To test this conjecture, we made two attempts at a functional "double-lesion" of area MT and the superior colliculus. Both methods yielded radical diminution of (blindsight) performance, thus implicating the superior colliculus in sustaining visual behavior in the absence of visual awareness.

The focus of Chapter 3 then shifts onto the notion of awareness-related effects of visual practice. A common observation in psychophysics is "perceptual learning", that is the significant increase in sensitivity for simple visual discrimination tasks induced by sensory experience (Karni & Sagi, 1991). There is a traditional conception of visual experience as inferential knowledge of our visually evoked behavior that manifests - in addition to external feedback on behavioral responses - the improvement of a subject's perception of the world over time (Poggio *et al.*, 1990). Here we attempt to show that perceptual learning does indeed occur in situations where no conglomerate visual experience exists (*e.g.*, induced blindsight). The psychophysical data obtained indicate that performance in visual discrimination tasks improves at comparable rates for conscious and unconscious vision, suggesting that perceptual learning and plasticity do not require visual awareness.

The final section of Chapter 3 is concerned with the gathering of additional evidence for the putative involvement of striate cortex in unconscious discrimination. We replicate - in a preliminary manner, equipped with visual displays that induce blindsight in normal observers - clinical findings of the McCollough effect in scotoma patients (Humphrey *et al.*, 1995). In our psychophysical displays an orientation contrast is barred from conscious perception but appears "as stripes of different color" after adaptation to the same orientation defined by color contrast. Our situation thus resembles the clinical case in that both patients and normal observers have no visual awareness of the display orientation but can reliably report the orientation-contingent aftereffect color. Given the massive damage to extrastriate cortex in scotoma patients who exhibit the McCollough effect, the anatomical site of this effect is likely to be within striate cortex.

1.3 Unconscious perception: pattern discrimination and priming effects

If unconscious perception of "conflicting" visual information permits discrimination of complex patterns, this raises the problem of how perceptual grouping is accomplished in the absence of visual awareness. In Chapter 4 we demonstrate various instances of visual pattern discrimination in the absence of visual awareness ("blindsight"). Two large arrays of local orientation elements are presented dichoptically. Fore- and background elements have orthogonal orientation (monocular). Foreground elements are arranged to form four letter shapes along the horizontal midline of the display. The left and right eye view orthogonal local elements at every array location. When left and right eye views are superimposed, the array subjectively appears uniform with no indication of the letter shapes whatsoever since presentation times are too short for one eye to dominate the other.

In one of our experiments, observers discriminate a sequence of four identical letters (4AFC) and rate their confidence (scale of 1 to 10). Letter discrimination is performed well above chance without visual awareness (no correlation between confidence and performance). In a similar experiment, the trial is preceded by a normally visible primer letter (50% valid, 50% invalid). A valid prime significantly increases performance, and invalid prime reduces it to chance. Priming effects are thus found to be much larger than in normal vision. In another experiment, observers discriminate a sequence of four different letters forming a word (4AFC) and rate their confidence. Word discrimination is performed well above chance without visual awareness (no correlation between confidence and performance). In a similar experiment, observers are visually or auditorily presented with a target word, view a sequence of "conflicting" displays and identify the one that conceals the target word. Spontaneous identification of a subjectively non-apparent word is also significantly above chance, indicating that blindsight in normal observers is not limited to forced-choice situations.

1.4 Utrocular identification

Studies of utrocular ("which eye") discrimination have offered the promise of insight into which aspects of neural activity in the visual cortex humans can be aware of. Helmholtz (1866) understood that utrocular information is necessary for stereopsis, but stated that we nonetheless have no conscious awareness of the origin of the eye to which a visual stimulus is presented ("eye-of-origin"). In brief, the dominant thought in Chapter 5 is that utrocular information is an essential part of the input but not the output of binocular (high-level) representation. So the suggestion - on ecological grounds - is that humans are not aware of eye-of-origin because it is not the output of behaviorally relevant computation. Notwithstanding, we show that in certain *unecological* situations observers may correctly identify eye-of-origin even in

the absence of vivid utrocular awareness.

In macaques and a variety of other monkeys a substantial portion of neurons in primary visual cortex (V1) are strongly dominated by one eye (Hubel & Wiesel, 1968). Humans share with Old World primates the characteristic of segregation of the inputs from the two eyes into parallel bands in area V1. And on the basis of evidence that in extrastriate cortical areas most neurons are roughly equally excited through both eyes (Maunsell & Van Essen, 1983; Burkhalter & Van Essen, 1985), it has been inferred that eye-of- origin information is conserved mainly in area V1 in humans as well. If we are aware of information represented within the firing activity of neurons in area V1, then we would expect to be able to report the eye-of-origin of a visual stimulus under normal circumstances. Our apparent failure to do so can be explained in one of two ways: first, due to the absence of direct projections from V1 to parietal, inferotemporal or frontal cortex (Crick & Koch, 1995); or second, in terms of masked ocularity by way of percept-dependent binocular feedback onto monocular V1 neurons. Although these two hypotheses may have different consequences, they are not (necessarily) mutually exclusive. Indeed, at the end of the chapter, we push for a particular reading of the latter that will endorse the hypothesis by Crick and Koch (1995).

In summary, simply eliminating binocular activity in extrastriate cortex is not sufficient for eye-of-origin identification. Our psychophysical data imply that utrocular identification is possible only under conditions where monocular neurons are differentially activated with respect to binocular neurons in striate cortex. Assuming that visual awareness is not associated with neural activity in striate cortex, a satisfactory account of (phenomenally impoverished) eye-of-origin extraction must hence revolve around the idea of eye-specific feedback originating at higher cortical levels. In a similar vein, Ishai and Sagi (1995) recently demonstrated that observers employing imagery of a previously primed visual target were significantly better at

detecting the target than when not instructed to employ imagery. The enhancement was eye-specific thus implying that imagery (*i.e.*, higher-level processing) can affect monocular neurons in lower visual cortices (presumably V1).

The results of previous studies of utrocular perception have been decidedly mixed (Porac & Coren, 1986). Ono and Barbeito (1985) have shown that earlier studies frequently contained artifactual cues that permitted reliable utrocular discrimination (Smith, 1945; Pickersgill, 1961; Blake & Cormack, 1979; Marten *et al.*, 1981). Moreover, Ono and Barbeito (1985) demonstrated that they could reverse an observer's utrocularity decision by systematically manipulating these cues. Chapter 5 represents our attempt at defeating the technical problems associated with earlier experimental paradigms (Smith, 1945; Blake & Cormack, 1979). Because equally (finely tuned) energetic stimuli are shown to both eyes, observers in our experiments do not experience an asymmetric "feeling in the eye" (Brueckner & von Brueke, 1902; Enoch *et al.*, 1969) or what Helmholtz (1866) referred to as "außerordentliches Organgefühl". Furthermore, the fact observers display differential performance across experimental conditions implies that no general artifact of our display can be exploited.

1.5 Interocular integration of motion signals

Neural events underlying perception of coherent motion are generally believed to be hierarchical (Movshon, 1990; Braddick, 1993); information about local motion is registered by spatio-temporal coincidence detectors (Adelson & Bergen, 1985; Van Santen & Sperling, 1984) whose outputs are then integrated at a subsequent stage (Chang & Julesz, 1984; Nawrot & Sekuler, 1990). Specific stimulus conditions capable of affecting image segmentation (*i.e.*, perceptual motion coherency) may cause systematic differences in the directional tuning of those neurons presumed to underlie the integration of component motion signals (Albright (1992). Reliable motion inte-

gration must satisfy two apparently conflicting demands. First, motion signals from neighboring locations must be spatially integrated for reasons of noise-reduction and for the aperture problem to be overcome. Second, sensitivity to small velocity differences ("motion contrast") must be preserved for the segmentation of image portions belonging to distinct objects.

Early visual processing represents the visual field as an undifferentiated array of signals that encode properties of light intensities at small image regions, but at some point in the cortical hierarchy an explicit representation should account for visual features as forming distinct perceptual entities, such as objects and surfaces. A wealth of psychophysical evidence points to the existence of both integration and segmentation mechanisms, but it is not clear how both, integration and segmentation can be accommodated in one computational framework. Chapter 6 presents an attempt to identify the cortical stages involved in human perception of coherent motion. Our psychophysical results endorse a functional distinction between motion segmentation and integration that relates to anatomically distinct areas V1 and MT.

Chapter 2 Perception without attention

2.1 Segregation of dynamic textures at different levels of attentional and cortical processing

2.1.1 Background

Fast grouping of features that specify textures and events (movement, change) compatible with the visual environment antecedes the segmentation of objects and background surfaces (Nakayama *et al.*, 1985). A prerequisite for initial scene segmentation is that static and dynamic features be extracted in parallel across visual space, that permit effortless and preattentive segregation of regions that contain them from regions that do not. Fast and parallel perception of texture contrasts and surface boundaries may involve grouping of local features, such as color, brightness, binocular disparity, line orientation and motion (Beck, 1966, 1967, 1982; Olson & Attneave, 1970; Attneave, 1971; Julesz, 1975, 1984; Treisman & Gelade, 1980; Nakayama *et al.*, 1985; Dick *et al.*, 1987). In that respect, static and dynamic textures afford similar levels of detectability, provided the spatial arrangement of local features is sufficiently dense. For example, an entire array of stimulus elements is processed in parallel in the detection of texture borders and singularities and similarly, regions with a common direction of motion mediate perceptual "pop-out" against a background of dissimilar movement (Julesz, 1981; Bergen & Julesz, 1983; Nakayama *et al.*, 1985; Treisman & Gormican, 1988; Braun & Sagi, 1990).

It seems likely that parallel processing subserves a priviledged class of feature detections that concern the initial stages of object segmentation and surface formation,

perceptual functions commonly attributed to early visual cortex, such as areas V1, V2, V3, V4 and MT. As yet, however, there is no physiological evidence *directly* relating parallel, preattentive perception to single-cell responses in early visual areas. Possible mechanisms are (indirectly) suggested by receptive field properties in visual cortical areas with topographic organization, but little attempt has been made to identify the neuronal correlates of parallel feature detection in humans or subhuman primates.

Cells selective for specific features (*e.g.* orientation) appear to be inhibited by similar features in the near surround of their classical receptive field ("surround inhibition"), at least in early visual cortex (Hubel & Wiesel, 1974; Miezin *et al.*, 1982; Allman *et al.*, 1985). Hence surround inhibition could partake in setting up salient boundaries between two adjacent visual textures by attenuating uniform regions significantly more than discontinuous or singular regions (Sagi & Julesz, 1987; Sagi, 1990; Rubenstein & Sagi, 1990; Malik & Perona, 1990; Bacon & Egeth, 1991; Bravo & Nakayama, 1992). An opportunity to study the cortical level at which dynamic visual texture is processed is provided by recent work of Qian and Andersen (1994). They describe dynamic visual textures that differentially stimulate areas V1 and MT in the macaque - whose visual system seems to closely resemble our own (Snowden *et al.*, 1992). In brief, the basis for this effect is that equal and opposite motion at the same point in space interact and attenuate responses at the level of MT but not V1.

Detection of texture boundaries may be classified as either parallel or serial depending on whether the foreground (small region) is more or less salient than the background (large region). This dichotomy is ascribed to local-global comparisons at some stage in the segmentation process. Comparisons of feature contrasts across larger distances of visual space, necessary for parallel figure-ground segmentation, are thought to be accomplished by surround inhibitions from the "non-classical" surround (Allman *et al.*, 1985). For example, some cells selective to feature contrasts in

areas V1, V2, V4 and MT are inhibited by feature contrasts in the far surround of their classical receptive field (Nelson & Frost, 1978; Allman *et al.*, 1985; Knierim & Van Essen, 1992; Malach *et al.*, 1993; Desimone *et al.*, 1993). Although, on the one hand, it is often assumed that surround inhibition in area V4 serves to "sharpen" the orientation contrast between neighboring texture elements, it is not evident whether those orientation-selective cells respond merely to local features, or global orientation contrasts between textures or surfaces, or both (Hammond, 1978, 1985; Nothdurft & Li, 1985). On the other hand, area MT has been implicated in both perceptual decisions concerning the single direction of visual motion at one image location as well as figure-ground discrimination based on multiple directions of motion across the field of view (Allman *et al.*, 1985; Newsome *et al.*, 1989; Salzman *et al.*, 1990). Hence the central question of this chapter: are the different stages of image segmentation (parallel *vs* serial) correlated with differential activation in one particular, identifiable cortical area (*e.g.*, strong *vs* weak) or do they reflect an overall activation difference across various stages of cortical processing (*e.g.*, V1 *vs* MT)?

A common behavioral test for visual processing of texture is fast and parallel visual search (Treisman, 1983; Treisman & Souther, 1985; Treisman & Gormican, 1988). This technique has some short-comings in that it does not distinguish between processing at the level of early vision and processing that requires divided attention (Nakayama & Bravo, 1992). Another short-coming is that it requires manipulation of stimulus set-size, a manipulation to which a dynamic visual texture does not (readily) lend itself. In our alternative technique, observers are required to focus their attention at display center, leaving the visual periphery largely unattended. In this situation, perception of the visual periphery is based entirely on parallel processing at the level of early vision. It has been shown that this perception includes the presence and position of singularities and discontinuities of visual texture.

In our experiments, human observers located a small target texture embedded in

a large background texture. Target and background texture were chosen to originate different activity levels, either in area V1 or MT, or both. For some texture pairs, activity was expected to be larger in the target region while for other pairs, activity in the target region was expected to be smaller than elsewhere. The extent to which these activity differences are processed at the level of early vision was assessed by asking observers to locate the target region with attention focused elsewhere in the display.

2.1.2 Materials and methods

Displays were generated by an SGI Indigo 2 on a high-resolution color monitor (SGI). The resolution was 1024×1024 pixels and the frame rate $60Hz$, permitting presentation times to be varied in steps of $16.6ms$. Viewing was binocular at a distance of $57cm$, resulting displays that subtended $10 \times 10^\circ$ of visual angle. Thus, a single pixel corresponded to approximately 0.01° of visual angle (neglecting projective distortion). No chin-rest was used. Before each trial, observers fixated a cross-shaped mark at display center (see Figure 2.1, *Fixation*). Because of the presentation times used, there was no need to otherwise monitor eye movements. Ambient illumination was approximately $5cd/m^2$ and maximal luminosity was $10cd/m^2$. Responses were unspeeded and were entered on a computer keyboard, with incorrect responses eliciting immediate auditory feedback.

Six Caltech undergraduates served as subjects (DE, JG, SK, HL, AR, AV). Each subject enrolled for at least 10 sessions of 1-1.5 hours and received payment of $120. All subjects had normal or corrected to normal vision.

Moving dots (size 0.01°, life-time $50ms$, velocity $2^\circ/s$, density $10\,\mathrm{deg}^{-2}$) populated all of our displays. In spite of the short lifetime of dots, dot density remained constant because every dot that "died" was instantly "reborn" elsewhere in the display. Dots moved in one of eight possible directions: 0, $\pi/4$, $\pi/2$, $3\pi/4$, $-\pi/4$, $-\pi/2$, $-3\pi/4$, and

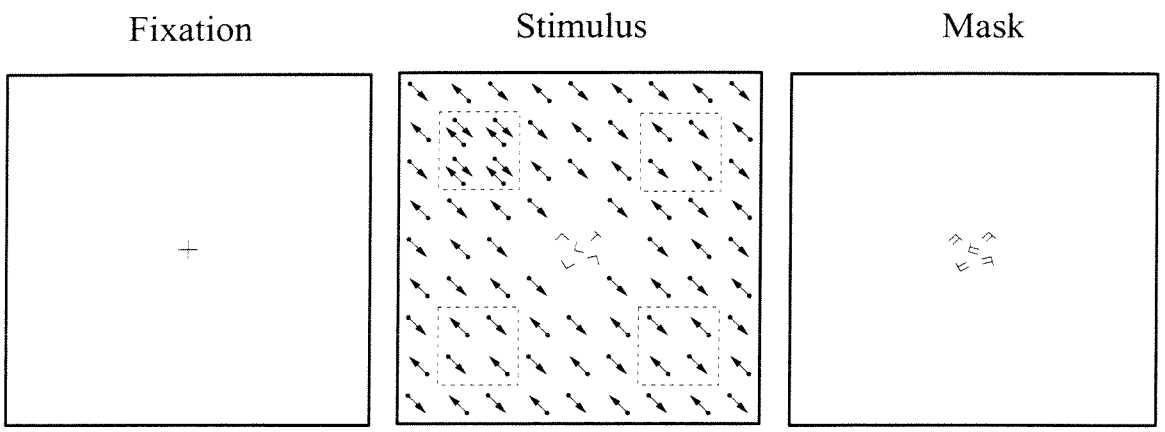

Figure 2.1: Schematic of display used in Experiment 2. The basic schema depicted here applied to all experiments. After a brief period of fixation ($\approx 1s$), the stimulus appeared for some time interval and was immediately followed afterwards by the letter mask (╔-shaped elements). Stimulus display size was $10 \times 10°$ with the foreground (target) subtending $2 \times 2°$ of visual angle. The target appeared randomly in one of the four background quadrants. Broken lines represent the four possible target locations. In this particular case, target texture was locally-balanced motion (LB) and background texture was globally-balanced motion (GB). The localization task involved the discrimination of the "odd" target region (*i.e.*, here upper left corner), that differed from the background either by orientation or texture contrast. The letter task concerned the discrimination of five ⊤- and ∟-shaped elements near display center. The stimulus protocol was identical in all experiments.

$-\pi$. Each display consisted of a $2 \times 2°$ foreground embedded in a $10 \times 10°$ background, the foreground being centered in one of the four quadrants of the background (see Figure 2.1, *Stimulus*). Generally, moving dots in the fore- and background formed qualitatively different dynamic visual textures. In Experiment 1, however, fore- and background textures were qualitatively the same but differed in the direction of motion. Four basic dynamic visual textures as well as several mixed textures were used. The four basic textures were unbalanced motion ("UB"), globally balanced motion ("GB"), locally balanced motion ("LB") and random motion ("RA"). The UB-texture consisted of a single surface of randomly placed dots moving with a single velocity, perceived as a coherent moving surface. The GB- texture consisted of two spatially *uncorrelated* sets of dots with two equal and opposite velocities, respectively, perceived as two surfaces sliding coherently over each other ("motion transparency"). The LB-texture consisted of two spatially *correlated* sets of dots with two equal and opposite velocities, respectively, perceived as incoherent flicker rather than coherent motion (Qian *et al.*, 1994a). Spatially correlated dots were "born" in pairs at a fixed separation of approximately 0.2° and moved towards (and past) each other for the duration of their lifetime. The RA-texture consisted of randomly placed dots with independent (and random) velocities, perceived as flicker noise.

The letter task involved the discrimination of five ⊤- and ⊔-shaped elements in an area subtending $1 \times 1°$ of visual angle near the center of the display (see Figure 2.1, *Stimulus*). Each line of the ⊤- and ⊔-shaped elements measured $0.16 \times 0.02°$. These elements could appear at seven possible location (r, θ): the exact center of the display and six locations at 1° of eccentricity, spaced evenly around the center ($r = 0$ or 34 pixels, $\theta = 0, \pi/6, \pi/3, \ldots, 5\pi/6$). On any one trial, five ⊤- or ⊔-shaped elements were assigned randomly to the seven possible locations and, in addition, were rotated randomly and independently. This resulted in a large number of possible configurations. Either five Ts, five Ls, four Ts and one L, or four Ls and one T appeared. The

masking pattern contained five ⌐- shaped display elements which were of identical dimensions and appeared at the same locations as the ⊤- and ⌊-shaped elements but were rotated independently (and randomly) (see Figure 2.1, *Mask*).

The *localization task* involved a four-alternative forced-choice (4AFC) localization of the foreground in one of the four quadrants of the display. Possible responses were "upper left corner", "upper right corner", "lower left corner", and "lower right corner".

The *letter task* involved a two-alternative forced-choice (2AFC) discrimination of letter shapes. Observers were asked to report whether all letters were the same (*i.e.*, five Ts, five Ls) or whether one was different from the other four (*i.e.*, four Ts and one L, four Ls and one T). The possible responses were "same" or "different".

When instructed to perform two tasks concurrently, subjects responded twice in every trial, resulting in two performance values called *double-task performances.* When instructed to perform only one task, either they responded only once in every trial, resulting in one performance value called *single- task performance.*

To prevent planned saccades, the trial sequence began with a fixation interval (background at mean luminance) of variable duration ($100 - 250ms$). Next, the stimulus pattern was presented for a fixed duration, and was immediately followed by the letter mask (of equal duration). After viewing the trial sequence, observers responded either once or twice, depending on instructions. All responses were entered as a single keystroke on the computer keyboard.

Stimulus elements belonging to both localization- and letter-task were present at all times, even during single-task blocks. When performing a double task, observers were instructed to treat as *primary* the letter task and as *secondary* the localization task. Instructions strongly encouraged subjects to achieve the highest possible performance on the letter task.

Averaged over all observers in all experimental conditions, the letter task was

performed almost as well in double ($89.94 \pm 2.19\%$ correct) as in single task conditions ($90.77 \pm 1.90\%$ correct). This difference was not significant. As single and double task performance on the letter task was generally comparable for each observer and experimental condition, we do not report letter task performance separately. Note however, the single and double task performance of the letter task enter into the "compatibility index" (see below) which is reported separately for each experiment.

The degree to which performance of the letter task removed visual attention from the periphery of the display has been quantified elsewhere (Braun, 1994). Using the discrimination of a single ⊤ or ⊥ as a probe task, to measure availability of attention in the visual periphery, it was found that little or no attention remained (see Figure 2.2). The letter task did not noticeably detain resources other than visual attention, and for approximately $200ms$, visual attention was prevented from shifting elsewhere (Bergen & Julesz, 1983; Kröse & Julesz, 1989).

Although subjects were practiced, performance generally continued to improve somewhat during data collection. To ensure that all critical comparisons were based on comparable states of practice, double and single task performance were investigated during the same session for any given trial. Data were collected in blocks of 100 trials. To obtain comparable observer performance near the level of 84% correct ("criterion performance"), a suitable display duration was chosen for every task. Differences between observers were generally small compared to differences between tasks.

When the two tasks were carried out concurrently, localization double-task performance was often lower than single-task performance. One way to quantify this decrease in performance is to directly compare single and double task performance of each task and to assess the statistical significance of any decrease using Kendall's τ. Another way is to define the *compatibility index* C_i

$$C_i = \frac{r_A^i - c_A}{\overline{s_A} - c_A} + \frac{r_B^i - c_B}{\overline{s_B} - c_B} - 1,$$

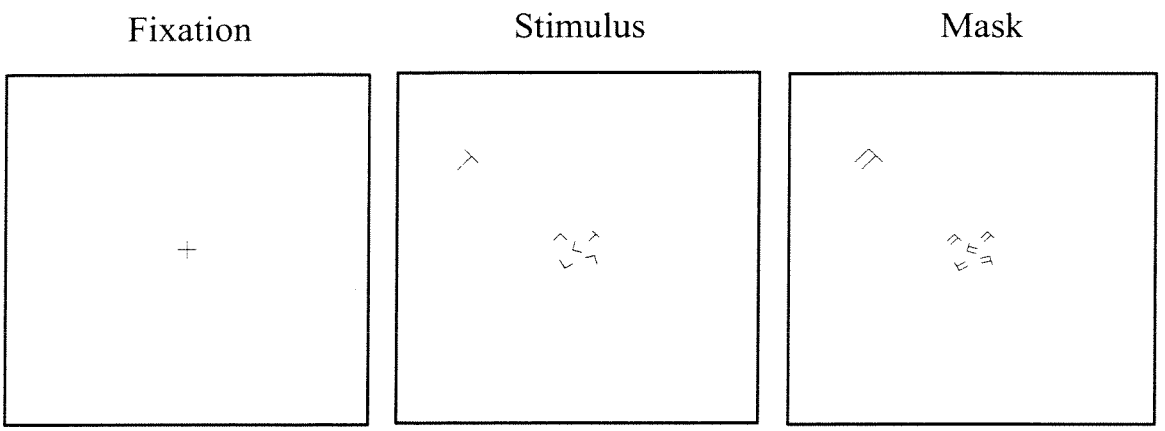

Figure 2.2: Schematic of stimulus used to probe the secondary task paradigm in removing visual attention from the display periphery (Braun, 1994). After a brief period of fixation ($\approx 1s$), the stimulus appeared, followed by the letter mask (see Figure 2.1) and probe mask (large ⊓). Perception with divided attention (multiple letters) was examined for the discrimination of a single ⊤ or ⊔. A mask was employed to terminate visual persistence. Since the discrimination of letter shapes is known to involve active attention, a task involving a cluster of such shapes is expected to show evidence of serial processing. When active attention is divided between two tasks (*e.g.*, letter and probe task), the performance of at least one of the two tasks is expected to decrease. The probe task is designed to be relatively undemanding but nevertheless require (active) visual attention. When presented concurrently, successful execution of both tasks becomes virtually impossible.

where r_A^i and r_B^i are the respective performance of tasks A and B in double task block i, $\overline{s_A}$ and $\overline{s_B}$ are the respective average performance in all single task blocks, and c_A and c_B are the respective levels of chance performance (letter-task chance performance was 25% and localization-task chance performance was 50%). If double task performance equals single task performance for both tasks, $C_i = 1$. If double task performance equals single task performance for one task but chance performance for the other, $C_i = 0$ (see Figure 2.3).

2.1.3 Results

Experiment 1

To gain insight into the cortical level at which the contrast between two dynamic textures is processed, we examined the perception of orientation contrasts in UB, GB and LB textures (see Figure 2.4). Single and double task performances were determined in all three conditions (UB, GB and LB) for four subjects (84,000 trials). Observers AR and AV served in all three conditions. Subjects DE and SK participated only in condition UB, and subjects JG and HL participated only in conditions GB and LB.

All three conditions were investigated at stimulus presentation times of $200ms$. For conditions UB, GB, and LB single localization-task performance was comparable at $99.60 \pm 0.69(0.28)\%$, $89.54 \pm 3.90(1.72)\%$, and $89.53 \pm 3.39(0.69)\%$ correct, respectively (see Figure 2.6, A). However, double task performance varied greatly and compatibility was 0.98 ± 0.005, 0.51 ± 0.018, and 0.014 ± 0.004, respectively.

When asked about their experience in the three single task situations, subjects consistently reported a "degradation of visibility", ranging from perceived *high* visibility for UB textures, *medium* visibility for GB textures to *low* visibility for LB textures. Note that at least the decrease in visibility from GB to LB textures did

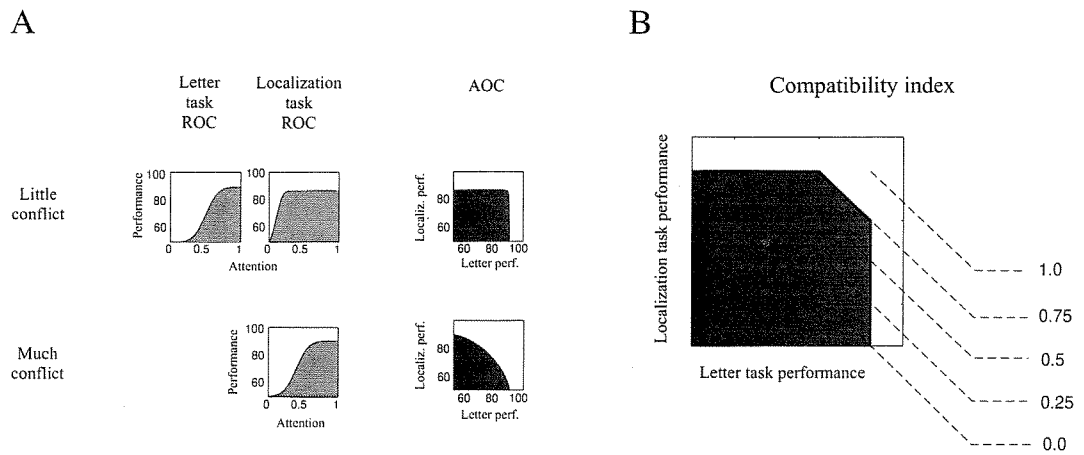

Figure 2.3: (A) Schematic ROC and AOC for several hypothetical tasks. The relationship between task performance and the amount of resources (*e.g.* attention) available to that task is called the "resource-operating characteristic" or *ROC*. Here, performance is measured by the percentage of correct responses. Chance performance is assumed to be 50%. The amount of attention available to the task is measured as a fraction of the total amount of attention, which is assumed to be constant. If attention is divided between tasks, the two ROCs determine how performance of one task (*e.g.*, *letter performance*) varies with performance of the other (*e.g.*, *localization performance*) and *vice versa*. This relationship is called the "attention-operating characteristic" or *AOC*. If performance of the letter task requires a much greater amount of attention than performance of the localization task, attentional resources remain effectively undivided. The resulting AOC shows that both tasks can be performed well (little conflict). For the case where performance of both tasks requires the same amount of attention, the resulting AOC shows that both tasks cannot be performed well (much conflict). (B) Schematic compatibility index for two concurrent tasks. The larger the area spanned by localization and letter task performance (dotted area) the less interference there is between the two tasks (compatibility = 1). If there is total interference between tasks the area spanned by the performance values will have a triangular shape compatibility = 0).

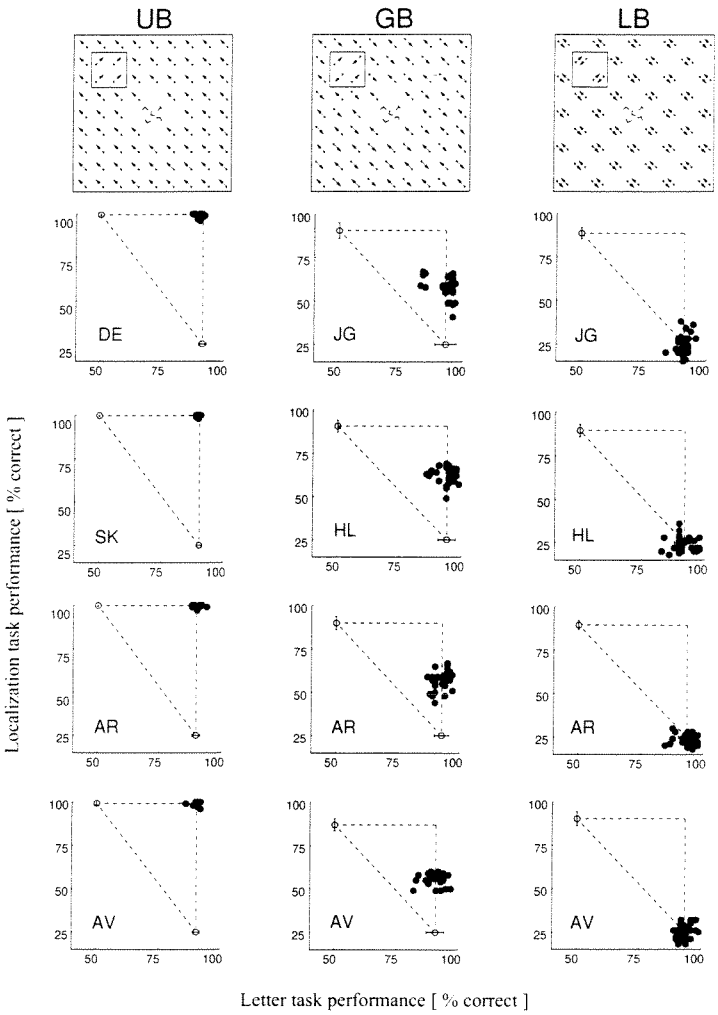

Figure 2.4: Displays and results of Experiment 1 (motion-defined orientation contrast only). First row from top: schematic of displays for the three conditions, from left to right, UB (unbalanced motion), GB (globally balanced motion) and LB (locally balanced motion). Columns contain results for each condition and observer (as identified by labeling). All conditions were performed at stimulus durations of $200ms$. The individual symbols in each scatter plot represent one block of 100 trials. Letter task performance is represented along the horizontal axes and localization task performance along the vertical axes. Open symbols (◯) show separate performance of a particular task (single task) and are positioned along the axes of the plot, together with respective single task standard errors (⊢◯⊣). Closed symbols (●) show concurrent performance of both tasks (double task) and occupy the plane of the scatter plot. Mean performance is indicated by broken lines. When the two tasks conflict, the closed symbols are found in the lower right corner of the scatter plot; when they do not, the closed symbols are located in the upper right corner of the plot.

not correspond to any decrease in performance. This dissociation between subjective visibility and performance will be addressed in detail in Chapter 3 (Kolb & Braun, 1995).

When active attention was available, orientation contrasts were readily detected in all three conditions. However, when visual attention was otherwise engaged a *continuum* of attentional demands emerged. Performance in condition UB was clearly independent of attention suggesting parallel processing, whereas double task performance in condition LB was overall at chance implying attentive and serial processing (see Figure 2.4). Although performance was drastically reduced in condition GB, it was still significantly above chance, indicating moderate demands on visual attention.

Average V1 and MT cell responses for textures UB, GB and LB are shown in Figure 2.8, A and B, respectively (Qian & Andersen, 1994). Apparently, the stronger the response in MT the greater the compatibility index was, implying that a strong activation in area MT was necessary for parallel processing. Since Qian and Andersen (1994) found that 75% of V1 cells tested could not "differentiate" between the GB and LB textures, it seems unlikely that an activity difference in area V1 should give rise to the observed difference in double-task performance. On the other hand, average MT cell responses to the GB and LB textures were significantly different, and among those cells that responded better to the GB than LB texture (39.6%), suppression for the LB texture was about 70%. We reasoned that if double task compatibility was indeed correlated with the amount of overall MT activation, then differential MT stimulation from fore- and background, respectively, could possibly account for previously observed double-task performance asymmetries with respect to which texture represented fore- and background. In other words, the question became whether a positive or negative difference in MT stimulation was responsible for performance asymmetries in texture discrimination (parallel *vs* serial).

Experiment 2

To determine whether parallel texture perception was correlated with the amount of overall MT activation or rather with the extent of differential MT activation (positive *vs* negative), we investigated the effect of the concurrent letter task on the detection of borders between dissimilar textures. The two basic textures involved in this experiment were GB and LB. In two conditions, fore- and background consisted of textures GB and LB (condition GB/LB), respectively and *vice versa* (LB/GB). In five other conditions, fore- and background consisted of mixtures of GB and LB textures (see Figure 2.5). Single and double task performances were determined in all seven conditions (*i.e.*, GB/LB, $3GB+1LB/1GB+3LB$, LB/GB, $2GB+2LB/LB$, $LB/2GB+2LB$, $2GB+2LB/GB$, and $GB/2GB+2LB$) for two to four subjects in 72,000 trials in total. Subjects JG and HL participated in only one condition, and subject DE participated in all but one condition. Observers SK and AR served in two and three conditions, respectively, and observer AV served in all cases.

Conditions GB/LB and LB/GB were investigated at stimulus presentation times of $200ms$ and the other conditions (all mixtures) were investigated at $250ms$. For conditions GB/LB and LB/GB single task performance was $88.20\pm0.35(1.60)\%$ and $84.75\pm3.41(4.61)\%$ correct, respectively (see Figure 2.6, B and D). For conditions $3GB+1LB/1GB+3LB$, $2GB+2LB/LB$, $LB/2GB+2LB$, $2GB+2LB/GB$, and $GB/2GB+2LB$ single task performance was $81.10\pm2.94(3.55)\%$, $82.60\pm1.54(4.10)\%$, $83.24\pm4.14(2.15)\%$, $81.10\pm3.20(3.65)\%$, and $85.54\pm1.32(2.70)\%$ correct, respectively (see Figure 2.6, C). Compatibility in conditions GB/LB and LB/GB was 0.95 ± 0.038 and 0.31 ± 0.035, respectively, and 0.41 ± 0.067, 0.28 ± 0.040, 0.20 ± 0.034, 0.21 ± 0.056, and 0.30 ± 0.062 for the mixtures.

When attention was available, all texture contrasts were detected comparably well, although at slightly different presentation times ($200ms$ for GB/LB and LB/GB, and $250ms$ for cases involving mixed textures). However, when attention was fully en-

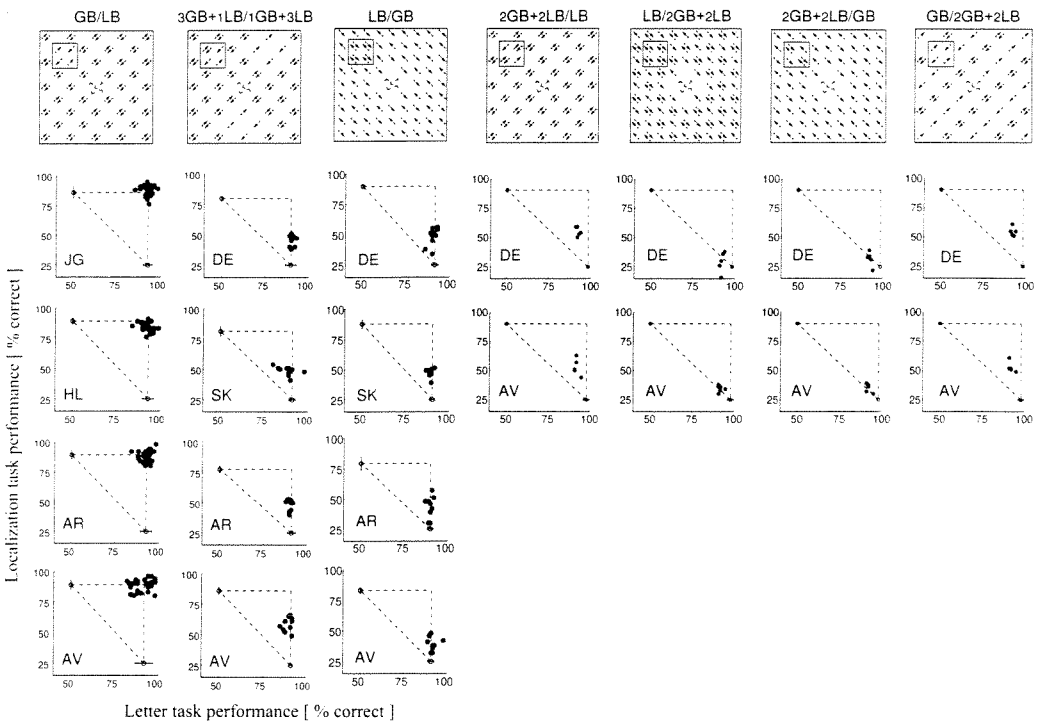

Figure 2.5: Displays and results of Experiment 2 (motion contrast only). Detailed schematic of the seven displays involving GB and LB textures and various mixtures. First row from top, from left to right, conditions GB/LB, $3GB+1LB/1GB+3LB$, LB/GB, $2GB+2LB/LB$, $LB/2GB+2LB$, $2GB+2LB/GB$, and $GB/2GB+2LB$. Mixtures refer to four-part ratios of GB and LB textures as indicated by the numbers describing each mixture. For example, $3GB+1LB/1GB+3LB$ refers to a target mixture of three parts GB texture and one part LB texture against a background of one part GB texture and three parts LB texture. Columns contain results for each condition and observer (as identified by labeling). Conditions GB/LB and LB/GB were performed at stimulus durations of $200ms$. The other conditions (all mixtures) were performed at $250ms$ stimulus duration. The individual symbols in each scatter plot represent one block of 100 trials. Letter task performance is represented along the horizontal axes and localization task performance along the vertical axes. Open symbols (○) show separate performance of a particular task (single task) and are positioned along the axes of the plot, together with respective single task standard errors (⊢○⊣). Closed symbols (●) show concurrent performance of both tasks (double task) and occupy the plane of the scatter plot. Mean performance is indicated by broken lines. When the two tasks conflict, the closed symbols are found in the lower right corner of the scatter plot; when they do not, the closed symbols are located in the upper right corner of the plot.

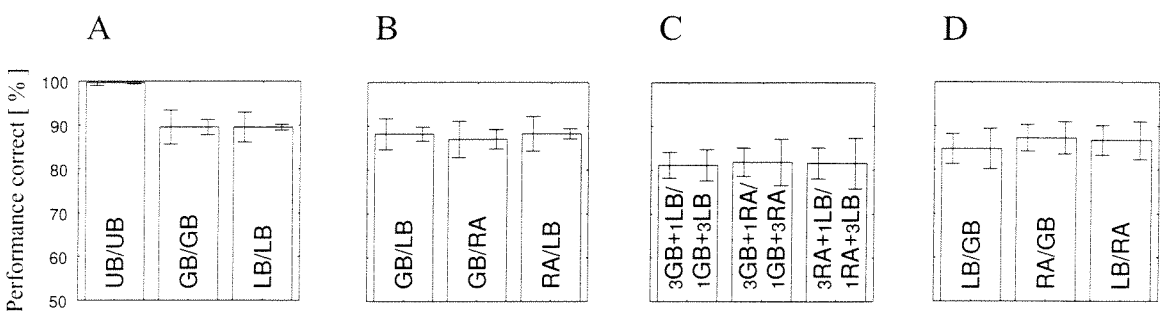

Figure 2.6: (A-D) Single localization task performance for all conditions studied in Experiments 1,2, and 3 across all relevant observers. Conditions are labeled to indicate target and background textures. For example, GB/LB refers to the case where fore- and background consisted of GB and LB textures, respectively. Note that in Experiment 1 fore- and background consisted of the same texture but differed in orientation (*e.g.*, UB/UB). Standard deviation (error between observers) and standard error (error within observers) are drawn on the left and right hand side of each bar, respectively.

gaged by the letter task, only in one condition (GB/LB) performance came close to single task results suggesting nonattentive and parallel processing. In all the other conditions, performance was dramatically impoverished, implying strong overall attentional demands.

Apparently, double task compatibility was correlated with the sign of differential MT stimulation from fore- and background, respectively. For example, a positive differential of 44 (as obtained from averaging MT cell responses for the GB and LB textures, respectively) resulted in double task compatibility of 0.95, whereas a negative differential of equal magnitude (-44) resulted in a compatibility index of 0.32. When the overall differential was relatively small (*e.g.* ± 22), double task compatibility was generally small, yet in cases with a differential of $+22$, compatibilities were slightly higher (average 0.33) as compared to cases with a negative differential of -22 (average 0.20). Since LB and RA textures elicit similar average responses in MT we would expect little if no difference in performance for displays containing RA and LB textures if our predictions about the role of differential MT activation were correct. On the other hand, we would predict an asymmetric outcome for fore- and background combinations of GB and RA textures, respectively.

Experiment 3

In the final experiment of this chapter, we studied texture segregation in displays consisting of RA and either GB or LB textures, respectively. Accordingly, fore- and background combinations were GB and RA textures and a mixture between the two, and RA and LB textures and a mixture between the two (see Figure 2.7). In total, six conditions were investigated with four subjects in 120,000 trials: GB/RA, $3GB+1RA/1GB+3RA$, RA/GB, RA/LB, $3RA+1LB/1RA+3LB$, and LB/RA. Subjects JG and HL participated only in conditions where GB was fore- and RA was background and conditions where RA was fore- and LB was background, and

subjects DE and SK participated in all but those two conditions. Observers AR and AV served in all six conditions.

All conditions were investigated at $200ms$ presentation times, with the exception of two ($3GB + 1RA/1GB + 3RA$ and $3RA + 1LB/1RA + 3LB$) that were tested at $250ms$. For conditions GB/RA, RA/GB, RA/LB, and LB/RA single localization-task performance was $87.01 \pm 4.16(2.22)\%$, $87.54 \pm 3.90(1.72)\%$, $88.28 \pm 3.98(1.16)\%$, and $86.67 \pm 3.39(0.68)\%$ correct, respectively (see Figure 2.6, B and D). For the mixtures $3GB + 1RA/1GB + 3RA$ and $3RA + 1LB/1RA + 3LB$ single localization-task performance was $81.80 \pm 3.03(3.70)\%$ and $81.52 \pm 3.43(4.33)\%$ correct, respectively (see Figure 2.6, C). Double-task compatibility in aforementioned non-mixtures were 0.86 ± 0.045, 0.26 ± 0.071, 0.28 ± 0.031, and 0.17 ± 0.041. For the mixtures double-task compatibility was 0.29 ± 0.088 and 0.17 ± 0.065.

All texture contrasts were detected comparably well when attention was not otherwise engaged, although presentation times varied slightly across conditions ($200ms$ for non-mixtures and $250ms$ for mixtures). However, when active attention was divided between the two, only in the GB/RA condition double-task performance was close to single-task performance, suggesting nonattentive and parallel processing. On the other hand, performance was relatively poor in all other conditions, including the three non-mixtures RA/GB, RA/LB, and LB/RA. In those cases and the conditions involving mixed textures, performance was crucially dependent on attentional resources.

These results confirmed our findings of the previous experiment that a positive differential in cortical MT activation was correlated with preattentive processing, while a negative differential (of equal magnitude) was not. This general rule is graphically depicted in Figure 2.8, D, where we plot double- task compatibilities against the corresponding levels of MT activation.

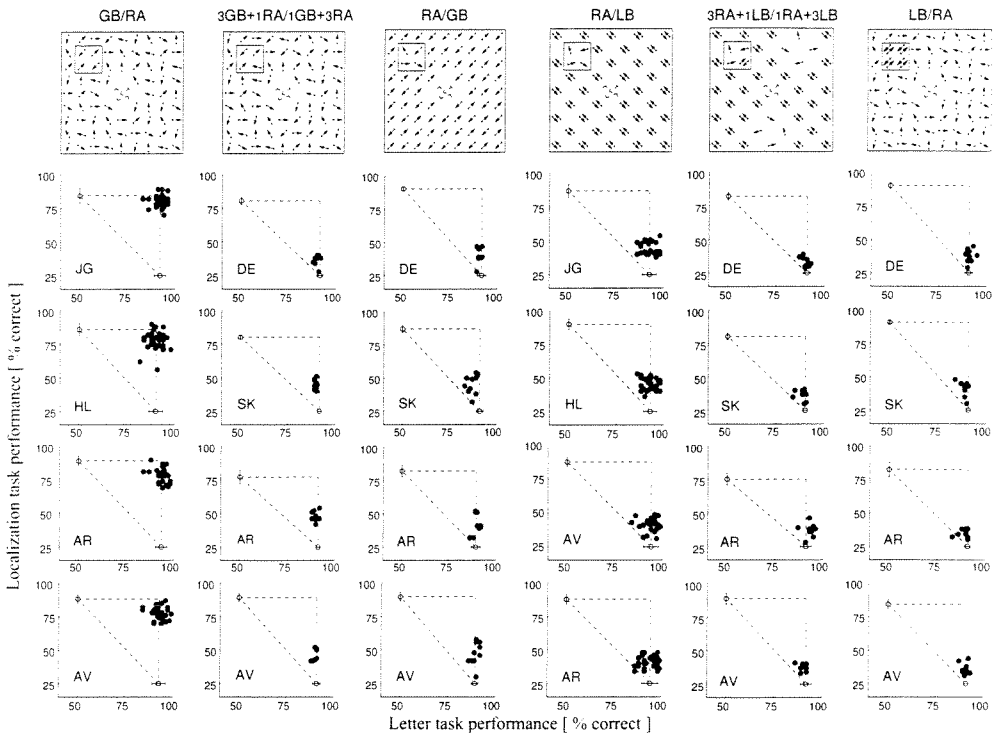

Figure 2.7: Displays and results of Experiment 3 (motion contrast only). Detailed schematic of the six displays involving GB, LB and RA textures. First row from top, from left to right, GB/RA, $3GB+1RA/1GB+3RA$, RA/GB, RA/LB, $3RA+1LB/1RA+3LB$, and LB/RA. Mixtures refer to four-part ratios of GB and RA textures or LB and RA textures as indicated by the numbers describing each mixture. For example, $3GB+1RA/1GB+3RA$ refers to a target mixture of three parts GB texture and one part RA texture against a background mixture of one part GB texture and three parts RA texture. Conditions GB/RA, RA/GB, RA/LB, and LB/RA were performed at $200ms$. The other conditions (mixtures) were performed at $250ms$ stimulus duration. The individual symbols in each scatter plot represent one block of 100 trials. Letter task performance is represented along the horizontal axes and localization task performance along the vertical axes. Open symbols (◯) show separate performance of a particular task (single task) and are positioned along the axes of the plot, together with respective single task standard errors (⊢◯⊣). Closed symbols (●) show concurrent performance of both tasks (double task) and occupy the plane of the scatter plot. Mean performance is indicated by broken lines. When the two tasks conflict, the closed symbols are found in the lower right corner of the scatter plot; when they do not, the closed symbols are located in the upper right corner of the plot.

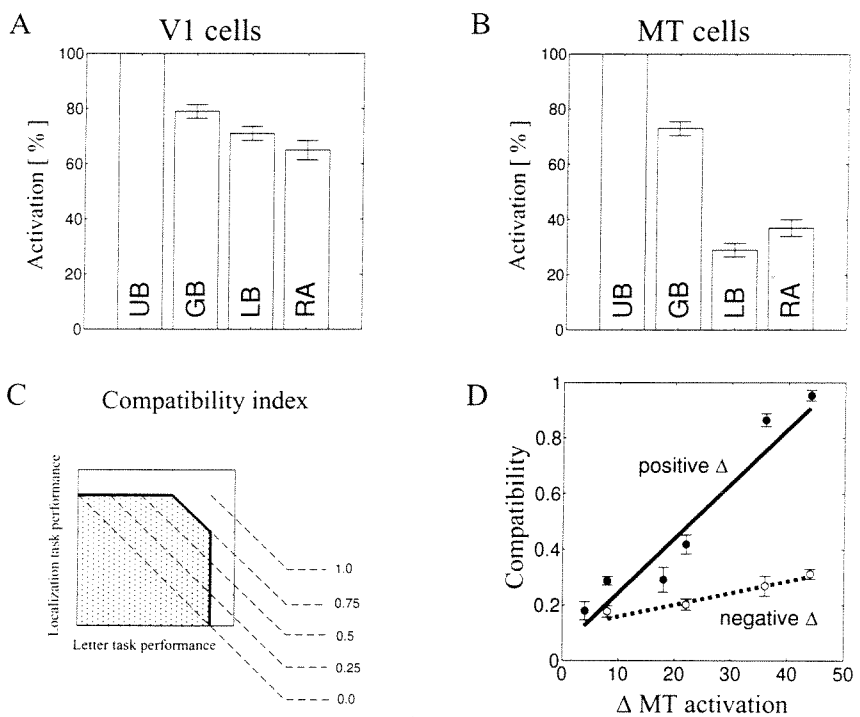

Figure 2.8: (A) Average direction-selective cell responses in area V1 to UB, GB, LB and RA textures. (B) Average responses from direction-selective MT cells to UB, GB, LN and RA textures - both with permission from Qian and Andersen (1994). The MT-cell responses to the GB texture were significantly larger than to the LB texture. Note that the RA texture examined by Qian and Andersen (1994) was stationary flicker derived from either the GB or the LB texture. For practical reasons, we chose a noise stimulus whose spatio-temporally uncorrelated component was velocity rather than intensity distribution. Since both stimuli generate isotropic motion noise (*i.e.*, "flickering in all directions") we use RA to denote both the flicker stimulus in the context of single-cell physiology and the random direction-of-motion stimulus in the context of our psychophysics. (C) Double task compatibility, see Figure 2.3, B. (D) Difference between MT activation occasioned by fore- and background, respectively, plotted against double-task compatibility where positive differential (solid line) and negative differential (broken line) are plotted separately.

2.1.4 Discussion

Attentional demands are typically studied with visual displays that necessitate the selection of some stimuli at the expense of others ("visual search"). In visual search, observers attempt to determine as quickly as possible the presence or absence of a target among numerous distractors, and reaction time is measured as a function of the number of distractors in the display. Depending on the particular target and distractors, reaction time is largely independent of distractor number ("parallel search"), or increases with rising number of distractors ("serial search"), or anything in-between.

Previous experiments using visual search among stimuli of different intensity have established performance asymmetries with respect to the *relative* intensity of target and distractors (Treisman & Gelade, Treisman, 1983; Treisman & Souther, 1985; Treisman & Gormican, 1988; Treisman, 1993). As a general rule, depending on whether the target is either more or less intense than the distractor items, visual search is said to be either parallel or serial, respectively.

To investigate the capabilities of preattentive processing in situations that do not lend themselves to the search-task paradigm, for example texture segregation, it becomes necessary to directly test performance in the absence of attention. In the present chapter we report a series of experiments in which subjects attempt to carry out two visual tasks simultaneously, the discrimination of a letter shape (letter task) and the localization of a texture contrast on an otherwise uniform background (localization task). Subjects are instructed to give different weights to the tasks, treating the letter task as primary and the localization task as secondary ("secondary task paradigm", Kahneman, 1973). An important aspect of the secondary task paradigm is that the primary task is particularly demanding of visual attention. Accordingly, when the primary task is performed well, little or no attentional capacity should be left over for the secondary task. In agreement with previous findings, we here report the existence of two classes of visual tasks, one that is subject to attentional capac-

ity limitations (serial), and another one that somehow escapes attentional capacity limitations (parallel) (Braun, 1994, Braun, 1995).

In what respect precisely do these two classes of visual tasks differ? Why should attention be required to detect a textural discontinuity in one case (*e.g.*, Experiment 2, condition LB/GB), and why should divided attention suffice to discriminate target from background in another case (*e.g.*, Experiment 2, condition GB/LB)? One relevant factor pertaining to the distinction between parallel and serial processing is *signal strength*. Signal strength is commonly thought to induce task performance as ranging from a "data-limited" to a "resource-limited" regime (Norman & Bobrow, 1975). When sensory factors become sufficiently weak, every visual task is thought to become dependent upon the availability of attention. This would imply that preattentive processing eventually requires undivided attention (*i.e.*, serial processing), once the signal strength becomes sufficiently weak. Hence it could be argued that differential activation of area MT as the purported distinguishing factor in preattentive *vs* attentive dynamic-texture segregation may merely reflect the difference in overall signal strengths occasioned by fore- and background textures. For example, if the background did not stimulate area MT (*e.g.*, GB/LB), the total noise level might have simply been lower than in the reverse case (*i.e.*, LB/GB), in other words, the greater the differential cortical activation the greater also the sensory signal variance.

To test this prediction, we evaluated signal-to-noise ratios for all types of displays used in Experiment 2. Our calculations are based on the model proposed by Qian *et al.* (1994b) to account for the strong suppression between locally balanced motions in area MT. Detection of motion signals is occasioned by two spatiotemporally oriented pairs of linear filters (Adelson & Bergen, 1985). In this manner, motion is represented as "orientation in space-time". Recent results from single-cell studies in cat visual cortex support the assumption of a linear mechanism for generating motion sensitivity (Jagadeesh *et al.*, 1993; but see Douglas *et al.*, 1995 for an opposing view).

The model's first stage computes the unidirectional motion energies by squaring and then summing the outputs of a quadrature pair of oriented filters (with 90° phase difference). Thus the first stage simply measures the Fourier power within a given spatiotemporal frequency window to yield the phase-independent motion energy. The model's second stage derives the *opponent energy* from opposite directions of motion via substractive inhibition (see Figure 2.9).

The first stage of the Bergen-Adelson model (Bergen & Adelson, 1985) - as described in Qian *et al.* (1994b) - assumes a quadrature pair of linear filters with even and odd phases tuned to leftward (-) and rightward (+) directions of motion as given by

$$g_e^{\pm}(x,t) = \frac{1}{2\pi\sigma_x\sigma_t}\exp\left(-\frac{x^2}{2\sigma_x^2}-\frac{t^2}{2\sigma_t^2}\right)\cos(\omega_x x \mp \omega_t t)$$

$$g_o^{\pm}(x,t) = \frac{1}{2\pi\sigma_x\sigma_t}\exp\left(-\frac{x^2}{2\sigma_x^2}-\frac{t^2}{2\sigma_t^2}\right)\sin(\omega_x x \mp \omega_t t).$$

The phase-insensitive leftward (-) and rightward (+) motion energies for a given spatiotemporal pattern $f(x,t)$ are defined as

$$\begin{aligned} E^+(x,t) &= [f * g_e^+]^2 + [f * g_o^+]^2 \\ E^-(x,t) &= [f * g_e^-]^2 + [f * g_o^-]^2, \end{aligned}$$

where $*$ denotes convolution. Responses at this stage are thought to match directionally selective complex cells (Qian *et al.* (1994b). The opponent motion energy (second stage) is then defined as the algebraic difference of the two:

$$E(x,t) = E^+(x,t) - E^-(x,t).$$

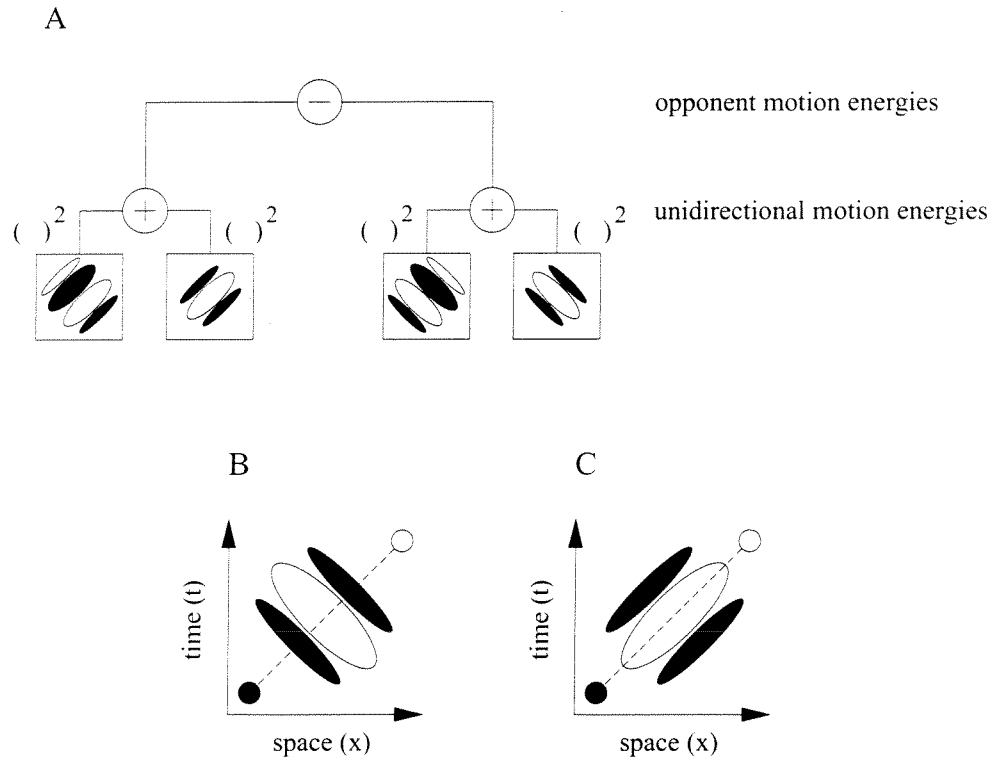

Figure 2.9: (A) Schematic of motion energy model used by Qian *et al.* (1994) to account for the perceptual difference between transparent (locally unbalanced motion signals) and nontransparent (locally balanced motion signals) displays. Detection of motion signals is accomplished by two spatiotemporally oriented pairs of linear filters (inside of square boxes) (Adelson & Bergen, 1985). In this fashion, motion is represented as "orientation in space-time". Recent results from single-cell studies in cat visual cortex support the assumption of a linear mechanism for generating motion sensitivity (Jagadeesh *et al.*, 1993). The model's first stage computes the *unidirectional motion energies* by squaring and then summing the outputs of a quadrature pair of oriented filters (with 90° phase difference). Thus the first stage simply measures the Fourier power within a given spatiotemporal frequency window to yield the phase-independent motion energy. The model's second stage derives the *opponent motion energies* from opposite directions of motion via substractive inhibition. Here motion signals in different (opposite) directions from each small region are assumed to inhibit each other. (B) Example of spatiotemporally oriented filter in the antipreferred direction of motion. For each spatial location there is a population of motion detectors tuned to either left or right direction of motion. In all calculations, the average dot trajectory length was assumed to be 8 pixels. (C) Example of spatiotemporally oriented filter in the preferred direction of motion.

For reasons of computational convenience, we rewrite the unidirectional and opponent motion energies using the complex Gabor function:

$$g_c^{\pm}(x,t) = \frac{1}{2\pi\sigma_x\sigma_t}\exp\left[-\frac{x^2}{2\sigma_x^2} - \frac{t^2}{2\sigma_t^2} + i(\omega_x x \mp \omega_t t)\right]$$

whose real and imaginary parts are the even and odd Gabor functions $g_c^{\pm}(x,t)$ and $g_c^{\pm}(x,t)$. Since the convolution of any real function $f(x,t)$ with the even and odd Gabor filters is equal to the real and imaginary parts of the convolution of that function with the complex filters, we will confine our analysis to the responses of the complex filters. Hence the unidirectional and opponent motion energies are now

$$\begin{aligned} E^+(x,t) &= [f * g_c^+]^2 \\ E^-(x,t) &= [f * g_c^-]^2, \end{aligned}$$

and

$$E(x,t) = [f * g_c^+]^2 - [f * g_c^-]^2,$$

respectively. A dot with initial position (x_0, y_0) and moving in the $+x$ direction with speed v from time t_1 to t_2 $(t_2 > t_1)$ can therewith be represented by the following equation

$$f_d^+(x,t) = c\delta(x - x_0 - vt)\delta(y - y_0)H(t - t_1)H(t_2 - t),$$

where H is the step function and c is a constant with the dimension of the inverse of length squared. With the 3-D extension of the Gabor filters in $g_c^{\pm}(x,t)$, Qian *et al.* (1994b) show that

$$
\begin{aligned}
f_d^+ * g_c^+ &= \exp\left[-\frac{(x-x_0-vt)^2+\sigma_x^2\sigma_t^2(\omega_t \mp \omega_x v)^2}{2(v^2\sigma_t^2+\sigma_x^2} - \frac{(y-y_0)^2}{2\sigma_y^2}\right] \\
&\quad \cdot \exp\left[-i(x-x_0+vt)\frac{\omega_x\sigma_x^2 \pm \omega_t\sigma_t^2 v}{v^2\sigma_t^2+\sigma_x^2} + i\omega^y(y-y_0)\right] \\
&\quad \cdot \frac{c}{(2\pi)^{3/2}\sigma_x\sigma_y\sigma_t}\int_{t-t_1+b/2a}^{t-t_2+b/2a}\exp(-ax^2)dx,
\end{aligned}
$$

where

$$
a = \frac{1}{2}\left(\frac{v^2}{\sigma_x^2}+\frac{1}{\sigma_t^2}\right),
$$

and

$$
b = \frac{(x-x_0-vt)v}{\sigma_x^2} + i(\omega_t - \omega_x v).
$$

If $f_d^+ * g_c^-$ is neglected, then $f_d^+ * g_c^+$ can be simplified - as Qian *et al.* (1994b) do in their equation (35) - to

$$
\begin{aligned}
f_d^+ * g_c^+ &= \frac{c}{2\pi\sqrt{v^2\sigma_t^2+\sigma_x^2}}\exp\left[-\frac{(x-x_0-vt)^2}{2(v^2\sigma_t^2+\sigma_x^2)} - \frac{(y-y_0)^2}{2\sigma_y^2}\right] \\
&\quad \cdot \exp\left[i\omega_x(x-x_0-vt)+i\omega_y(y-y_0)\right] \\
&\quad \cdot \{\mathrm{erf}[\sqrt{a}(t-t_2+b'/2a)] - \mathrm{erf}[\sqrt{a}(t-t_1+b'/2a)]\},
\end{aligned}
$$

with $f_d^+ * g_c^- \approx 0$, where

$$
b' = \frac{(x-x_0-vt)v}{\sigma_x^2}.
$$

Equation (35) in Qian *et al.* (1994b) describes a three-dimensional complex Gabor filter $f^+ * g^+$ whose response is a complex function of spatial position x and y, and

time t. We determined the spatial variability of these detectors from the density of a particular dot pattern, that is we computed the average empty neighborhood around each dot (or pair of dots, as in LB). Using equation (35) we obtained mean and variance of V1 and MT activation, respectively, occasioned by the following dot textures: GB, $3GB + 1LB$, $2GB + 2LB$, $1GB + 3LB$, and LB (see Figure 2.10, A and B). The model results for the basic textures GB and LB (V1: $79.00 \pm 4.67\%$ and $82.03 \pm 5.19\%$; MT: $79.00 \pm 4.67\%$ and 0) are in (overall) good agreement with the physiological data (see Figure 2.8, A and B).

A qualitatively similar picture canvassing the effect of differential MT activation on preattentive texture segregation can be seen in the model data (see Figure 2.10, C), as compared to the psychophysics (see Figure 2.8, D). However, model MT response signal-to-noise values show no significant correlation with previously determined double-task compatibility, implying that it is indeed the difference in cortical MT activation and *not* in signal strength that is functionally related to performance asymmetries in texture-discrimination tasks.

2.1.5 Conclusion

Motion-defined orientation contrasts were detected preattentively in cases where either both target and background were thought to elicit strong responses in area MT (Experiment 1). Textural contrasts were detected preattentively in cases where the target strongly stimulated area MT but the background did not (Experiments 2 and 3). Serial and attentive performance was required in cases where either both target and background were thought to selectively elicit responses in area V1, or in cases where the target caused putatively weaker responses in area MT than the background. In general, we found a pronounced asymmetry in performance depending on whether the target texture elicited more or less activity than the background texture. When both textures elicited comparable activity (orientation difference only) performance

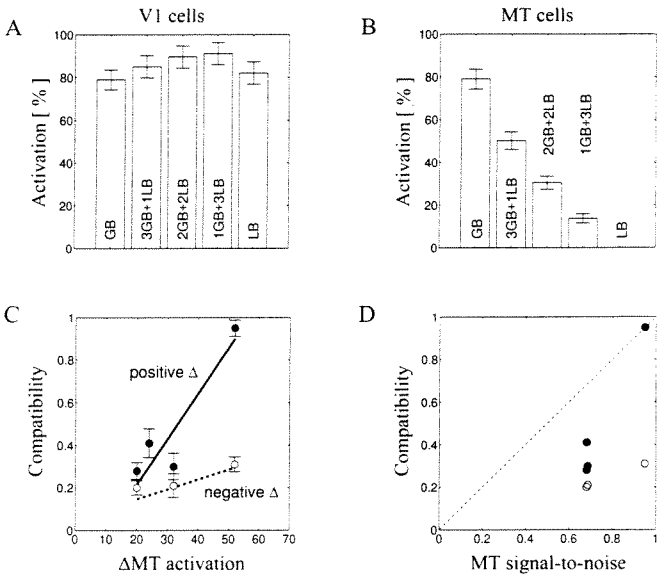

Figure 2.10: (A) Model V1 cell responses to GB and LB textures and various mixtures. We assume that for each location there is a population of motion energy detectors tuned to either left or right direction of motion. This stage may be identified with V1 cells (Qian *et al.*, 1994). (B) Model MT cell responses to GB and LB textures and various mixtures. Here the opponent energy is computed within each spatial frequency channel (left or right) from the initial motion measurement. Qian *et al.*(1994) proposed this stage is performed by subunits in MT cells' receptive fields. All calculations are based on equation (35) in Qian *et al.* (1994, pp 7391). For the GB texture we estimate a density of 2000 dots per 1024×1024 pixels and a nearest-neighbor separation of 18 pixels. For the LB texture we estimate a density of 1000 dots per 1024×1024 pixels and a nearest-neighbor separation of 13 pixels. For all displays involving GB and LB textures (or the mixtures) we derive the mean and variance (spatial) of activity occasioned by a dynamic-dot texture by determining the average empty neighborhood around each dot (GB) or pair of dots (LB). For the filter responses, we only consider the preferred and antipreferred directions and assume that the variance between these two subpopulations will be a good estimate of the variance between all subpopulation (*i.e.*, between all direction). (C) Difference between model MT activation occasioned by fore- and background, respectively, plotted against double-task compatibility where positive differential (solid line) and negative differential (broken line) are plotted separately. Model results are in good agreement with our psychophysical results (see Figure 2.8, D). (D) Model MT response signal-to-noise values plotted against double- task compatibility. No significant correlation is observed. Signal-to-noise ratios are expressed in terms of decision-probability (0 to 1) that the simulated neural activity occasioned by a display will be larger than zero. We consider both the difference in mean and variance between fore- and background texture (Rubenstein & Sagi, 1990). The decision is based on an area of 205×205 pixels. In this area, we assume a subunit spacing of 4×4 pixels, corresponding to 1/2 of the filter's wavelength. Hence the decision is based upon approximately 2500 subunits.

required MT activation. In summary, preattentive target localization required either equal MT activation and an orientation difference, or higher MT activation in the target area. Discrimination improved with positively but not negatively differential activity at the cortical level of area MT but not at V1, suggesting that an activity difference at area MT is required for parallel and preattentive dynamic- texture segregation. Furthermore, attentional demands of dynamic-texture segregation are not determined by sensory signal strength (signal-to-noise ratio), but by competition for the most conspicuous (salient) texture.

Chapter 3 Perception without awareness

3.1 Blindsight in normal observers: Psychophysics of visual segmentation and integration tasks without awareness

3.1.1 Background

Some patients with lesions in visual cortex that produce a homonymous visual field defect within which the patient is experientially blind, respond to stimuli confined to the blind field when they are persuaded to "guess". These patients lack conscious visual experience but, when tested, exhibit a significant ability, termed "blindsight", to discriminate visual stimuli (Pöppel *et al.*, 1973; Weiskrantz *et al.*, 1974; Stoerig & Cowey, 1993). Patients with blindsight may be able to detect and localize stimuli presented at various eccentricities within the defect. In some cases, patients may be able to distinguish moving from stationary stimuli and discriminate stimulus attributes, such as line orientation, direction of motion and color (Cowey & Stoerig, 1991; Blythe *et al.*, 1951).

The visual field defects caused by striate cortical lesions can be clinically classified with respect to size, density and position within the visual field (Weiskrantz *et al.*, 1974). Unlike relative defects where some (amblyopic) vision persists, absolute field defects (scotoma) are experienced as blind. Despite the lack of visual awareness, visual stimuli are apparently processed in a manner that allows the patient to respond to them. It is has therefore been frequently asked whether the residual vi-

sual functions that persist after the striate cortical lesion can be attributed to the variety of visual subsystems associated with normal vision (*e.g.*, magnocellular *vs* parvocellular), provided forced-choice behavioral responses are employed that require the patient to guess - for example, where a stimulus has been presented (Pöppel *et al.* 1973; Weiskrantz *et al.*, 1974; Perenin & Jeannerod, 1978), whether or not a stimulus has been presented (Stoerig *et al.*, 1985; Magnusson & Mathiesen, 1989), or which one of a limited number of stimuli has been presented (Weiskrantz *et al.*, 1974; Perenin, 1978; Ptito *at al.*, 1987; Stoerig, 1987).

A striate cortical lesion destroys the major source of anatomical input to extrastriate visual cortical areas (V2, V3, V4 and MT). Such a lesion also destroys the striate cortical input to subcortical nuclei such as the superior colliculus and the pulvinar nucleus and, in addition, causes massive retrograde degeneration of the dorsal lateral geniculate nucleus (dLGN), which loses approximately 99% of its projection neurons within just three months (Mihailovic *et al.*, 1975). The remaining dLGN neurons survive, apparently permanently, due to direct projections to extrastriate cortical areas (Yukie & Iwai, 1981; Cowey & Stoerig, 1989). Retrograde staining of surviving dLGN projection neurons from area V4 reveals a direct input from the superior colliculus and an indirect input via the GABAergic genuculate interneurons (Kisvarday *et al.*, 1991), implying the existence of a sparse retino-colliculo-geniculo- extrastriate pathway that survives striate cortical damage (see Figure 3.1).

The magnocellular pathway begins with Pβ ganglion cells (Leventhal *et al.*, 1981; Perry *et al.*, 1984), passes through the two magnocellular layers of the LGN to layer 4Cα (Hubel & Wiesel, 1972) and 4B of area V1 (Fitzpatrick *et al.*, 1985; Lund, 1973, 1987, 1988, 1991; Lund & Boothe, 1975) (see Figure 3.2), which projects directly to the V2 thick stripes (Hubel & Livingstone, 1987), V3 (Felleman & Van Essen, 1984), and MT (Lund & Boothe, 1975; Spatz, 1977; Zeki, 1969). Subsequent projections are primarily to parietal cortex (Maunsell & Van Essen, 1983; Ungerleider & Desimone,

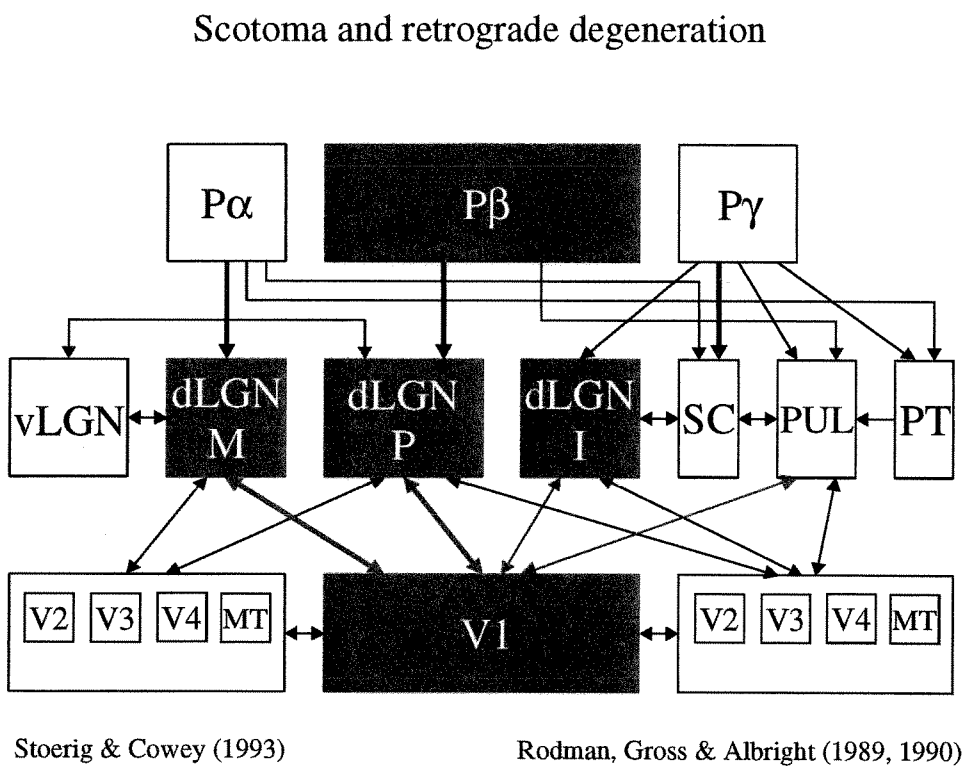

Figure 3.1: Although virtually all Pα and Pβ ganglion cells project to the magno- and parvocellular layers of the dLGN, respectively, these populations are not equally affected by transneuronal degeneration following striate cortical destruction (red boxes). Classification of surviving ganglion cells on the basis of morphological criteria in transneuronally degenerated retinae, which were retrogradely labeled with horseradish peroxidase from the optic nerve, showed the transneuronal degeneration to be selective for Pβ cells. Whereas the normal retina contains about 10% Pα, 80% Pβ and 10% Pγ cells, the selectivity of the degeneration produces an unusual ganglion cell population which consists of approximately equal numbers of the three cell types. The Pγ cell population is unaffected, indicating that there is no retrograde degeneration of the retino-colliculo-striate cortical pathway. Surprisingly, the Pα cell population appears equally unaffected, despite the fact that these cells project primarily to the magnocellular layers of the dLGN.

1986). The parvocellular pathway begins with the Pα retinal ganglion cells (Leventhal *et al.*, 1981; Perry *et al.*, 1984), passes through the four parvocellular layers of the LGN to V1 where it first synapses onto layer 4Cβ and continues primarily to the interblob regions of layers 2 and 3 (Fitzpatrick *et al.*, 1985; Lund, 1973, 1988; Lund & Boothe, 1975) (see Figure 3.2). The interblobs project to the interstripes of area V2 (Livingstone & Hubel, 1984), which in turn project to area V4 (DeYoe & Van Essen, 1985; Shipp & Zeki, 1985). Subsequent projections are mainly to inferotemporal cortex (Felleman & Van Essen, 1991). Physiologically, there are some striking differences between the two pathways. Cells in the magnocellular stream at the retinogeniculate level are characterized by transient responses, larger receptive fields, fast conduction velocity, sensitivity to low luminance contrasts, and lack of color selectivity (De Monasterio, 1978; De Monasterio & Gouras, 1975; Derrington *et al.*, 1984; Derrington & Lennie, 1984; Kaplan & Shapley, 1982; Schiller & Malpeli, 1978; Shapley *et al.*, 1981; Shapley & Perry, 1986). In striate cortex, layer 4B cells are highly selective for direction of orientation (Blasdell & Fitzpatrick, 1984; Dow, 1974; Livingstone & Hubel, 1984; Movshon & Newsome, 1984) and somewhat selective for disparity (Poggio & Fischer, 1977; Poggio *et al.*, 1985). In the thick stripes of V2 there is a shift in emphasis with cells showing high disparity and orientation selectivity, and somewhat less direction selectivity (De Yoe & Van Essen, 1985; Hubel & Livingstone, 1987; Shipp & Zeki, 1985). By contrast, cells in the parvocellular stream are characterized by sustained responses, smaller receptive fields, slower conduction velocities, lack of response to low-contrast stimuli (below 10% contrast), and high color selectivity. In the cortical continuation of the parvocellular stream, the interblob cells acquire several new response properties, being highly orientation selective, mostly complex, and somewhat selective for end- stopping, disparity, and color (Gouras & Kruger, 1979; Hubel & Wiesel, 1968; Micheal, 1985; Poggio, 1984; Thorell *et al.*, 1984). In area V2, cells in the interstripe regions are again selective for orientation, and may be highly

selective for end-stopping (Hubel & Livingstone, 1985, 1987).

In extrastriate cortex, the functional segregation continues. Area V4 neurons are selective for aspects of form (*e.g.*, length, orientation, spatial frequency) and color (Desimone & Schein, 1987; Desimone *et al.*, 1985; Zeki, 1978). In contrast, area MT contains neurons primarily selective for the direction and speed of stimulus motion, and binocular disparity (Albright, 1984; Baker *et al.*, 1981; Felleman & Kaas, 1984; Maunsell & Van Essen, 1983; Zeki, 1974). The form/color pathway terminates in the inferior temporal cortex, while the motion/spatial relations pathway terminates in the posterior parietal cortex. Lesions of infereotemporal cortex in humans and monkeys impair the ability to locate objects and judge their spatial relationship. Lesions also affect visuomotor coordination, visuospatial attention, and motion processing (Andersen, 1987; Dean, 1982; Gross, 1973; Hyvärinen, 1982; Iwai, 1985; Lynch, 1980; Maunsell & Newsome, 1987; Mishkin & Ungerleider, 1982; Mishkin *et al.*, 1983). Anatomically, there exist cross-connections between streams. Some examples include (i) projection of layer 4B of V1 to V3 then to both V4 and MT (Felleman & Van Essen, 1987); (ii) lateral connections between MT and V4 (Maunsell & Van Essen, 1983); and (iii) projections from 4B to superficial layers in V1 (Blasdel & Fitzpatrick, 1984) (see Figure 3.3).

Although all Pα and Pβ ganglion cells project to the magno- and parvocellular layers of the dLGN respectively, the two populations are not equally affected by transneuronal degeneration. Audiograph analysis of the degenerated dLGN revealed that the magnocellular part of the nucleus received substantially larger retinal input, although the projection neurons in both parts of the dLGN are equally affected by retrograde degeneration (Weller *et al.*, 1979; Dinnen *et al.*, 1982). This finding is consistent with selective depletion of the parvocellular input fibers and it could hence be argued that magnocellular labeling in the normal thalamus is relatively so dense that even a large diminution is unlikely to be recorded by autoradiography. However,

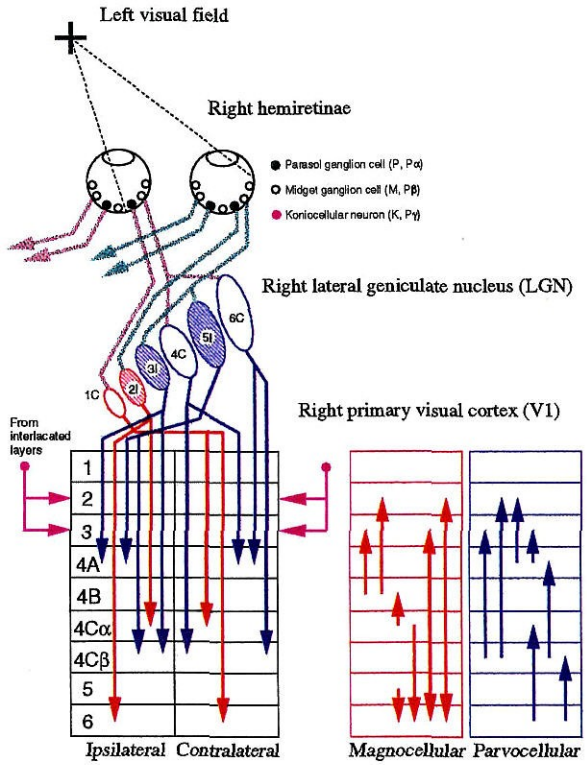

Figure 3.2: Anatomical and physiological evidence points to the existence of partially segregated processing streams within the visual cortical hierarchy - one for motion and spatial relations (the "where" pathway), and one for color and form analysis (the "what" pathway). The two streams diverge at the lowest level of the cortical hierarchy, comprising separate subdivisions of the lateral geniculate nucleus (LGN) and primary visual cortex (V1). Specifically, at the level of LGN, V1, and V2 three somewhat parallel streams exist. The magnocellular pathway begins with Pβ retinal ganglion cells, passes through the two magnocellular layers of the LGN to layer 4Cα. The parvocellular pathway begins with Pα retinal ganglion cells, passes through the four parvocellular layers of the LGN to layer 4Cβ of V1 and continues primarily to the interblob regions of layers 2 and 3. A third processing stream, the interlaminar pathway begins with Pγ retinal ganglion cells, some of which project to the six interlaminar (interlacated) layers of the LGN and subsequently to the blobs in layer 3 of V1.

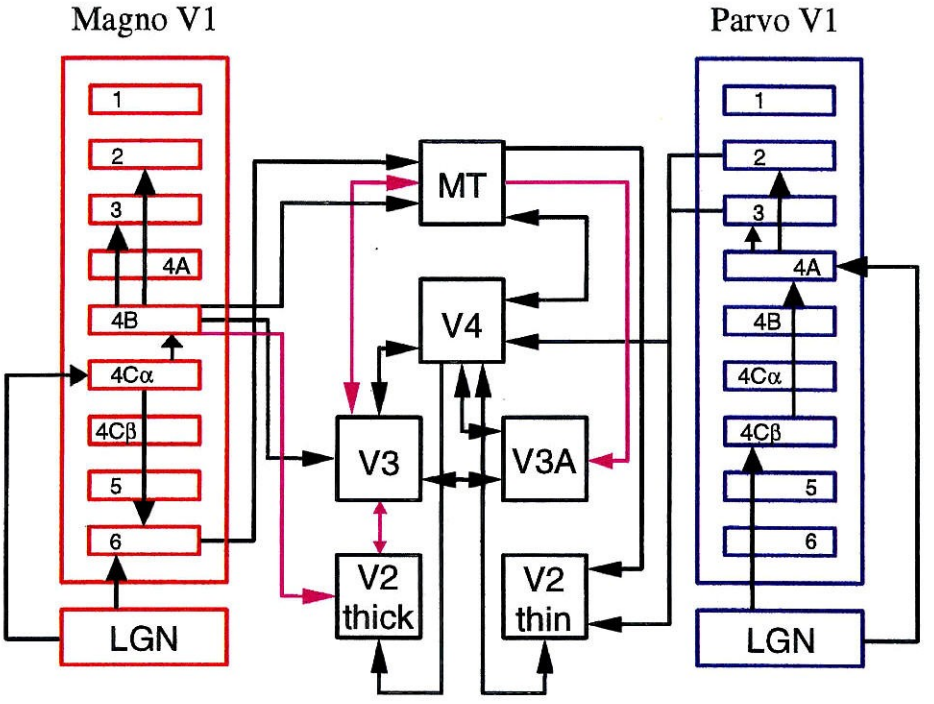

Figure 3.3: Anatomically, there exist cross-connections between the different processing streams. Signals from the magnocellular layers of the LGN are directed predominantly at layer 4α of V1 which then connects with layers 4B and 6, the latter also receiving a direct geniculate input. The two layers project directly to MT and layer 4B projects, in addition, to the thick stripes of V2 and V3. The thick stripes project in turn to V3 and MT. Signals from the parvocellular layers of the LGN are directed mainly to layers $4C\beta$ and 4A, themselves interconnected. The signals are then communicated to layers 2 and 3 which project to V4 directly from the foveal region of V1 and indirectly through the thin stripes and interstripes of V2. Pink lines show possible sites of interactions between the two systems. Cross-connections include projections from layer 4B of V1 to V3 and then both to V4 and MT; lateral connections between MT and V4; and projections from layer 4B to superficial layers in V1 (Zeki, 1987).

there is no room for doubt that retinal ganglion cells are differently affected. Classification of surviving ganglion cells based on morphological criteria in transneuronally degenerated retinae (horseradish peroxidase labeling from the optic nerve) showed the transneuronal degeneration to be selective for Pβ ganglion cells (Cowey *et al.*, 1989). Both Pγ and Pα cells were found in normal numbers in the degenerated hemiretinae. Unlike the normal distribution of retinal ganglion cells (10% Pα, 80% Pβ, and 10% Pγ) (Leventhal *et al.*, 1981; Perry & Cowey, 1981), the selectivity of the transneuronal degeneration produces an unusual ganglion cell population which consists of approximately equal numbers of the three morphological ganglion cell classes.

The Pγ cell population is unaffected, implying survival of the retino-colliculo-extrastriate pathway. Many of the (otherwise functionally heterogeneous) Pγ ganglion cells respond preferentially to moving stimuli (DeMonasterio, 1978). Via the pulvinar, they project directly to area MT which is mainly involved in the processing of stimulus motion. Not surprisingly, the visual responsitivity of area MT that survives striate cortical ablation, depends on collicular input (Rodman *et al.*, 1989).

The Pα cell population appears equally unaffected, despite the fact that these cells project mainly to the magnocellular layers of the dLGN. However, since their number appears to be unaffected by the massive degeneration, these cells are likely to project to extrageniculate targets as well, although the Pα projection to the midbrain is rather sparse (Leventhal *et al.*, 1981; Perry & Cowey, 1984). Pα cells could also project to additional and as yet unidentified target nuclei, for example dLGN interneurons. Due to their large terminal aborization Pα cells would be better suited to synapse onto the surviving dLGN projection neurons and interneurons than the comparatively small Pβ cells with their much more restricted terminals (Micheal, 1988). Note that the survival of a subgroup of Pβ cells implies that these cells possibly also have additional and as yet unidentified targets.

Different lines of evidence point to perceptual phenomena that were uncovered in

visual field defects and are usually thought to reflect information processing in the magnocellular system. Barbur *et al.* (1980) demonstrated detection of fast moving stimuli and low frequency spatial and high frequency bandpass temporal responses in the blind hemifield. Richards (1973) provided evidence for coarse stereopsis in the field defect, and Stoerig and Cowey (1993) showed that in blindsight patient luminance sensitivity curves very similar to the ones in normals - under conditions that favor the color-opponent system - can indeed be recovered in the blind hemifield.

Clinical blindsight has most often been attributed to the retino-colliculo-extrastriate pathway (Pöppel *et al.*, 1973; Weiskrantz *et al.*, 1974; Perenin & Jeannerod, 1978; Lepore *et al.*, 1975, Barbur *et al.*, 1980). Although the superior colliculus like pulvinar nucleus, loses its input from striate cortex, a retino-colliculo-pulvino-extrastriate pathway remains that could mediate visual functions in the absence of striate cortex. For example, clinical studies of a patient with a unilateral colliculectomy (Heywood & Ratcliff, 1975) and a patient who suffered severe damage to his left pulvinar (Zihl & von Cramon, 1979) have implicated the superior colliculus in the mediation of saccadic eye movements. The patient studies showed that saccadic eye movement latency to the hemifield contralateral to the lesion was increased, and that spontaneous eye movements into the same hemifield were rare (attentional neglect). That it is indeed the superior colliculus that is involved in saccadic localization within a field defect was demonstrated by Mohler and Kurtz (1977) who produced a circumscribed visual field defect by removing a small part of striate cortex in monkeys. Soon after the lesioning the monkey learned to make saccades to targets within the field defect. Then in a second operation, the retinotopically corresponding portion of the superior colliculus was removed, resulting in a collicular field defect superimposed on the cortical one. After the second lesion, the monkey was unable to learn (*i.e.* relearn) saccadic localization (Wurtz & Albano, 1980).

Two laboratories have examined the visual responsivity in area MT after striate

cortex lesion. Both Rodman *et al.* (1989) and Bullier and Girard (1988) found that neurons in area MT retain some level of responsivity when area V1 is inactivated. Since only very few LGN neurons project to cortical targets other than area V1 (Benevento & Yoshida, 1981; Yukie & Iwai, 1981), and these projections avoid area MT (Benevento & Standage, 1982), it is likely that the remaining responses are mediated via thalamic structures such as the pulvinar (Rodman *et al.*, 1989).

Rodman *et al.* (1989) examined the dependence of visual responses in area MT on the functional integrity of area V1. They recorded from neurons in area MT following striate cortical ablation or reversible inactivation (cooling) of topographically corresponding portions of area V1. They found that striate cortex removal or inactivation did not completely abolish visual responses in area MT, but MT cell responses were considerably weakened. Moreover, substantial direction selectivity was seen in MT cells devoid of striate cortical input, in other words, both strength and sharpness of directional tuning was found comparable to normal MT activity. In addition, the binocularity of the responsive cells and the size of the overall topographic organization of their receptive fields were not substantially altered.

Studies of the laminar pattern of reciprocal connections of area MT with other visual cortical areas have shown that MT receives ascending (feedforward) projections from striate cortex and extrastriate areas V2 and V3, and descending (feedback) projections from the medial superior temporal area (MST), the floor of the superior temporal area (FST), the lateral intraparietal area (LIP), and the ventral interparietal sulcus (VIP), and lateral projections from area V4 and possibly V3A and the parietal-occipital sulcus (PO) (Cragg & Ainsworth, 1969; Ungerleider & Mishkin, 1979; Montero, 1980; Rockland & Pandya, 1981; Maunsell & Van Essen, 1983; Ungerleider & Desimone, 1986). Several lines of evidence indicate that sriate cortex plays an important or even an exclusive role in the genesis of visual responses of area MT. First, the majority of MT's ascending projections derive either directly from area V1

or from V1-recipient regions V2 and V3. V1's layers 4B and 6 project directly to MT; layer 4B also projects to V3 and the V2 thick stripes which in turn project to MT (see Figure 3.3). Second, other extrastriate visual cortical areas lose their responsivity following striate cortical removal, such as V2 (Schiller & Malpeli, 1977) and inferior temporal cortex (Rocha-Miranda *et al.*, 1975). Third, the antidromic experiments of Movshon and Newsome (1984) suggest that the V1 projection neurons have receptive field organization and direction selectivity very similar to their MT targets.

There are, however, also reasons for believing that regions other than V1 are capable of sustaining visual responsitivity in area MT. For example, the superficial (visual) layers of the superior colliculus receive direct retinal input and project to topographically organized subdivisions of the pulvinar, the inferior and lateral pulvinar (Hubel *et al.*, 1975; Pollack & Hickey, 1979; Benevento & Fallon, 1975; Harting *et al.*, 1980; Benevento & Standage, 1983). Since the superficial layers of the superior colliculus remain visually responsive following striate cortex removal (Schiller *et al.*, 1974), area MT may thus receive visual information via a tectopulvinar pathway. Although striate cortex removal has devastating consequences for both lateral and inferior divisions of the pulvinar, about 15% of the cells in both divisions of the pulvinar remain responsive (Burman *et al.*, 1982; Bender, 1983). Further support for a tectopulvinar-MT pathway is the discovery of a polysensory cortical region, the superior temporal polysensory area (STP), where some visual responsiveness survives striate cortex removal but is abolished by an additional superior colliculus lesion (Bruce *et al.*, 1986). Deep (motor) layers of the superior colliculus and the pretectum project to nontopographic subdivisions of the pulvinar, including the dorsolateral and medial pulvinar, which in turn project to cortical areas MST, 7a, LIP and the dorsal intraparietal sulcus (DIP) (Rodman *et al.*, 1989). Furthermore, many areas in the dorsal cortical pathway (the "where" pathway) project to the pontine reticular formation. For example, areas MT and MST project to the dorsolateral pontine nuclear areas of the brainstem, which

in turn project to the contralateral cerebellar flocculus, and then to the brain stem oculomotor centers in the pons. Although area MT itself does not receive projections from the dLGN (Standage & Benevento, 1981; Maunsell & Van Essen, 1983), there are weak projections from the interlaminar divisions of the LGN to extrastriate areas V4 and possible V3 (Benevento & Yoshida, 1981; Yoshida & Benevento, 1981; Yukie & Iwai, 1981), both of which project to area MT (Maunsell & Van Essen, 1983; Ungerleider & Desimone, 1986).

Another possible source of visual input to area MT after striate cortical removal are the descending projections from visual cortical areas such as MST, LIP, and VIP. Areas MST and LIP project to area 7a (Andersen *et al.*, 1990; Rodman *et al.*, 1989; Colby *et al.*, 1988; Desimone & Ungerleider, 1986). At least MST is connected to area STP which contains some neurons responsive in the hemifield contralateral to the striate cortical lesion (Bruce *et al.*, 1986). It seems unlikely, however, that descending projections from an area such as MST, with its large receptive and rather crude topography (Desimone & Ungerleider, 1986), could regenerate the spatially restricted receptive fields and topography of MT devoid striate cortical input. Nonetheless there exists a substantial flow of information from parietal visual areas to inferior temporal cortex (Andersen *et al.*, 1990; Boussaoud *et al.*, 1990).

Rodman *et al.* (1990) also found that in addition to striate cortical ablation destruction of the superior colliculus eliminates the residual responsiveness in area MT. This finding implies there is input to area MT from a portion of the visual system that receives visual signals in parallel with those reaching striate cortex. Moreover, the sensitivity of MT neurons to stimulus motion and their relative insensitivity to stimulus form suggests a potentially important role for pathways involving the SC in the genesis of visual response properties in area MT. Rodman *et al.* (1990) also showed that destruction of the superior colliculus alone produces only minor alterations in the characteristic properties of neurons in area MT. Although Rodman *et al.* (1990)

reported a tendency for increased responsitivity to slit stimuli, there were no apparent effects on direction selectivity, orientation tuning, and receptive field size and other properties. As in the normal monkey, almost all MT neurons in monkeys with superior colliculus lesion alone responded to visual stimulation.

In species with geniculocortical systems less developed than those of the higher primates, the tectofugal pathways play a dominant role in visual processing (Trevarthen, 1968; Karten, 1979; Diamond *et al.*, 1985). Because of this fact, and because of the strong reciprocal connections from area MT with the inferior and lateral pulvinar, Rodman *et al.* (1989, 1990) have suggested that the residual responses found in area MT after striate cortical removal derive from superior colliculus inputs via the pulvinar. A small subpopulation of cells in both the inferior and lateral pulvinar remain responsive after striate cortex removal (Burman *et al.*, 1982; Bender, 1983).

Therefore, a pathway from the retina to area MT passing through only the superior colliculus and its pulvinar targets via a minimal number of synapses is quite plausible. However, the portions of the inferior and lateral pulvinar that project to area MT may not be the same subdivisions that receive superior colliculus input (Kaas & Huerta, 1988). Moreover, there are several other potential routes through the midbrain and diencephalon which may be affected by superior colliculus damage and which may contribute to the effects of such damage on area MT. In particular, the pretectum and the LGN may play a role in the effects of superior colliculus lesions on visual responsiveness in area MT. Lesions of the superior colliculus often produce direct damage to the pretectal region, which lies just anterior to the foveal representation in the superior colliculus. Efferents of the pretectum project to a number of subcortical visual structures, including the superior colliculus, inferior and lateral pulvinar, and LGN (Carpenter & Pierson, 1973; Benevento *et al.*, 1977; Benevento & Standage, 1983). Moreover, since some of these efferents pass through the brachium of the superior colliculus (Carpenter & Pierson, 1973), even lesions limited to the

superior colliculus might interrupt axonal connections from the pretectum to the pulvinar and LGN (Benevento & Fallon, 1975). A possible role for the pretectum in the visual behavior that survives striate cortical damage is suggested by Pasik and Pasik (1973). They found that monkeys were unable to relearn a light/no-light discrimination after striate damage only when additional midbrain lesions were large and included extensive pretectal damage. Thus, it is not possible to rule out a role for the pretectum in the effects of superior colliculus damage on area MT.

Although area MT does not receive direct projections from any portion of the LGN (Standage & Benevento, 1981; Maunsell & Van Essen, 1983), there are weak projections from primarily the interlaminar and magnocellular divisions of extrastriate V4 and possibly V3 (Benevento & Yoshida, 1981; Yukie & Iwai, 1981). Both these extrastriate areas project to area MT (Maunsell & Van Essen, 1983; Ungerleider & Desimone, 1986). This LGN-extrastriate pathway remains intact years after striate cortex removal (Cooper & Cowey, 1988). Two additional pieces of evidence suggest that the LGN may play a role in MT responses and in visual behavior above and beyond that serving as a relay from the retina to striate cortex. First, reversible inactivation of the magnocellular layer of the LGN produces a nearly complete recess of activity in retinotopically corresponding parts of area MT (Maunsell *et al.*, 1989), whereas reversible inactivation of striate cortex does not (Rodman *et al.*, 1985, 1989; Bullier & Girard, 1988). Second, lesions of the LGN abolish the visually guided eye movements that persist after striate cortex lesions (Schiller *et al.*, 1985). Whatever role the LGN may have in the MT responses that survive striate cortex damage is obviously undetermined by the superior colliculus lesion, since this lesion completely abolishes the residual responsiveness. In addition, Benevento and Yoshida (1981) showed that intraocular injections of amino acids label all projection structures of the LGN expect extrastriate cortex, suggesting that the LGN cells which project to extrastriate visual areas do not receive direct retinal input, but rather, as Benevento

and Yoshida (1981) hypothesized, the LGN- extrastriate projection may be analogous to the pulvinar-extrastriate system which receives visual inputs from the midbrain and cortex.

The residual responsiveness in area MT after a striate cortex lesion is rather striking in view of the weakness of the pathways likely to be involved in relaying visual information from the midbrain to area MT. Only a small proportion of the cells in the lateral and inferior pulvinar remain visually responsive after a striate lesion, and none are directionally selective, and the LGN-MT pathway is rather sparse indeed. Thus MT appears able to generate a surprising amount of neural function on the basis of rather weak signals from pathways originating in the midbrain. This relationship between area MT and the midbrain may reflect the role of MT in spatial functions. The notion that anatomically separable pathways subserve spatial and pattern vision in primates was introduced (among others) by Trevarthen (1968). Originally, spatial functions, such as the detection and localization of brief visual stimuli, were attributed to a tectopulvinar system, whereas pattern vision, such as the identification of objects, was attributed to a geniculocortical system. We now know that there is degree of separation of pathways subserving spatial and pattern vision at the cortical level (Ungerleider & Mishkin, 1982) (see Figure 3.3). Pattern vision is now thought to be represented cortically by a pathway that originates within certain subdivisions of striate cortex (see Figure 3.2), goes next to V4 via subdivisions of V2, and then connects ventrally to areas in the inferior temporal lobe, whereas spatial vision is believed to be subserved by a pathway that originates in other compartments of V1 (see Figure 3.2) and V2 and then connects dorsally to parietal cortex via area MT and other divisions within the superior temporal sulcus.

Bruce *et al.* (1986) have suggested that while cortical areas are involved in pattern vision (the ventral pathway) and may be dependent solely on visual information deriving from geniculostriate projections, the superior colliculus may influence visual

processing within the spatial pathway (the dorsal pathway). Major components of the dorsal vision system, namely area MT and surrounding divisions in the superior temporal sulcus (Rodman *et al.*, 1989, 1990; Bullier & Girard, 1988) retain visual responsitivity devoid of striate cortex input. Similarly, area STP, which receives converging input from both the dorsal and ventral cortical systems (Jones & Powell, 1970; Seltzer & Pandya, 1978; Baizer *et al.*, 1988), contains visually responsive cells after striate lesions (Bruce *et al.*, 1988). On the other hand, insofar as it has been examined, it appears that components of the ventral pathway (V2, inferior temporal cortex) are completely dependent on striate cortex for visual responsiveness (Rocha-Miranda *et al.*, 1975; Schiller & Malpeli, 1977; Bullier & Girard, 1988).

In this chapter we introduce two different visual displays that induce blindsight in normal observers. Using an objective measure, we show that conscious experience remains defective at presentation times much longer ($1s$) than the onset of visual sensitivity ($\approx 60ms$). To obtain this effect, we generate a contrast between visual textures and then conceal the contrast by superimposing "complementary" textures. Complementarity can involve either opposite motion (see Figure 3.4) or binocular rivalry and orthogonal orientation (see Figure 3.5). In both cases, observers locate the texture contrast reliably but do not, by either subjective or objective measures, consciously experience it. Taken together with present knowledge of the visual cortical site(s) at which opposite motion and rivalrous orientation interact (Qian & Andersen, 1994; Logothetis & Schall, 1989; Leopold & Logothetis, 1995; Dobbins *et al.*, 1994) (see Figure 3.6), this observation bears upon the functional anatomy of conscious visual experience. We further attempt - in analogy to the double-lesion experiments by Rodman *et al.* (1990) - to implicate the superior colliculus as an essential component in the subcortical-cortical pathway involved in *artificial* blindsight.

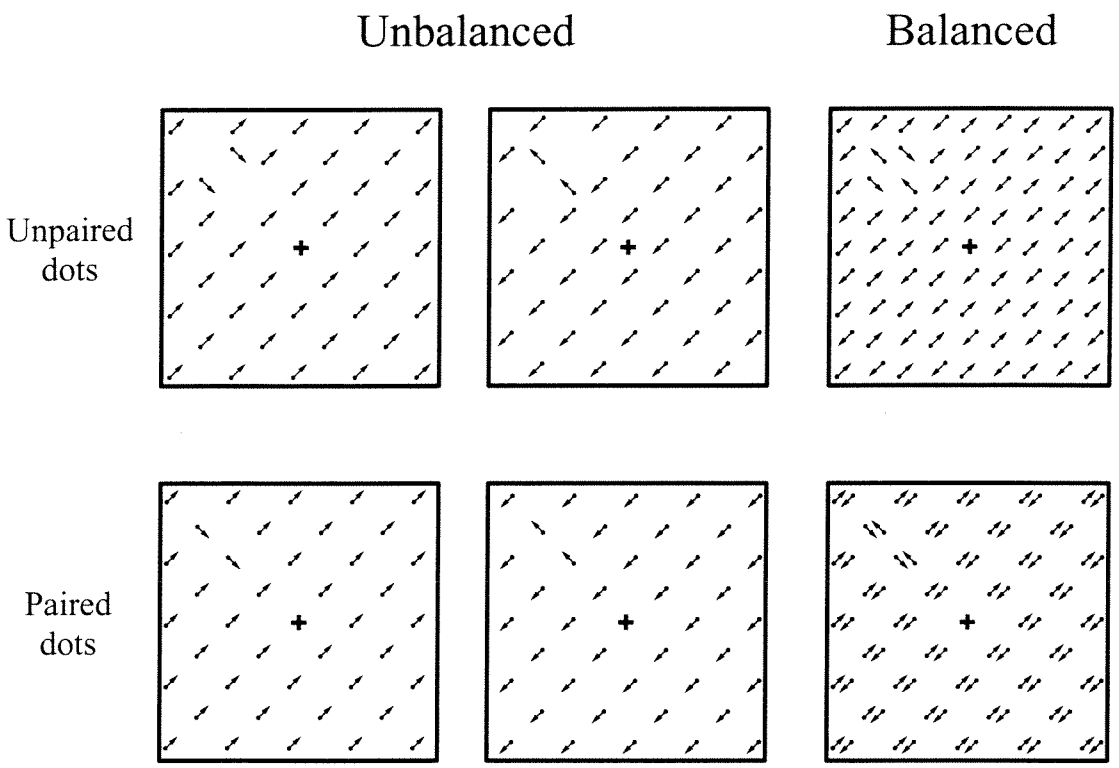

Figure 3.4: Schematic of display used to investigate unconscious perception. Unpaired dots, when balanced (globally balanced) give rise to the percept of motion transparency. The area defined by orthogonal motion perceptually "pops out" and is readily detected at short presentation times. Paired dots, when balanced (locally balanced) appear perceptually intermediate in order between motion transparency and flicker noise. Both fore- and background appear nontransparent and may appear perceptually distinct only upon closer inspection. Observers are asked to locate the foreground (target) in a cluttered background in a 4-alternative forced-choice (4AFC) procedure. When confronted with conflicting visual information, *i.e.*, dots of opposite motion at every location, observers can locate the target reliably although they experience the display as uniform and are subsequently unaware of the target. Why do the paired dots merely allow unconscious discrimination while the unpaired dots permit phenomenal vision? Evidence from single-cell recording in macaque monkeys suggests differential stimulation of direction selective cell populations in visual cortical area MT as a possible reason. In MT, more direction selective cells respond significantly less to paired than to unpaired dot patterns (Qian & Andersen, 1994).

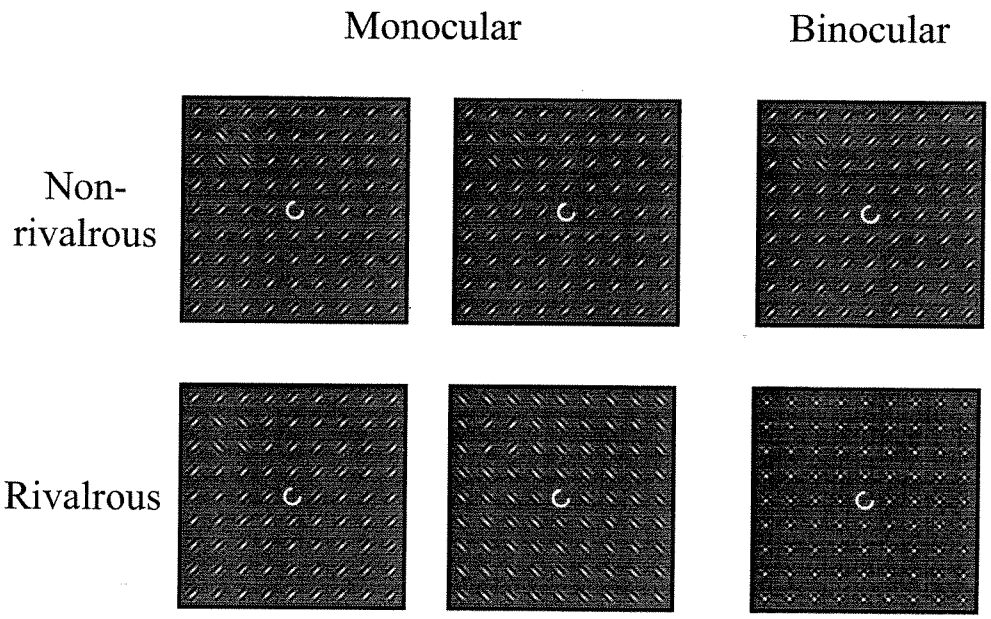

Figure 3.5: Schematic of display used to investigate unconscious perception. When non-rivalrous displays of oriented line elements (Gabor patches) are presented to both eyes (binocular), the foreground defined by elements of orthogonal orientation with respect to the background is readily detected ("pop-out"). When rivalrous displays are presented dichoptically, the foreground will escape visual awareness at short presentation times. At longer presentation times, one eye gains dominance and elements presented to the other eye are barred from subjective awareness. Observers are asked to locate the foreground (target) in a cluttered background in a 4-alternative forced-choice (4AFC) procedure. When presented with conflicting information, *i.e.*, binocular rivalry between orthogonal line elements at every retinal location, observers can locate the target reliably although they experience the display as uniform and are subsequently unaware of the target. The ability to locate a texture contrast without being aware of it, may be based upon responses in striate cortex (and possibly unknown pathways to higher cortical levels). Striate cortical cells respond more strongly to a texture contrast than to a uniform texture, presumably because of the ubiquitous surround inhibition in this area. In our rivalrous display, the visual textures viewed by the left and right eyes may be processed independently, as many striate cortical cells are dominated by input from one eye and as the intrinsic connections that are likely to mediate surround inhibition appear to be eye-specific (Mallach *et al.*, 1993).

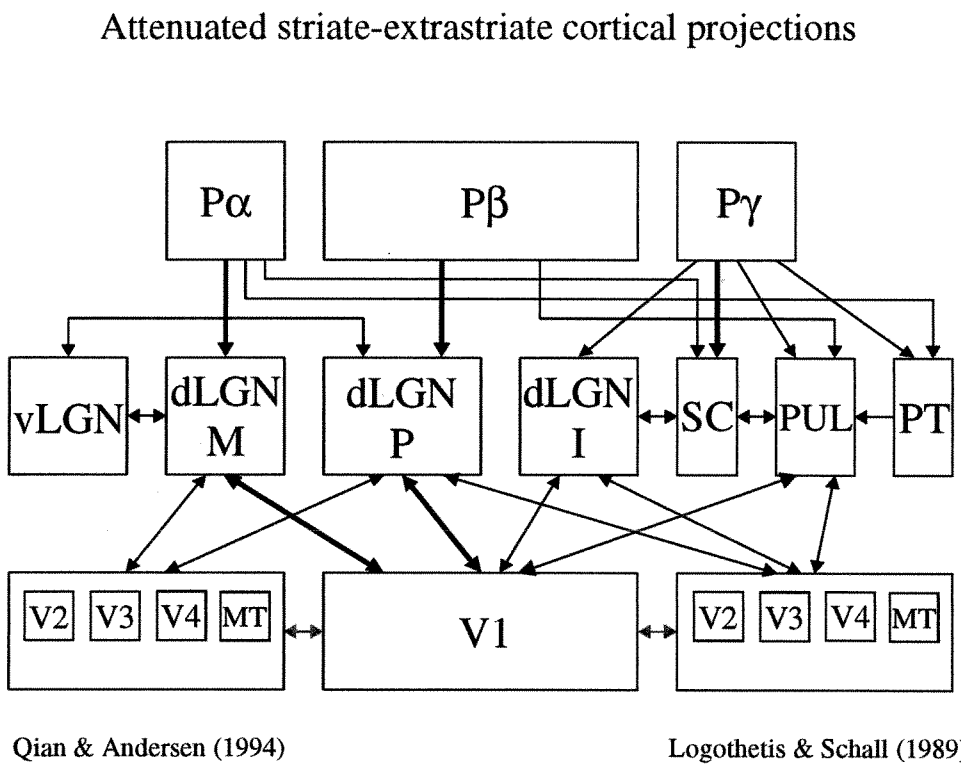

Figure 3.6: Work in non-human primates suggests that, in the presence of conflicting visual information, extrastriate input from striate cortex is reduced and much of the remaining input derived from subcortical sources (red arrows). Note that this pattern of extrastriate inputs is similar to that obtained after damage to striate cortex (see Figure 3.1). Examples of attenuated striate-extrastriate cortical projections are mutual inhibition of opposite directions of motion in small regions (Qian & Andersen, 1994) and binocular rivalry between elements of orthogonal orientation (Logothetis & Schall, 1989). Specifically, in extrastriate visual cortical area MT, more direction selective cells respond only approximately half as much to paired than to unpaired dot textures whereas responses in striate cortex are comparable (Qian & Andersen, 1994). Similarly, dichoptic stimulation with rivalrous patterns has been found to suppress responses in extrastriate areas V4 and MT (Logothetis & Schall, 1989; Leopold & Logothetis, 1995), but apparently not in striate cortex (Dobbins *et al.*, 1994).

3.1.2 Materials and methods

Our paradigm randomly interleaves two matched displays within each block of trials (Experiments 1-3). Both displays contain a target of uniform visual texture and a background of contrasting texture. In one display, the target is subjectively visible whereas in the other it is not (as is evident by inspection). In spite of this difference, performance turns out to be comparable when practiced observers locate the target in a forced-choice task.

The letter task in Experiment 4 involved the discrimination of five ⊤- and ⊔-shaped elements in an area subtending $1 \times 1°$ of visual angle near the center of the display (see Figure 2.1, *Stimulus*). Each line of the ⊤- and ⊔-shaped elements measured $0.16 \times 0.02°$. These elements could appear at seven possible location (r, θ): the exact center of the display and six locations at 1° of eccentricity, spaced evenly around the center ($r = 0$ or 34 pixels, $\theta = 0, \pi/6, \pi/3, \ldots, 5\pi/6$). On any one trial, five ⊤- or ⊔-shaped elements were assigned randomly to the seven possible locations and, in addition, were rotated randomly and independently. This resulted in a large number of possible configurations. Either five Ts, five Ls, four Ts and one L, or four Ls and one T appeared. The masking pattern contained five ⊓-shaped display elements which were of identical dimensions and appeared at the same locations as the ⊤- and ⊔-shaped elements but were rotated independently (and randomly) (see Figure 2.1, *Mask*).

The *letter task* involved a two-alternative forced-choice (2AFC) discrimination of letter shapes. Observers were asked to report whether all letters were the same (*i.e.*, five Ts, five Ls) or whether one was different from the other four (*i.e.*, four Ts and one L, four Ls and one T). The possible responses were "same" or "different".

When instructed to perform two tasks concurrently, subjects responded twice in every trial, resulting in two performance values called *double-task performances.* When instructed to perform only one task, either they responded only once in every

trial, resulting in one performance value called *single- task performance.*

To prevent planned saccades, the trial sequence in Experiment 4 began with a fixation interval (background at mean luminance) of variable duration ($100-250ms$). Next, the stimulus pattern was presented for a fixed duration, and was immediately followed by the letter mask (of equal duration). After viewing the trial sequence, observers responded either once or twice, depending on instructions. All responses were entered as a single (unspeeded) keystroke on the computer-keyboard.

Stimulus elements belonging to both localization- and letter-task were present at all times, even during single-task blocks. When performing a double task, observers were instructed to treat as *primary* the letter task and as *secondary* the localization task. Instructions strongly encouraged subjects to achieve the highest possible performance on the letter task.

3.1.3 Results

Experiment 1

Our first pair of matched displays uses moving-dot textures (Figure 3.7, A and B), and target and background differ in that dots in the two regions move along orthogonal trajectories. In one ("paired") display, each dot is paired with a nearby dot (separation $< 0.1°$) of equal and opposite motion. Observers report seeing a uniform texture of incoherently flickering dots (Qian *et al.*, 1994a) without any impression of a target whatsoever. In the other ("unpaired") display, dots exhibiting equal and opposite motion are placed at random distances ($< 10°$) from the original dots. Observers report seeing two coherent sets of dots sliding over each other like two surfaces ("motion transparency") (Qian *et al.*, 1994a) with the target appearing as smaller surfaces moving orthogonally. After viewing each trial, observers (i) report the target position (1 of 4 possibilities) and (ii) rate their confidence that the reported position

is correct (scale of 1 to 10). Instructions encourage observers to use all confidence ratings, independent of whether their overall confidence is high or low. Accordingly, confidence ratings tend to reflect *relative* rather than *absolute* confidence levels. Here, the ROC is defined as the conditional probability of a confidence rating $r > \theta$, $\theta = 0, 1, \ldots, 10$, given that the response is correct, $P_{(r>\theta \mid correct)}$, plotted against the conditional probability of $r > \theta$ given that the response is incorrect, $P_{(r>\theta \mid incorrect)}$, where $P_{(r>\theta \mid correct)} = \sum_{r>\theta} c_r / \sum_r c_r$ and $P_{(r>\theta \mid incorrect)} = \sum_{r>\theta} i_r / \sum_r i_r$.

Surprisingly, the percentage of trials in which the position is correctly reported is comparable for paired ($69.9 \pm 0.9\%$ correct) and unpaired displays ($74.4 \pm 1.1\%$) and well above chance (25%) in both cases (presentation time $250ms$). Observers report that they "guess" target position in paired trials. Confidence ratings document this dissociation of performance and awareness. Figure 3.7, C, shows confidence ratings obtained with subjectively visible targets. The distribution is skewed towards higher ratings (Figure 3.7, C, thick line and arrow) and the fraction of correct responses increases monotonically with confidence (Figure 3.7, C, bar histogram), exhibiting a highly significant correlation (Kendall's $\tau = 0.99$, $p < .0001$). Figure 3.7, D shows the very different outcome obtained with subjectively invisible targets. The distribution is skewed towards lower ratings (Figure 3.7, D, thick line and arrow) and the fraction of correct responses bears little or no relation to confidence (Figure 3.7, D, bar histogram, $\tau = -0.61$, $p < .05$). Instructions make the difference in average ratings artificially small. The correlation between the fraction of correct responses and confidence is best visualized with the receiver-operating characteristic (ROC) (Green & Swets, 1967). A highly curved ROC reflects a high degree of correlation and also, it seems, normal subjective awareness of the target Figure 3.7, E, unpaired). A straight ROC reflects the absence of a correlation and betrays the lack of subjective awareness of the target (Figure 3.7, E, paired).

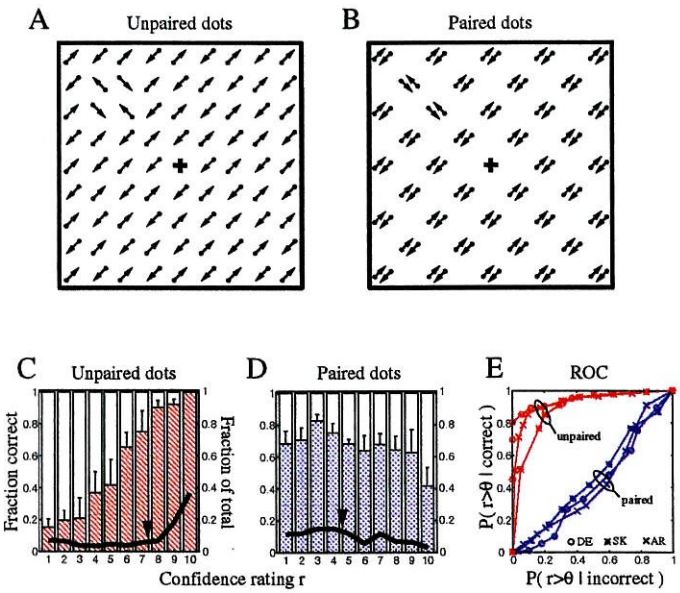

Figure 3.7: Psychophysical displays (schematic) with moving-dot textures and results for three observers (DE, SK, AR; 1,500 trials total, $250ms$, presentation time). Equal and opposite motion conceals a target from visual awareness but does not prevent its localization. Displays are generated on an SGI Indigo 2 (1024×1024 pixels, subtending $10 \times 10°$, viewing distance $57cm$). Parameters of moving dots are similar to ones described in Qian *et al.* (1994) (size $0.01°$, life-time $50ms$, velocity $2°/s$, density $10\,\mathrm{deg}^{-2}$). Dot trajectories (polar directions $\pi/4$ and $-3\pi/4$ or $\pi/4$ and $-\pi/4$) are orthogonal in the target (size $2 \times 2°$, centered in one of the four quadrants of the display) and background regions. Observers fixate the center of the display, report the target position (4-alternative forced-choice), and rate their confidence that the reported position is correct (scale of 1 to 10). (A) Unpaired display (dots of equal and opposite motion placed at random distances $< 10°$) with visible target. (B) Paired display (dots of equal and opposite motion separated by $< 0.1°$) with concealed target. Paired and unpaired displays are randomly interleaved. (C-E) Analysis of performance and confidence. Let n_r, c_r, and i_r be the number of all trials, correct trials, and incorrect trials with confidence rating r, respectively, with $n_r = c_r + i_r$ and $r = 1, \ldots, 10$. (C) and (D) Thick line and arrow: fraction of trials with confidence rating r, γ_r (mean of all observers, $\gamma_r = n_r / \sum_r n_r$). The arrow marks the distribution mean. Bar histogram: fraction of correct responses among trials with confidence rating r, ξ_r (mean and standard error of all observers, $\xi_r = c_r/n_r$). For unpaired displays, the fraction f_r increases almost monotonically with the confidence rating (C) whereas, for paired displays, there is no significant relation (D). (E) Receiver-operating characteristics (ROCs) for paired and unpaired trials (individual observers). The ROC of paired trials is essentially straight, showing failed awareness of the target, while the ROC of unpaired trials is highly curved, showing normal awareness of the target.

Experiment 2

Our second pair of matched displays uses oriented-element textures (Figure 3.8, A) and target and background differ with respect to element orientation. Observers wear polarizing goggles, permitting independent stimulation of left and right eyes. To ensure spatial register and prevent observers from simply closing one eye, observers discriminate a Landolt C at display center, a task that is performed best with binocular vision (not shown). In one ("rivalrous") display, corresponding elements impinging upon the left and right eye have orthogonal orientation. Observers report seeing a uniform texture of small "stars" without any impression of a target whatsoever (presentation time $250ms$). (At longer presentation times, one eye gains dominance and elements presented to the other eye are barred from subjective awareness (Fox, 1991).) In the other ("non-rivalrous") display, corresponding left and right eye elements have the same orientation. Observers report seeing a texture of oriented elements with a contrasting target that is readily apparent. Otherwise, the experimental protocol is the same as with our first pair of matched displays. Again, performance is well above chance for both rivalrous ($75.2\pm1.1\%$ correct) and non-rivalrous ($83.3\pm1.8\%$) displays (presentation time $250ms$), although observers believe themselves to be "guessing" on rivalrous trials. Again, subjectively visible and invisible targets produce differentially skewed distributions of ratings (Figure 3.8, B and C, thick line and arrow) and the correlation between success and confidence is strong for visible (Kendall's $\tau = 0.90$, $p < .0005$) and absent for invisible targets ($\tau = 0.02$, $p > .5$) (Figure 3.8, B and C, bar histogram). The curvature of the ROC again highlights this difference (Figure 3.8, D).

Experiment 3

As in Experiment 2, the current pair of matched displays uses oriented-element textures under heterochromatic isoluminant contrast condition. Figure 3.9, A, target

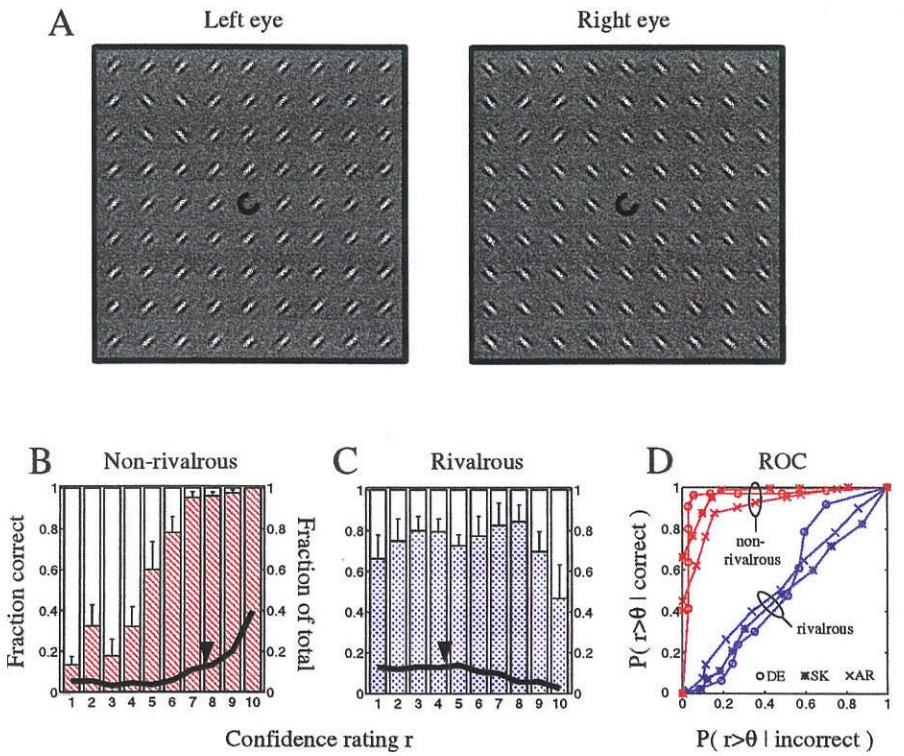

Figure 3.8: Psychophysical displays (schematic) with oriented- element textures and results for three observers (DE, SK, AR; 1,200 trials; 250ms). Binocular fusion of orthogonally oriented elements conceals a target from visual awareness but does not prevent its localization. Left and right eyes are stimulated dichoptically with the help of polarizing goggles. Both eyes view a 20 × 20 array of oriented elements (2-D Gabor functions with polar orientation $\pm\pi/4$, period 0.448°, σ = 0.224°, phase $\pm\pi/2$). Elements are oriented orthogonally in the target (size 2 × 2°, centered in one of four quadrants of the display) and the background region (for both eyes). To ensure binocular viewing and to control fixation, observers discriminate a small (0.5°) Landolt C at the center of the displays of both eyes. If the polar position of the opening of the C is reported correctly, the trial proceeds, if not, the trial is aborted. Next, observers report target position and rate their confidence. (A) Rivalrous display (corresponding left and right elements have orthogonal orientation) with concealed target. Not shown: non-rivalrous display (corresponding left and right eye elements have same orientation) with visible target. Rivalrous and non-rivalrous displays are randomly interleaved. (B, C) Thick line and arrow: fraction of trials with confidence rating r, γ_r (mean of all observers). The arrow marks the distribution mean. Bar histogram: fraction of correct responses among trials with confidence rating r, ξ_r (mean and standard error of all observers). (D), The ROCs for non-rivalrous trials are highly curved while those for rivalrous trials are essentially straight, showing the difference between normal and failed awareness of the target (individual observers) (see Figure 3.7).

and background differ with respect to element orientation. Observers wear polarizing goggles, permitting independent stimulation of left and right eyes. In one ("rivalrous") display, corresponding elements impinging upon the left and right eye have orthogonal orientation. Observers report seeing a uniform texture of small "stars" without any impression of a target whatsoever (presentation time $250ms$). (At longer presentation times, one eye gains dominance and elements presented to the other eye are barred from subjective awareness (Fox, 1991).) In the other ("non-rivalrous") display, corresponding left and right eye elements have the same orientation. Observers report seeing a texture of oriented elements with a contrasting target that is readily apparent. Prior to the experiment, observers adjusted the color contrast until a subjective point of isoluminance was reached. Otherwise, the experimental protocol is the same as with our first and second pair of matched displays (see Figure 3.7 and Figure 3.8). Unlike in Experiments 1 and 2, performance is essentially at chance level (25%) for the rivalrous ($25.1 \pm 2.3\%$ correct). Performance for the non-rivalrous display is slightly lower than in the previous experiment but also well above chance ($(72.2 \pm 4.3\%)$ (presentation time $250ms$).

Experiment 4

Both paired and rivalrous display types (see Figure 3.7, B and Figure 3.8, A) are combined with a concurrent letter task (see Figure 2.1) as in our previous attentional experiments from Chapter 2 involving locally balanced dot textures (see Figure 2.4, LB). In the first display type target and background differ in that dots in the two regions move along orthogonal trajectories. In this display each dot is paired with a nearby dot (separation $< 0.1°$) of equal and opposite motion (Qian *et al.*, 1994). The localization task involved the discrimination of the "odd" target region (orthogonal direction of motion). The concurrent letter task concerned the discrimination of five T- and L-shaped elements near display center (2AFC). In the second display target and

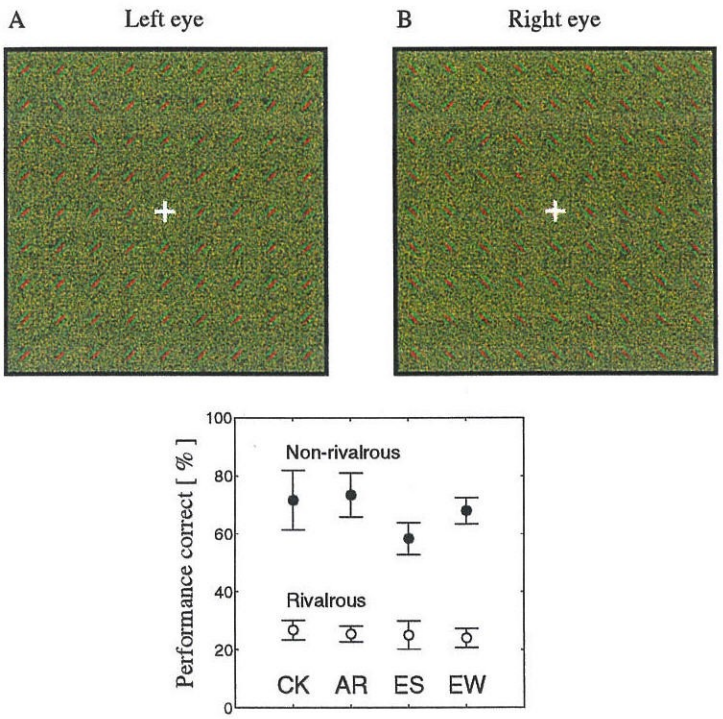

Figure 3.9: Psychophysical displays (schematic) and individual data from four observers (CK, AR, ES, EW; 2,400 trials; $250ms$). The display used was similar to that in Figure 3.8 except it contained a (stationary) fixation cross rather than a Landolt C in the center. Binocular fusion of orthogonally oriented elements conceals a target from visual awareness but does not prevent its localization. Left and right eyes are stimulated dichoptically with the help of polarizing goggles. Both eyes view a 20×20 array of oriented elements (2-D Gabor functions with polar orientation $\pm\pi/4$, period $0.448°$, $\sigma = 0.224°$, phase $\pm\pi/2$). Elements are oriented orthogonally in the target (size $2 \times 2°$, centered in one of four quadrants of the display) and the background region (for both eyes). Display values corresponding to the phase maxima and minima ($+\pi/4$ and $-\pi/4$) were the color values for red and green, respectively. To ensure isoluminant values for red and green, before each experiment observers adjusted the red value for rapidly phase-shifting Gabor patches ($\approx 50ms$) in the above display until a percept of "minimal flicker" was achieved, while keeping the green value constant (Cavanagh & Anstis, 1991). For the non-rivalrous display performance was significantly above chance (and indeed compatible with earlier results, see Figure 3.8, B), whereas performance for the rivalrous display was essentially at chance (*i.e.*, at 25 %).

background differ with respect to local element orientation. Observers wear polarizing goggles, permitting independent stimulation of left and right eyes. Corresponding elements impinging upon the left and right eye have orthogonal orientation. The localization task involved the discrimination of the "odd" target region (orthogonal orientation). The concurrent letter task concerned the discrimination of five ⊤- and ⊔-shaped elements near display center (2AFC). The protocol was identical in both cases. Instructions encouraged observers to treat as primary the letter task and to perform as well as if they had attempted to perform this task by itself. As a result, secondary task performance for both display types (paired and rivalrous) dropped essentially to chance level (at 25%).

3.1.4 Discussion

The dissociation of performance and awareness in paired and rivalrous displays is not limited to a narrow threshold region but holds over a wide range of performance (Figure 3.11). Increasing presentation time from $60ms$ to $1s$ raises performance from $31 \pm 1\%$ to $77 \pm 1\%$ for paired, and from $33 \pm 2\%$ to $80 \pm 1\%$ for unpaired displays, yet the respective ROCs remain straight, or curved, throughout this range (Figure 3.11, A and B). Similar results are obtained with rivalrous and non-rivalrous displays at $100ms$ and $250ms$ presentation time (Figure 3.11, C). Figure 3.12 and Figure 3.13 show both percentage correct and receiver-operating characteristics obtained over a 16-fold range of presentation time.

Even extensive visual practice ($>$ 20 sessions of $1h/day$) does not change the outcome (not shown). It appears that, without subjective awareness, the observer cannot gauge signal strength and thus cannot estimate the accurateness of his or her response. Among the psychophysical measures investigated (percentage correct, reaction time, confidence), the curvature of the receiver-operating characteristic appears to be best correlated with awareness (as judged by introspection and revealed

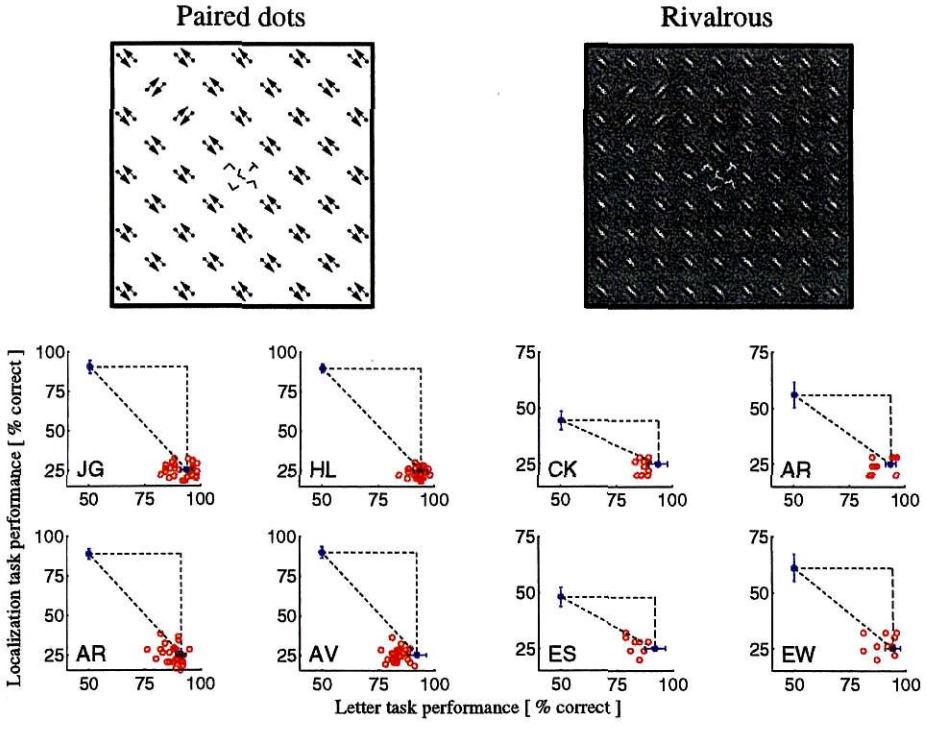

Figure 3.10: Psychophysical displays (schematic) and results for seven observers (JG, HL, AR, AV, CK, ES, EW; 12,000 trials; 200*ms*). Left, *Paired dots*, see Figure 2.4, LB. Right, *Rivalrous* see Figure 3.8, A. The individual symbols in each scatter plot (for each individual observer as identified by labeling) represent one block of 100 trials. Letter task performance is represented along the horizontal axes and localization task performance along the vertical axes (see Figure 2.1, *Stimulus*). Closed symbols (●) show separate performance of a particular task (single task) and are positioned along the axes of the plot, together with respective single task standard errors. Open symbols (○) show concurrent performance of both tasks (double task) and occupy the plane of the scatter plot. Mean performance is indicated by broken lines. When the two tasks conflict, the open symbols are found in the lower right corner of the scatter plot; when they do not, the open symbols are located in the upper right corner of the plot. Apparently, the concurrent letter task interferes with both paired dots and rivalrous tasks.

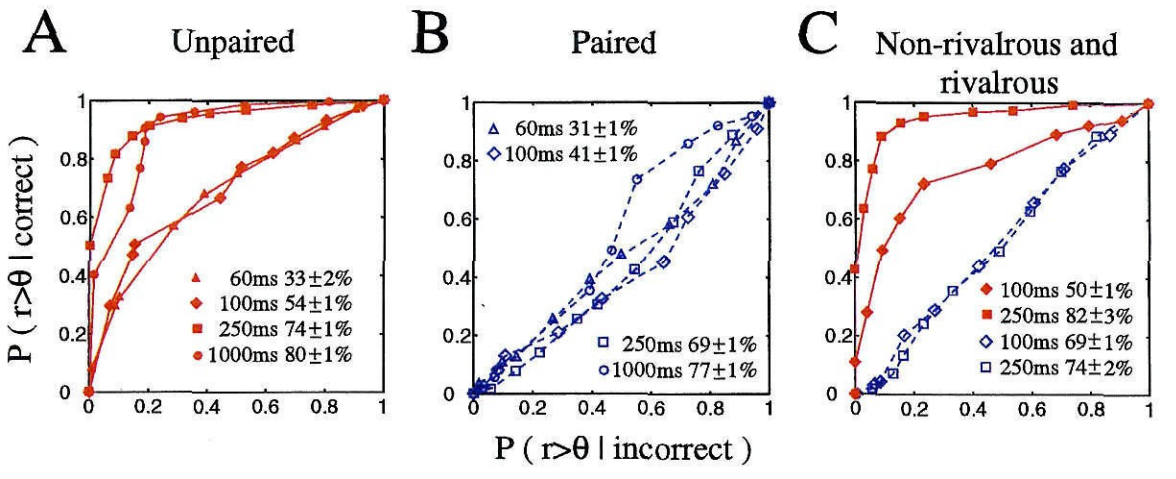

Figure 3.11: (A-C) Receiver-operating characteristics (ROCs) obtained over a 16-fold range of presentation time. Data from Figure 3.7 and Figure 3.8 at $250ms$ presentation time combined with additional data at $60ms$, $100ms$, and $1s$ presentation time (2200 trials, observers DE, SK). ROCs are drawn with different symbols, and insets give the respective presentation time and performance (mean of all observers). When moving-dot displays are presented for $1s$, it is necessary to prevent serial scrutiny of individual display regions. To this end, the orientation of dot trajectories changes every $250ms$ in both target and background regions. Oriented-element displays were not investigated at $> 250ms$ because one eye dominates perception at longer presentation times. (A) and (C), filled symbols and solid lines: curved ROCs indicate normal awareness of the target even at the lowest levels of performance (unpaired and non-rivalrous displays). (B) and (C), open symbols and dashed lines: essentially straight ROCs indicate failed awareness of the target even at the highest levels of performance (paired and rivalrous displays). (Here, the ROC is defined as the conditional probability of a confidence rating $r > \theta$, $\theta = 0, 1, \ldots, 10$, given that the response is correct, $P_{(r>\theta \mid correct)}$, plotted against the conditional probability of $r > \theta$ given that the response is incorrect, $P_{(r>\theta \mid incorrect)}$, where $P_{(r>\theta \mid correct)} = \sum_{r>\theta} c_r / \sum_r c_r$ and $P_{(r>\theta \mid incorrect)} = \sum_{r>\theta} i_r / \sum_r i_r$.)

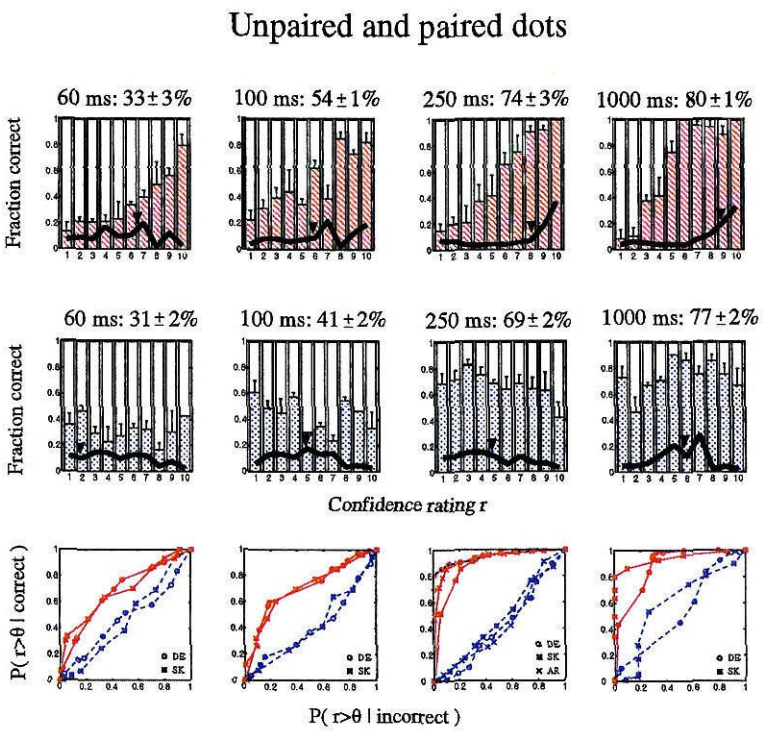

Figure 3.12: Performance values and receiver-operating characteristics (ROCs) obtained over a 16-fold range of presentation time. Data from Figure 3.7, C and D, combined with additional data at $60ms$, $100ms$ and $1000ms$ presentation time (2,200 trials, observers DE, SK, AR). Red-colored histograms and ROC curved represent data from "unpaired" trials, and blue-colored histograms and ROC curves represent data from "paired" trials. Let n_r, c_r, and i_r be the number of all trials, correct trials, and incorrect trials with confidence rating r, respectively, with $n_r = c_r + i_r$ and $r = 1, \ldots, 10$. Thick line and arrow: fraction of trials with confidence rating r, γ_r (mean of all observers, $\gamma_r = n_r / \sum_r n_r$). The arrow marks the distribution mean. Bar histogram: fraction of correct responses among trials with confidence rating r, ξ_r (mean and standard error of all observers, $\xi_r = c_r / n_r$). For unpaired displays, the fraction f_r increases almost monotonically with the confidence rating whereas, for paired displays, there is no significant relation (individual observers). The ROC of paired trials is essentially straight, showing failed awareness of the target, while the ROC of unpaired trials is highly curved, showing normal awareness of the target. (The ROC is defined as the conditional probability of a confidence rating $r > \theta$, $\theta = 0, 1, \ldots, 10$, given that the response is correct, $P_{(r>\theta \mid \mathit{correct})}$, plotted against the conditional probability of $r > \theta$ given that the response is incorrect, $P_{(r>\theta \mid \mathit{incorrect})}$, where $P_{(r>\theta \mid \mathit{correct})} = \sum_{r>\theta} c_r / \sum_r c_r$ and $P_{(r>\theta \mid \mathit{incorrect})} = \sum_{r>\theta} i_r / \sum_r i_r$.)

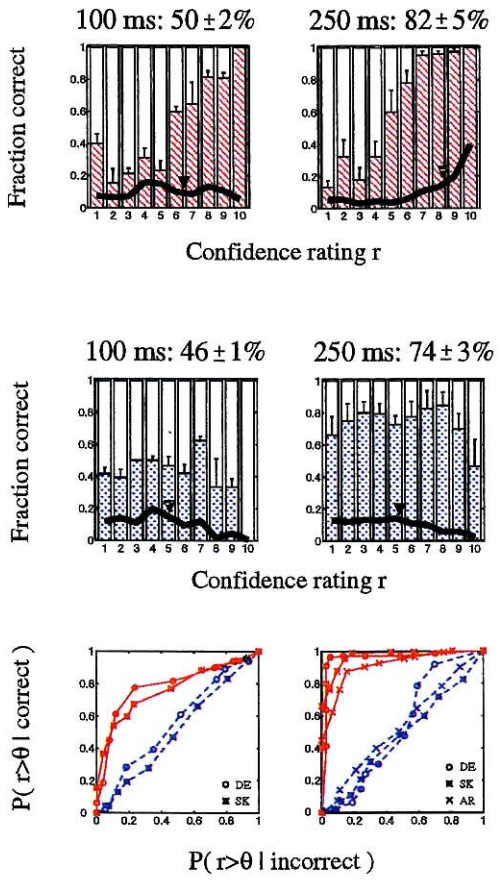

Figure 3.13: Performance values and receiver-operating characteristics (ROCs) obtained over a 8-fold range of presentation time. Data from Figure 3.8, B and C, combined with additional data at $100ms$ presentation time (2,000 trials, observers DE, SK). Red- colored histograms and ROCs represent data from "non-rivalrous" trials, and blue-colored histograms and ROCs represent data from "rivalrous" trials. Let n_r, c_r, and i_r be the number of all trials, correct trials, and incorrect trials with confidence rating r, respectively, with $n_r = c_r + i_r$ and $r = 1, \ldots, 10$. Thick line and arrow: fraction of trials with confidence rating r, γ_r (mean of all observers). The arrow marks the distribution mean. Bar histogram: fraction of correct responses among trials with confidence rating r, ξ_r (mean and standard error of all observers). The ROCs for non-rivalrous trials are highly curved while those for rivalrous trials are essentially straight, showing the difference between normal and failed awareness of the target over a range of different presentation times (individual observers).

by confidence measure), somewhat correlated with reaction-time (see Figure 3.14 and Figure 3.15), and least correlated with signal strength.

The capacity to locate a texture with blindsight crucially depends on a limited range of spatial frequencies that describe the local interactions between opposite directions of motion (see Figure 3.16) and orthogonal orientations (see Figure 3.17). For blindsight to occur in normal observers, it appears that dots traveling in opposite directions be confined to parallel trajectories not more than four pixels apart. Given the limited dot lifetime the range of spatial interactions matches the size of the classical V1 receptive field near the fovea (central 5°) of an estimated 0.2° - 0.45° of visual angle (VanEssen. *et al.*, 1984). Similarly, in the case of rivalrous orientations even a minute disparity offset (1 pixel) between the left and right eye images diminishes blindsight performance and causes conscious appreciation of the target, at least in one observer (ES). For the other observer (CK), blindsight was evident up to three pixels of shifted overlap between the two images (see Figure 3.17).

This seemingly complete lack of awareness far above the onset of visual sensitivity warrants comparison with blindsight (Pöppel *et al.*, 1973; Weiskrantz *et al.*, 1974; Stoerig & Cowey, 1993). In previous attempts to dissociate awareness and performance in normal observers "subliminal perception") (Sidis, 1898; Marcel, 1983), a direct measure (*e.g.*, a task like our 4AFC location task) typically shows zero or near-zero visual sensitivity (i.e., performance is at or near chance) while an indirect measure (*e.g.*, priming of a subsequent task) shows that some visual processing has taken place. Accordingly, this situation is not comparable to blindsight. In an explicit attempt to demonstrate blindsight in normal observers, a recent study dissociates detection and localization performance, showing that undetected stimuli are localized somewhat better than chance (Meeres & Graves, 1990; Graves & Jones, 1992). However, it has been argued that this dissociation may simply concern *performance* and be unrelated to *awareness* (Merikle, 1992). In general, controversy persists about whether perfor-

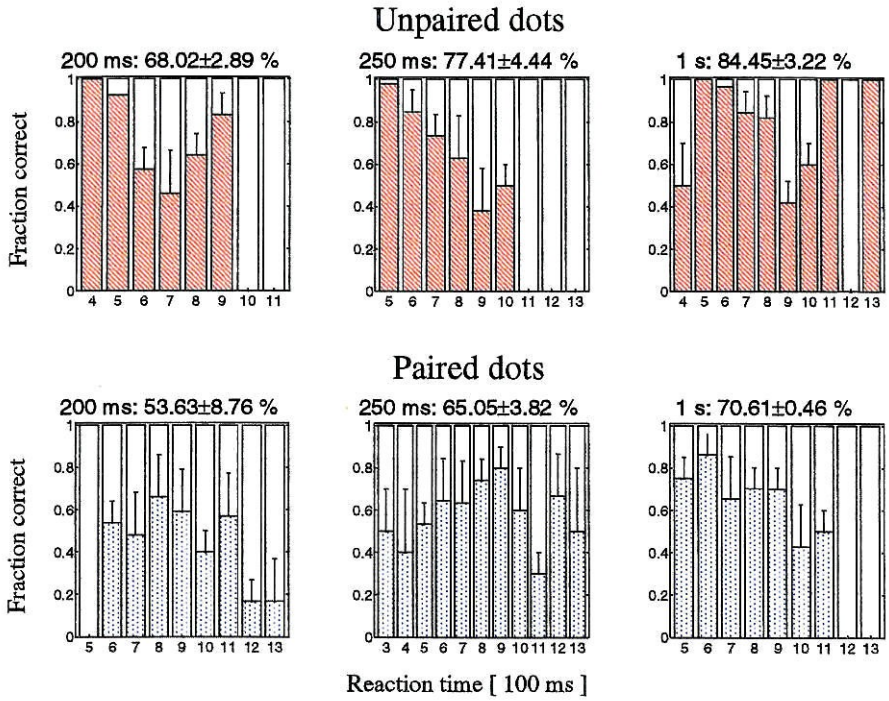

Figure 3.14: Reaction times data obtained over an 8-fold range of presentation time (2,100 trials, observers DE, AR). "Reaction time" was defined as the time from stimulus onset to the observer's key press indicating the target location (see Figure 3.7). For the "unpaired" trials there was an overall correlation between performance (expressed as fraction correct) and reaction time. For shorter reaction times, the fraction of correct responses was significantly higher for a stimulus duration of $250ms$, and only weakly significantly higher for presentation times of $200ms$ and $1s$. For the "paired" trials any significant correlation between performance and reaction time was observed only for a stimulus presentation of $1s$.

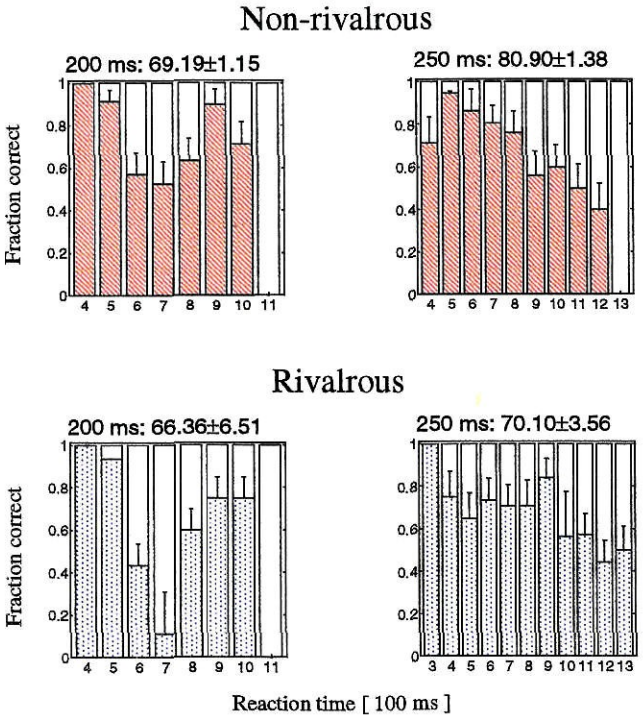

Figure 3.15: Reaction time data obtained over a 1.5-fold range of presentation time (1,600 trials, observers DE, AR). *Reaction time* was defined as the time from stimulus onset to the observer's key press indicating the target location (see Figure 3.8). In both "non-rivalrous" and "rivalrous" trials significant correlations between performance and reaction time were observed for a stimulus duration of $250ms$. Weakly significant correlations were observed for both display types at presentation times of $200ms$.

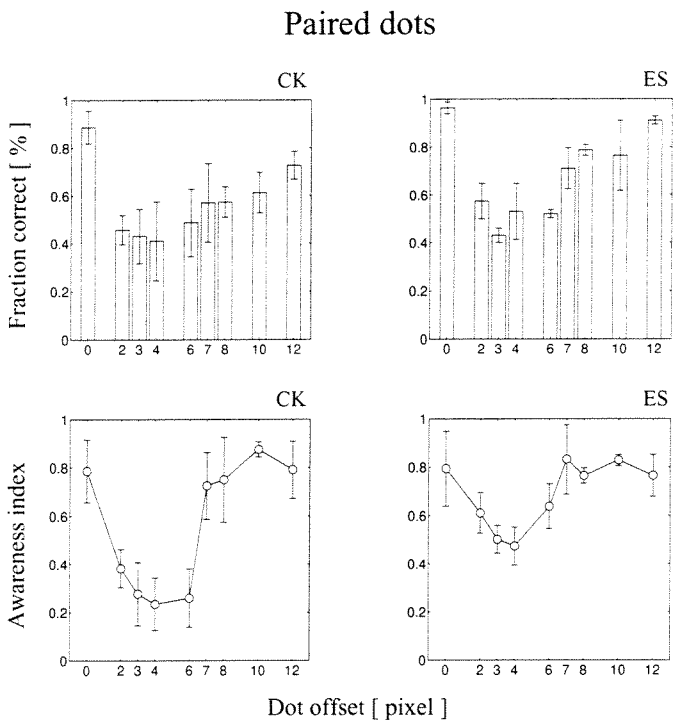

Figure 3.16: Dependence of blindsight performance on spatial frequency characteristics (5,400 trials, observers CK, ES). Stimulus consisted of paired dots similar to the display described in Figure 3.7, B. The vertical distance between two paired dots along their horizontal trajectories of motion (dot offset) was systematically varied from 0 to 12 pixels separation. Top row shows performance in fraction of correct responses for nine offset values (0, 2, 3, 4, 6, 7, 8, 10, 12 pixels). Bottom row shows the respective *awareness index* and standard deviation (⊢◯⊣), derived from the area underneath the associated (normalized as 1×1) ROC curve (see Figure 3.7 and Figure 3.8). An awareness index of 0.5 would thus signify a lack of correlation between performance and awareness (corresponding to a straight ROC), whereas an awareness index significantly larger than 0.5 would imply a certain degree of correlation between performance and awareness (corresponding to a curved ROC). Note that for vertical dot offsets of one pixel and less, "directional" motion aftereffects reveal the true target position, resulting in a high awareness index.

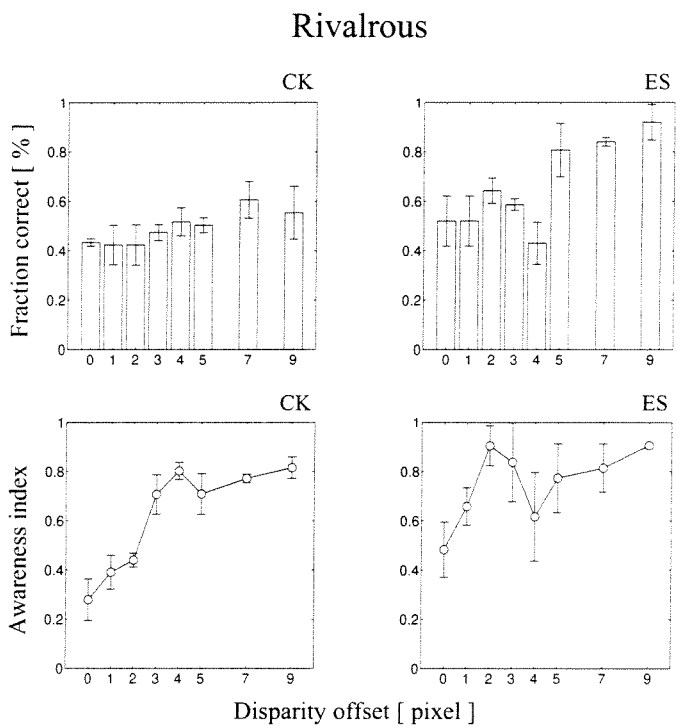

Figure 3.17: Dependence of blindsight performance on spatial frequency characteristics (4,800 trials, observers CK, ES). Stimulus consisted of rivalrous 2-D Gabor elements similar to the display described in Figure 3.8, A. The horizontal disparity (disparity offset) was systematically varied from 0 to 9 pixels (lateral) separation. Top row shows performance in fraction of correct responses for eight offset values (0, 1, 2, 3, 4, 5, 7, 9 pixels). Bottom row shows the respective *awareness index* and standard deviation (⊢◯⊣), derived from the area underneath the associated (normalized as 1×1) ROC curve (see Figure 3.7 and Figure 3.8). An awareness index of 0.5 would thus signify a lack of correlation between performance and awareness (corresponding to a straight ROC), whereas an awareness index significantly larger than 0.5 would imply a certain degree of correlation between performance and awareness (corresponding to a curved ROC).

mance can be convincingly dissociated from awareness with any paradigm (Merikle, 1992; Greenwald, 1992; Schacter, 1992; Farah *et al.*, 1991).

Why do two of our displays induce blindsight while two others support visual awareness of the target? Single-cell evidence from non-human primates who view similar stimuli suggests reduced or altered input to extrastriate cortex as a possible reason. This would imply that our observations and clinical blindsight (Pöppel *et al.*, 1973; Weiskrantz *et al.*, 1974; Stoerig & Cowey, 1993) may have a similar genesis. In general, striate cortex is thought to exhibit an increased response at the location of a texture contrast, presumably because of the surround inhibition intrinsic to this area (Malik & Perona, 1990; Rubenstein & Sagi, 1990; Knierim & VanEssen, 1992; Press *et al.*, 1994; Karni *et al.*, 1993). As opposite motion and rivalrous orientation appear to be processed independently at the level of striate cortex (Qian & Andersen, 1994; Logothetis & Schall, 1989; Leopold & Logothetis, 1995; Malach *et al.*, 1993), this increased response should be evident in direction-selective cells with both paired and unpaired displays and in orientation-selective cells with both rivalrous and non-rivalrous displays. In extrastriate cortex, however, opposite motions and rivalrous orientations seem to interact in an inhibitory manner: in extrastriate area MT, for example, paired dot textures elicit approximately half the activity (in direction-selective cells) of unpaired dot textures (Qian & Andersen, 1994) and, in extrastriate areas V4 and MT, rivalrous patterns elicit significantly less activity than non-rivalrous patterns (Logothetis & Schall, 1989; Leopold & Logothetis, 1995) (see Figure 3.18).

The underlying mechanism of blindsight in normal observers (Kolb & Braun, 1995) appears to be an inhibitory interaction between conflicting visual features. Here we attempt to obtain clues to possible neural sites by investigating the spatial range of this interaction. A first display consists of two arrays of Gabor elements viewed dichoptically. For each eye, all elements have identical orientation except those in

the target area, which are oriented orthogonally. However, orthogonal elements are presented to left and right eyes at every array location. Thus the target area is subjectively not apparent (presentation time 200ms, viewing distance 57cm, 2 observers). Nevertheless, observers are able to correctly "guess" the location of the target area. The degree of visual awareness of the target is quantified with the help of confidence ratings. A second display consists of randomly placed dots of limited lifetime, which appear in pairs at nearby locations, move in opposite directions past each other, and disappear. Dots in the target area move at right angles to dots in the rest of the display. Otherwise the procedure is the same (presentation time 200ms, viewing distance 85cm, 2 observers). In the first display, target awareness is nil when corresponding Gabor elements are presented to left and right eyes at exactly the same location, but recovers rapidly when corresponding elements are displaced from each other by less than 0.1°. In the second display, target awareness is nil when nearby dots pass each other at 0.05°, but rapidly recovers as this distance increases to 0.15° (Qian & Andersen, 1994). The spatial range of the interactions that suppress visual awareness is comparable to receptive field diameters in striate visual cortex. Thus, the interaction may be related to the "divisive inhibition" suggested by Heeger and Carandini (1994) and others.

However, a close comparison between some of the abilities that characterize clinical blindsight and the persistence of motion-sensitive properties in area MT after striate lesion warrants further studies in artificial blindsight (Kolb, 1995). For example, monkeys with striate cortical lesions are capable of detecting motion and even discriminating between angular velocities (Keating, 1980), and apparently blind human patients have also been shown to process rudimentary information regarding direction and speed of visual motion (Barbur *et al.*, 1980; Perenin *et al.*, 1980; Tychsen *et al.*, 1988). Detection of apparent motion has also been described within a scotoma (Blythe *et al.*, 1986). These abilities, as well as the recovery of visually

guided reaching behavior, are likely to be dependent upon the activity of directionally selective neurons somewhere in the visual system. Thus far, area MT is the only primate visual cortical structure known to have directionally selective units in the absence of striate cortex, implying a crucial role for MT in blindsight. On the other hand, there are behavioral dysfunctions in monkey following striate cortical ablation that may reflect the lowered gain of the motion signal arising from area MT in the destriated monkey. For example, after unilateral striate lesions, monkeys show oculo-motor deficits that suggest an inability to use information about the velocity of a moving target (Segraves *et al.*, 1987). In the intact animal such information is provided at least in part by MT neurons (Newsome *et al.*, 1985; Newsome & Pare, 1986).

3.1.5 Conclusion

Assuming that our paired and rivalrous displays impede the direct propagation of activity from striate to extrastriate cortex, the situation resembles damage to striate cortex and clinical blindsight in that extrastriate input is reduced and much of the remaining input is derived from subcortical sources (Stoerig & Cowey, 1993). Accordingly, a reduced amount or a subcortical source of extrastriate input, or both, may impoverish subjective awareness. This would be consistent with the recent suggestion, on anatomical grounds, that subjective awareness may correlate with neural activity in extrastriate but not striate cortex (Crick & Koch, 1995). Note that, even if paired and rivalrous displays would completely block the direct striate-extrastriate projection, activity in striate cortex could still affect activity in extrastriate areas indirectly by way of the superior colliculus, the pulvinar, or other subcortical nuclei (Stoerig & Cowey, 1993). In this way, a texture contrast registered in striate cortex could guide behavior without entering subjective awareness.

Rodman *et al.* (1990) demonstrated that adding a superior colliculus lesion to stri-

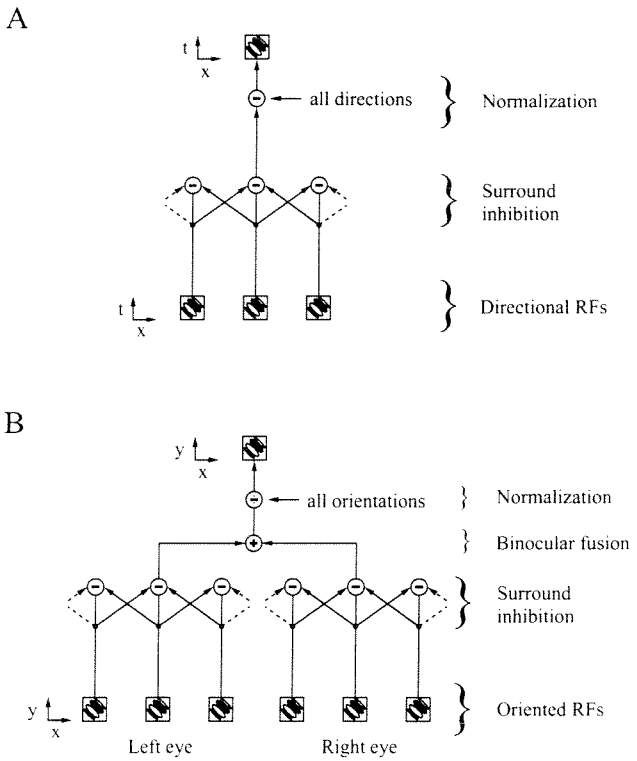

Figure 3.18: (A) and (B) Hypothetical processing stages of blindsight inducing displays. A texture contrast is though to elicit a robust response as a result of orientation or direction selective surround inhibition, which least attenuates responses where neighboring stimuli exhibit orthogonal orientation or direction of motion. (A) First, direction selective receptive fields (*RFs*) register local motion; second, direction-selective surround inhibition least attenuates responses in the target quadrant; and third, local inhibition across directions normalizes the response. (B) First, orientation selective RFs register local orientation separately for each eye; second, orientation selective surround inhibition differentiates responses in the target quadrant; and third, left and right eye responses are pooled, and subsequently local inhibition across orientation normalizes responses. Orientation selective surround inhibition is well documented in area V1. In addition, many cells in area V1 are dominated by one eye. Thus, the intrinsic connectivity of area V1 is ocular-dominance specific, potentially permitting right- and left-eye textures to be processed independently.

ate cortex removal obliterates the considerable visual responsiveness remaining in area MT after a (single) striate cortex lesion. Anatomical data indicate that the superficial (visual) layers of the superior colliculus receive direct retinal inputs (Hubel *et al.*, 1975; Pollack & Standage, 1983) which potentially gain access to extrastriate cortex via the pulvinar nucleus of the thalamus (Benevento & Standage, 1983). Portions of the inferior and lateral pulvinar project to area MT (Maunsell & Van Essen, 1983; Standage & Benevento, 1983), and some cells in the inferior and lateral pulvinar remain responsive in the absence of striate cortex input (Burman *et al.*, 1982; Bender, 1983). Pathways that might provide visual input to area MT and might be disrupted by superior colliculus lesions are 1) retina-colliculus-(inferior)pulvinar to (lateral)pulvinar-MT; 2) retina-pretectum to (inferior)pulvinar to (lateral)pulvinar-MT; 3) retina- pretectum-colliculus to (inferior)pulvinar to (lateral)pulvinar-MT; 4) retina-colliculus to LGN to extrastriate-MT; 5) retina-pretectum to LGN to extrastriate-MT.

Our two attempts at reproducing a functional superior colliculus lesion (heterochromatic isoluminance condition and "freezing" of visual attention) resulted in radical diminution of blindsight performance. Although our first result is somewhat at odds with a recent study by Stoerig and Cowey (1993) who demonstrated almost normal color vision in blindsight patients (in conditions that favored the color- opponent system), the difference in experimental outcome may be explained in terms of crosstalk between magno- and parvocellular streams at any of the variety of stages in the cortical hierarchy (Logothetis, 1991; Schiller & Colby, 1983). For example, motion processing clearly suffers when only chromatic form cues are present, and the perceived speed of motion is often slower (Cavanagh *et al.*, 1985). Under most conditions, however, motion is still perceived (Cavanagh & Favreau, 1985; Derrington & Badcock, 1985; Cavanagh & Anstis, 1991), and direction of motion can be accurately discriminated (Sato, 1988; Dobkins & Albright, 1993). The chromatic pathways that subserve motion detection, however, remain largely unknown. Recent studies, how-

ever, indicate that while MT neurons are not selective for color *per se*, they can detect the motion of isoluminant chromatic gratings, giving a reduced but significant response to these stimuli (Charles & Logothetis, 1989; Dobkins & Albright, 1991; Saito *et al.*, 1989).

The fact that removing visual attention from the periphery that contains background and target results in chance performance for both paired and rivalrous displays is again *prima facie* at odds with the classical notion of attention (James, 1890, Koch & Ullman, 1985). Thus far, information is said to be "attended" if it enters short-term memory and remains there long enough to be voluntarily reported (Kahneman, 1973; Neisser, 1967). Hence visual attention is closely linked to visual awareness. Since visual attention is thought to control access to levels of processing that guide behavior, it should be impossible for anything outside the focus of attention to be relevant to behavioral objectives and not also reach awareness. Thus, stimuli that win the competition for saliency (see Figure 1.1) may enter phenomenal awareness independently of focal attention. In other words, blindsight is thought to be non-attentive simply by stipulating a notion of attention that is operationally equivalent to awareness. We suggest that this apparent conflict may be resolved if blindsight performance in normal observers can be shown to operate top-down unlike perception outside the focus of attention that is known to operate bottom-up (see Figure 1.1). Thus we hypothesize a cancellation of mechanisms, one that selects on the basis of local stimulus information pitted against another mechanism whose selection criteria are based on prior information. This hypothesis is examined in Chapter 4.

3.2 Blindsight in normal observers: Perceptual learning and plasticity

3.2.1 Background

The overarching theme of the following psychophysical experiments is "contour integration", a form of perceptual organization in the Gestalt sense (see Figure 3.19, A). When observers view hundred or thousand contour displays over several days or weeks, performance on detecting the contour improves significantly (Kolb *et al.*, 1995). Consistent with the idea of perceptual learning in striate cortex (or beyond), practicing with on eye does not improve performance with the other (Karni & Sagi, 1991). Contour integration depends on both the local and global shape of a contour. The importance of global shape is evident from the fact that closed contours are more readily detected than open contours of equal length and curvature (Kovacs & Julesz, 1993). However, it is not obvious how "hard-wired" short- range interactions in striate cortex could account for this dependence on global shape.

With displays ("artificial blindsight") that putatively relegate contour integration to the functional level of striate cortex, we investigated the possibility of perceptual learning without the possibility of long-range interactions in extrastriate cortex (see Figure 3.19, left and right eye). In striate cortex, functional interactions have been demonstrated between cells that (i) receive input from the same eye, (ii) are sensitive to similar orientations and, (iii) are within $1 - 8mm$ of each other (corresponding to $0.5 - 1.5^{\circ}$ of visual angle). Such interactions may be mediated by lateral connections intrinsic to striate cortex and, possibly, by feedback from cells with similar selectivity in area V2. Perceptual learning of global shapes in the absence of activity in extrastriate cortical areas could then be explained in terms of the dynamic nature of short-range interactions in area V1 (Braun, 1995).

3.2.2 Materials and methods

Binocular fusion of orthogonally oriented elements conceals a target from visual awareness but does not prevent its localization. Left and right eyes are stimulated dichoptically with the help of polarizing goggles. In Experiment 1 both eyes view a display subtending $10 \times 10^{\circ}$ and filled with oriented elements (2-D Gabor functions with polar orientation $\pm\pi/4$, period 0.448°, $\sigma = 0.224^{\circ}$, phase $\pm\pi/2$). (A) A fixed number of elements are oriented to form a closed (circular) contour (*snake*), randomly located in a background filled with randomly oriented elements (see Figure 3.19). The snake could randomly appear at one out of eight positions across the display. In Experiment 2 both eyes view a display subtending $10 \times 10^{\circ}$ and filled with oriented elements (2-D Gabor functions with polar orientation $\pm\pi/4$, period 0.448°, $\sigma = 0.224^{\circ}$, phase $\pm\pi/2$). (A) and (B) A fixed number of elements are oriented to form a straight line, located in a background filled with randomly oriented. The length of a line was approximately 10°. Line orientation (global) was either horizontal or vertical depending on subject and condition (non-rivalrous *vs* rivalrous) and a line could randomly occur at 1 out of 16 positions across the display. Observers are presented with two quasi-successive stimulus presentation (separated by a $200ms$ blank interval of mean luminance). One of the two displays contained the line and the other consisted of merely randomly oriented elements (not shown here) (see Figure 3.20).

3.2.3 Results

Experiment 1

Observers are presented with two quasi-successive stimulus presentation (separated by a $200ms$ blank interval of mean luminance). One of the two displays contained the snake and the other consisted of merely randomly oriented elements. Observers report the presence of the snake in a 2-alternative forced- choice procedure , and rate their

confidence in their answer (scale of 1 to 10). Possible answers were "first display" or "second display". Rivalrous and non-rivalrous displays were randomly interleaved (see Figure 3.19). In the rivalrous case, corresponding elements impinging upon the left and right eye have orthogonal orientation. Observers report seeing a uniform texture of small "stars" without any impression of a target whatsoever (presentation time $150ms$). (At longer presentation times, one eye gains dominance and elements presented to the other eye are barred from subjective awareness (Fox, 1991).) In the non-rivalrous case, corresponding left and right eye elements have the same orientation. Observers report seeing a texture of oriented elements with a contrasting target that is readily apparent. Performance is well above chance for both rivalrous ($68.5 \pm 3.1\%$ correct) and non-rivalrous ($94.1 \pm 2.6\%$) displays (presentation time $150ms$), although observers believe themselves to be "guessing" on rivalrous trials. Subjectively visible and invisible targets produce differentially skewed distributions of ratings (Figure 3.19, B and C, thick line and arrow) and the correlation between success and confidence is strong for visible (Kendall's $\tau = 0.91$, $p < .0005$) and absent for invisible targets ($\tau = 0.03$, $p > .5$) (Figure 3.19, B and C, bar histogram). The curvature of the ROC again highlights this difference (Figure 3.19, D).

Experiment 2

Observers are shown two quasi-successive stimulus presentation (separated by a $200ms$ blank interval of mean luminance). Depending on experimental condition, displays were either rivalrous or non-rivalrous. One of the two displays contained the line (target) and the other consisted of merely randomly oriented elements (not shown here). Observers reported the presence of the snake in a 2- alternative forced-choice procedure (2AFC). Possible answers were "first display" or "second display". Four naive observers (AR, DE, HH, SK) participated in nine trial sessions on nine consecutive days. Each session consisted of twelve blocks of 100 trials. Half of the trials features

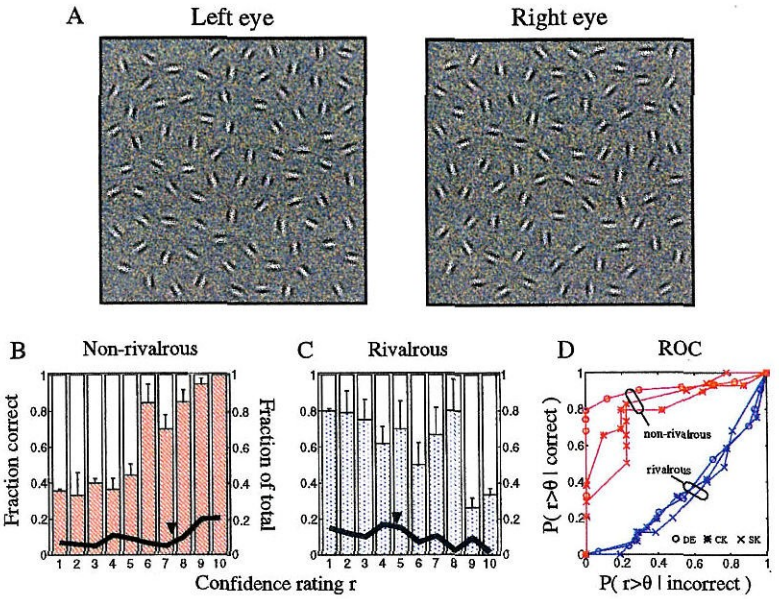

Figure 3.19: Psychophysical displays (schematic) with randomly oriented- element background texture and target contour and results for three observers (DE, CK, SK; 2,100 trials; $100ms$). Binocular fusion of orthogonally oriented elements conceals a target from visual awareness but does not prevent its localization. Left and right eyes are stimulated dichoptically with the help of polarizing goggles. Both eyes view a display subtending $10 \times 10°$ and filled with oriented elements (2-D Gabor functions with polar orientation $\pm\pi/4$, period $0.448°$, $\sigma = 0.224°$, phase $\pm\pi/2$). (A) A fixed number of elements are oriented to form a closed contour ("snake"), randomly located in a background filled with otherwise randomly oriented elements (for both eyes, see Figure 3.8, A). Observers are shown two quasi-successive stimulus presentations (separated by a $200ms$ blank interval of mean luminance). One of the two displays contains the snake and the other consists of merely randomly oriented elements (not shown here). Observers report the presence of the snake in a 2-alternative forced-choice procedure (first display or second display), and rate their confidence that the reported presence is correct (scale of 1 to 10). Rivalrous and non-rivalrous (not shown here) displays were randomly interleaved. (B-D) Analysis of performance and confidence. Let n_r, c_r, and i_r be the number of all trials, correct trials, and incorrect trials with confidence rating r, respectively, with $n_r = c_r + i_r$ and $r = 1, \ldots, 10$. (B) and (C) Thick line and arrow: fraction of trials with confidence rating r, γ_r (mean of all observers, $\gamma_r = n_r / \sum_r n_r$). The arrow marks the distribution mean. Bar histogram: fraction of correct responses among trials with confidence rating r, ξ_r (mean and standard error of all observers, $\xi_r = c_r/n_r$). For non-rivalrous displays, the fraction f_r increases almost monotonically with the confidence rating (B) whereas, for paired displays, there is no significant relation (C). (D) Receiver-operating characteristics (ROCs) for rivalrous and non-rivalrous trials (individual observers). The ROC of rivalrous trials is essentially straight, showing failed awareness of the target, while the ROC of non-rivalrous trials is highly curved, showing normal awareness of the target.

non-rivalrous displays, the other half featured rivalrous displays. The six blocks of both non-rivalrous and rivalrous trials involved different spacings between local elements (3, 4, 5, 6, 7, 8 Gabor λ units) (see Figure 3.21). For each individual observer, a "performance index" was computed as the area under the normalized (1×1) task-performance curve for each day. The red and blue curves in Figure 3.21 depict the results of perceptual learning for non-rivalrous and rivalrous displays, respectively. To avoid perceptual learning across different display types observers AR and DE were tested with horizontal non-rivalrous and vertical rivalrous lines, whereas observers HH and SK were tested with vertical non-rivalrous and horizontal rivalrous lines. Despite the characteristic difference in absolute performance between the two viewing conditions (rivalrous and non-rivalrous), perceptual learning slopes were almost identical when averaged across observers (see Figure 3.20, C).

3.2.4 Discussion

The significance of perceptual learning in cases of "conflicting" visual information is severalfold. First, the suggestion will be that short-range interactions at the level of striate cortex are crucial constituents of perceptual organization (contour integration). Second, perceptual learning may be explained without reference to long-range interactions at the level of extrastriate cortical areas but may instead involve dynamic, context-dependent response properties of striate cortical cells. And third, the predominantly subcortical input to extrastriate areas in "artificial" and clinical blindsight may further bear on the cortical specificity of visual plasticity (Cowey & Weiskrantz, 1963; Mohler & Wurtz, 1977). The latter point raises the important question of visual rehabilitation of scotoma patients, especially in the light of clinical evidence pointing to a significant improvement of visual performance after systematic practice (Weiskrantz, 1986).

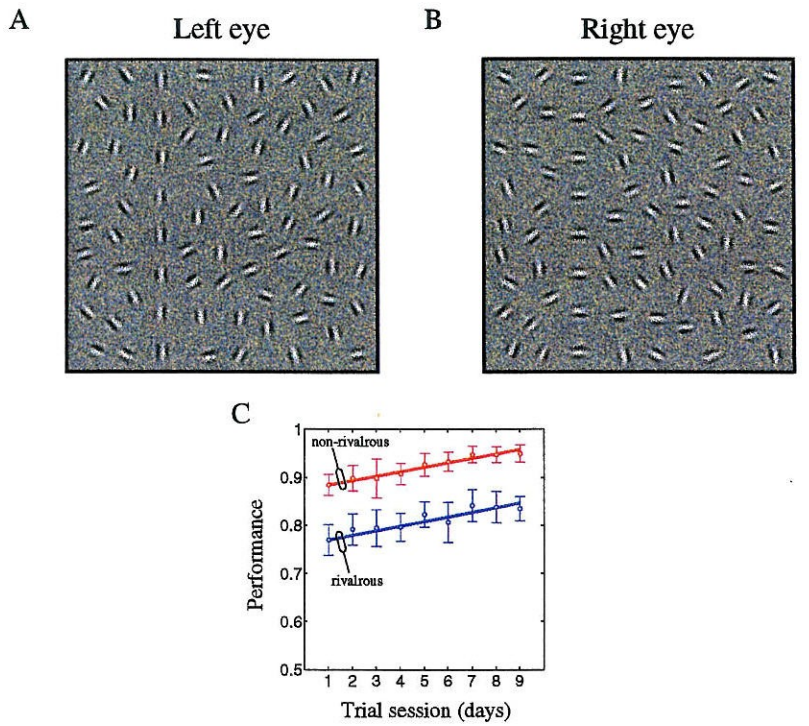

Figure 3.20: Psychophysical displays (schematic) with randomly oriented-element background texture and target contour and results for four observers (AR, DE, HH, SK; 43,200 trials; $200ms$). Binocular fusion of orthogonally oriented elements conceals a target from visual awareness but does not prevent its localization. Left and right eyes are stimulated dichoptically with the help of polarizing goggles. Both eyes view a display subtending $10 \times 10°$ and filled with oriented elements (2-D Gabor functions with polar orientation $\pm\pi/4$, period $0.448°$, $\sigma = 0.224°$, phase $\pm\pi/2$). (A) and (B) A fixed number of elements are oriented to form a straight line, located in a background filled with randomly oriented. The length of a line was approximately $10°$. Line orientation (global) was either horizontal or vertical depending on subject and condition (non-rivalrous *vs* rivalrous), and the line could randomly occur at 1 of 16 positions across the display. Observers are shown two quasi-successive stimulus presentations (separated by a $200ms$ blank interval of mean luminance). One of the two displays contained the line and the other consisted of merely randomly oriented elements (not shown here). Observers reported the presence of the snake in a 2-alternative forced-choice procedure (first display or second display). Local element spacings were systematically varied from 3 to 8 Gabor patch λ (wavelength) units. (C) Learning curves ("performance index") for nine trial sessions averaged across all subjects (see Figure 3.21). The performance index and standard deviation (⊢◯⊣) was computed from the area underneath the performance curves (corresponding to nine days) for various degrees of task difficulty (element separation: 3, 4, 5, 6, 7, 8 λ).

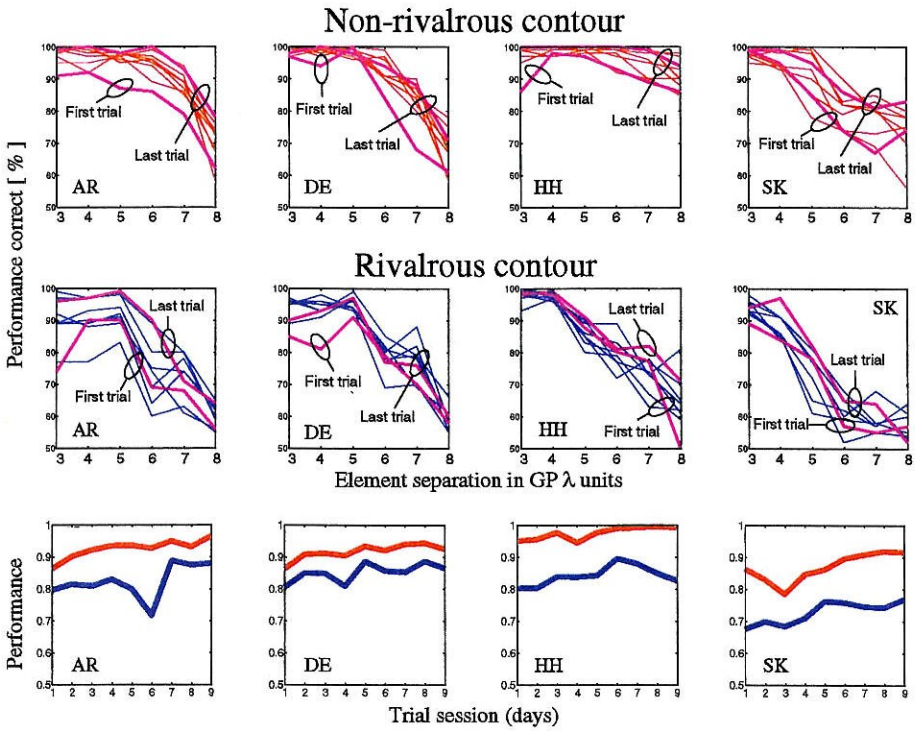

Figure 3.21: Perceptual learning data for four observers (individual). Task difficulty varies along the horizontal axes in the two upper rows (*Non- rivalrous contour* and *Rivalrous contour*) as a function of Gabor element spacing (3, 4, 5, 6, 7, 8 Gabor λ units). Vertical axes in the two upper rows indicate performance correct. Nine curves within each graph represent results from one to nine experimental session (corresponding to 1 to 9 days, or *First trial* to *Last trial*). A "performance index" was computed for each observer as the area under the normalized (1×1) task-performance curve for each day. The red and blue curves thus illustrate the effect of learning over time for non-rivalrous and rivalrous displays, respectively. Note that confidence measures (ROCs, see Figure 3.7 and Figure 3.8) were taken every three days to ensure the qualitative difference in perception (conscious *vs* unconscious perception) persisted (not shown here). To avoid perceptual learning across different display types observers AR and DE were tested with horizontal non-rivalrous and vertical rivalrous lines, whereas observers HH and SK were tested with vertical non-rivalrous and horizontal rivalrous lines.

3.2.5 Conclusion

Perceptual learning can be demonstrated in situations where what is being learned fails to present itself experientially to the learner. Our experimental data imply that discrimination in simple visual detection tasks improves at comparable rates for conscious and unconscious viewing, suggesting that perceptual learning and plasticity do not require visual awareness and activation of extrastriate cortex.

3.3 Blindsight in normal observers: Orientation discrimination and the McCollough effect

3.3.1 Background

McCollough (1965) discovered an orientation-contingent color aftereffect that offered indisputable evidence for some kind of interaction between color- and orientation-coding mechanisms in the visual system. In its original version, the McCollough effect is produced in observers who view two differently oriented grating patterns alternately for a few minutes, such as a red-and-black vertical grating and a black-and-green horizontal grating ("adaptation gratings"). When observers are subsequently shown black-and-white gratings of the same orientation as the adaptation gratings (vertical *vs* horizontal), the white stripes will appear as either pink or pale green, respectively.

Until recently the question of the cortical site of the McCollough effect has been subject of a variety of theories in the absence of anatomical evidence (Dodwell & Humphrey, 1990). Now clinical experiments by Humphrey *et al.* (1995) have shed light on the cortical mechanisms underlying this intriguing effect. Their patient P.B. who had suffered severe damage to extrastriate areas 18 and 19 and as a result, was unable to make any orientation discriminations showed a remarkable ability to dissociate

different colors, including those used to induce the McCollough effect. After viewing the adaptation gratings, P.B. was able to report the orientation-specific aftereffect colors for the test gratings, even though he could not discriminate their orientations. Given the specific extrastriate cortical destruction in patient P.B., Humphrey *et al.* (1995) have concluded that primary visual cortex must serve as the anatomical locus of the McCollough effect.

Using "conflicting" visual information to conceal the global orientation contrast in a (grating) display from consciousness, we first demonstrate unconscious orientation discrimination in normal observers thereby mimicking patient P.B.'s distinct perceptual impediment. In a second experiment, we probe for the McCollough effect in artificial (orientation) blindsight. Under certain unecological viewing conditions (again related to selective V1 activation), normal observers, like patient P.B. have no visual awareness of the orientation grating but can reliably describe the orientation-contingent aftereffect color.

3.3.2 Materials and methods

Binocular fusion of orthogonally oriented elements conceals an oriented grating pattern from visual awareness but does not prevent observers orientation (see Figure 3.22, A and B). Left and right eyes are stimulated dichoptically with the help of polarizing goggles. In both experiments left and right eye view a display subtending $10 \times 2^{\circ}$ (with the exception of various other display widths in Experiment 1) and filled with oriented elements (2-D Gabor functions with polar orientation $\pm\pi/4$, period 0.448°, $\sigma = 0.224^{\circ}$, phase $\pm\pi/2$). Local Gabor elements were oriented orthogonally alternately in large stripes that make up the grating that extends over the entire display. The width of the stripes measured orthogonal to their orientation is 2°. The grating had one of four principal orientations: 0, $\pi/4$, $\pi/2$, or $3\pi/4$ and appeared as uniformly gray in all displays used in Experiment 1 and in the test gratings of Experiment 2

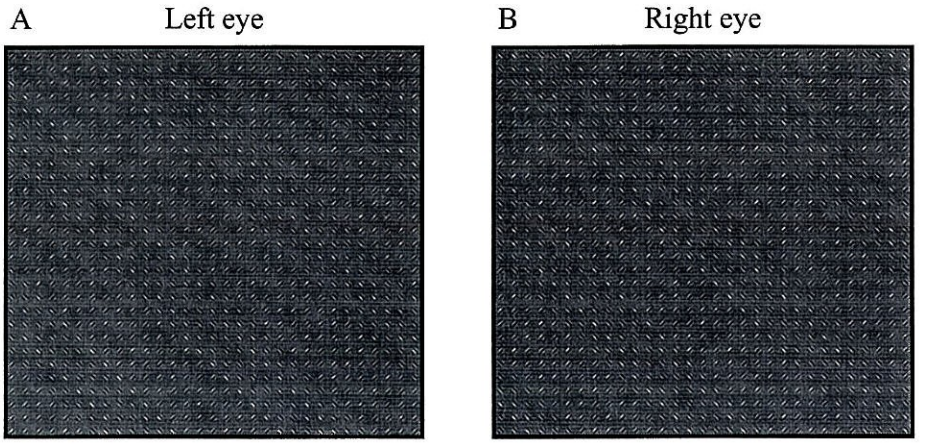

Figure 3.22: Psychophysical displays (schematic) with oriented-element textures. Binocular fusion of orthogonally oriented elements conceals global display orientation from visual awareness but does not prevent its discrimination. Left and right eyes are stimulated dichoptically with the help of polarizing goggles. Both eyes view a display subtending $10 \times 10°$ and filled with oriented elements (2-D Gabor functions with polar orientation $\pm\pi/4$, period $0.448°$, $\sigma = 0.224°$, phase $\pm\pi/2$). Elements are oriented orthogonally in large stripes that make up the grating that extends over the entire display. The width of the stripes measured orthogonal to their orientation is $2°$. The grating could have one of four principal orientations: 0, $\pi/4$, $\pi/2$, or $3\pi/4$. Observers are asked to indicate the orientation of the grating in a 4-alternative forced-choice (4AFC) procedure.

(see Figure 3.23, Figure 3.24, Figure 3.25, and Figure 3.26) . In Experiment 2, non-rivalrous adaptation gratings consisted of oriented elements (2-D Gabor functions with polar orientation $\pm\pi/4$, period $0.448°$, $\sigma = 0.224°$, phase $\pm\pi/2$) that appeared as either red/gray or green/gray gratings with polar orientation $\pi/4$ or $3\pi/4$, respectively (see Figure 3.27 and Figure 3.28) .

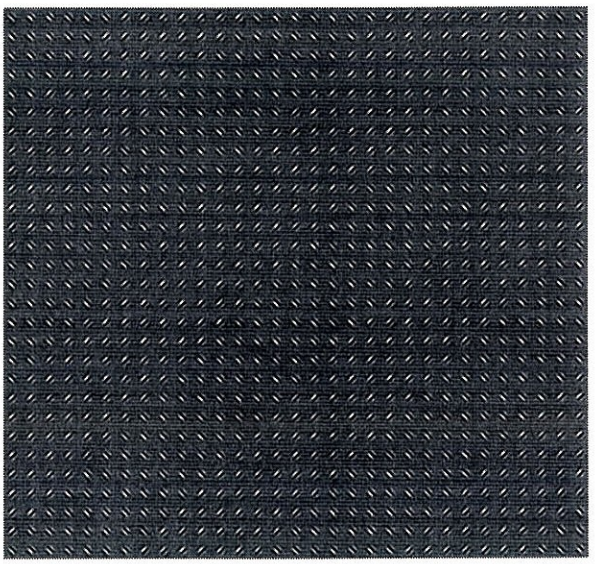

Figure 3.23: Illustration of test pattern for the McCollough effect using local Gabor elements to make up the grating pattern with polar orientation $\pi/4$ (2-D Gabor functions with polar orientation $\pm\pi/4$, period 0.448°, $\sigma = 0.224°$, phase $\pm\pi/2$). The width of the stripes measured orthogonal to their orientation is 2°. Observers briefly ($\approx 500ms$) view a rivalrous display (corresponding left and right elements have orthogonal orientation). Observers indicate the presence of a color aftereffect. Possible answers are "red" and "green".

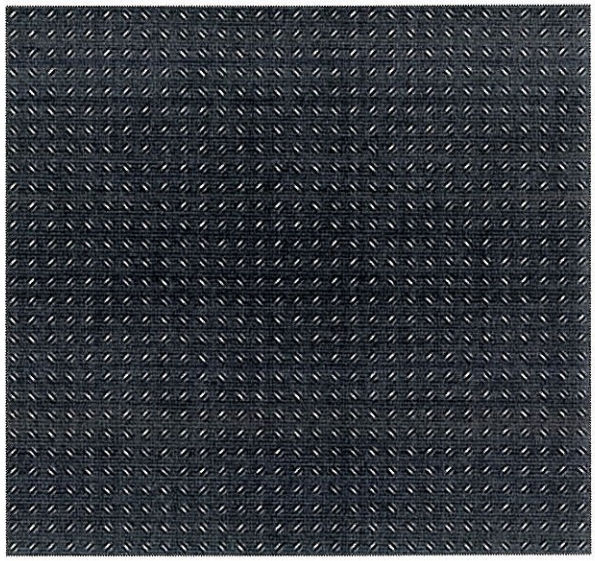

Figure 3.24: Illustration of test pattern for the McCollough effect using local Gabor elements to make up the grating pattern with polar orientation $3\pi/4$ (2-D Gabor functions with polar orientation $\pm\pi/4$, period $0.448°$, $\sigma = 0.224°$, phase $\pm\pi/2$). The width of the stripes measured orthogonal to their orientation is $2°$. Observers briefly ($\approx 500ms$) view a rivalrous display (corresponding left and right elements have orthogonal orientation). Observers indicate the presence of a color aftereffect. Possible answers are "red" and "green".

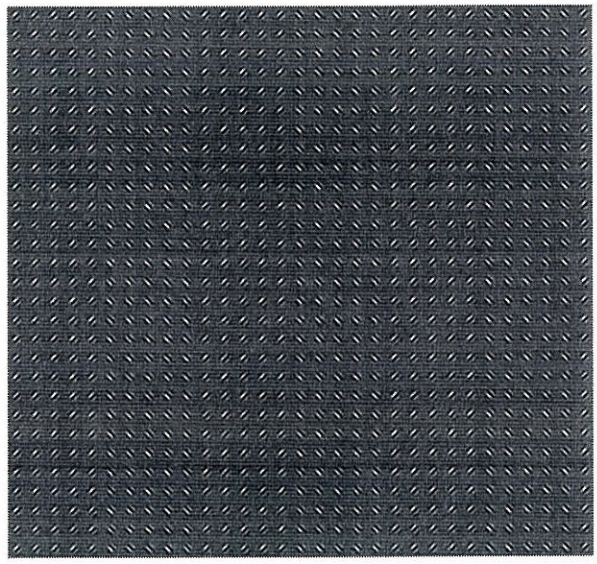

Figure 3.25: Illustration of test pattern for the McCollough effect using local Gabor elements to make up the grating pattern with polar orientation 0 (2-D Gabor functions with polar orientation $\pm\pi/4$, period $0.448°$, $\sigma = 0.224°$, phase $\pm\pi/2$). The width of the stripes measured orthogonal to their orientation is $2°$. Observers briefly ($\approx 500ms$) view a rivalrous display (corresponding left and right elements have orthogonal orientation). Observers indicate the presence of a color aftereffect. Possible answers are "red" and "green".

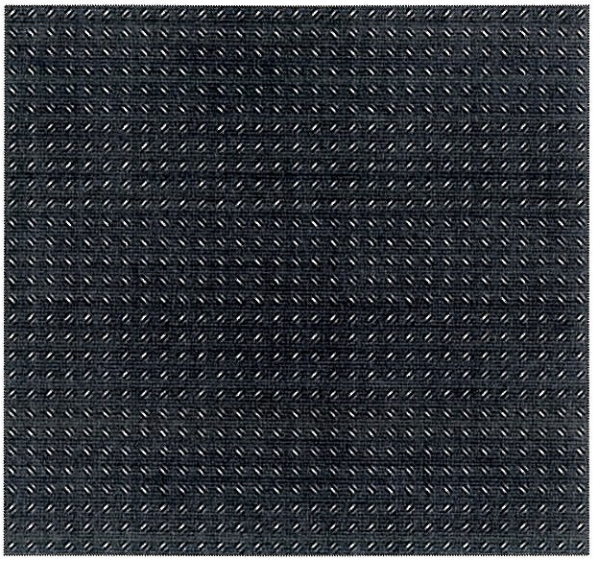

Figure 3.26: Illustration of test pattern for the McCollough effect using local Gabor elements to make up the grating pattern with polar orientation $\pi/2$ (2-D Gabor functions with polar orientation $\pm\pi/4$, period 0.448°, $\sigma = 0.224°$, phase $\pm\pi/2$). The width of the stripes measured orthogonal to their orientation is 2°. Observers briefly ($\approx 500ms$) view a rivalrous display (corresponding left and right elements have orthogonal orientation). Observers indicate the presence of a color aftereffect. Possible answers are "red" and "green".

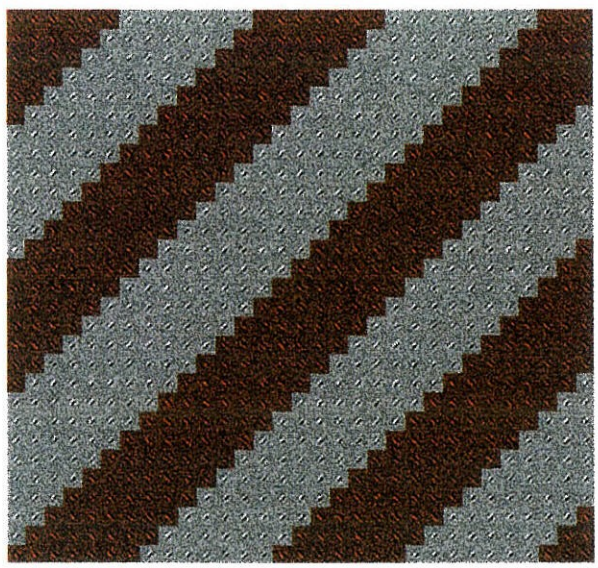

Figure 3.27: Illustration of induction stimulus for the McCollough effect using local Gabor elements to make up the grating pattern. Both eyes view identical displays subtending $10 \times 10°$ and filled with oriented elements (2-D Gabor functions with polar orientation $\pm\pi/4$, period $0.448°$, $\sigma = 0.224°$, phase $\pm\pi/2$) that constitute a red/gray grating with polar orientation $\pi/4$. The width of the stripes measured orthogonal to their orientation is $2°$. Induction time is $4min$.

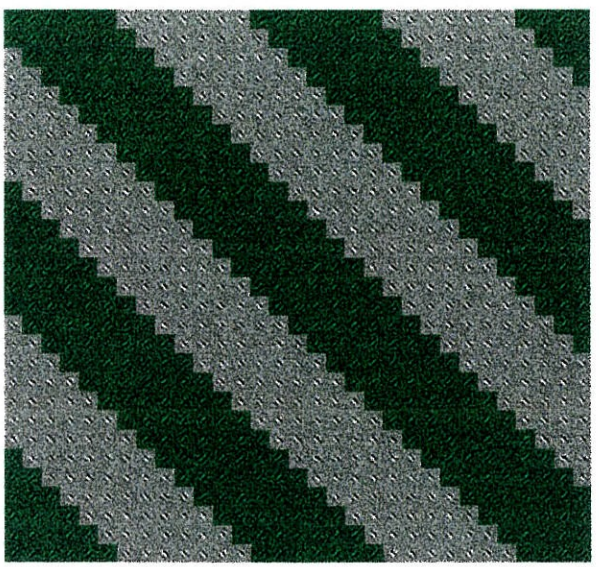

Figure 3.28: Illustration of induction stimulus for the McCollough effect using local Gabor elements to make up the grating pattern. Both eyes view identical displays subtending $10 \times 10°$ and filled with oriented elements (2-D Gabor functions with polar orientation $\pm\pi/4$, period $0.448°$, $\sigma = 0.224°$, phase $\pm\pi/2$) that constitute a green/gray grating with polar orientation $3\pi/4$. The width of the stripes measured orthogonal to their orientation is $2°$. Induction time is $4min$.

3.3.3 Results

Experiment 1

Observers are shown brief presentations ($60ms$) of a rivalrous grating and indicate its orientation in a 4- alternative forced-choice (4AFC) procedure. In addition, observers rate their confidence in their answer (scale of 1 to 10). Three different display widths were investigated (10°, 5°, and 2° of visual angle at a viewing distance of $57cm$). Both performance ($82 \pm 3\%$, $71 \pm 4\%$, and $49 \pm 4\%$ correct) and confidence (receiver-operating characteristics) varied as a function of display width (see Figure 3.29). The lack of curvature in the ROC for a grating width of 2° signifies unconscious orientation discrimination.

Experiment 2

The same stimulus parameters that induced (orientation) blindsight in normal observers in the previous experiment, were also used here. Observers viewed somewhat lengthy ($4min$) non-rivalrous presentations of the adaptation gratings (see Figure 3.27 and Figure 3.28) twice in alternating sequence. In a simpler version of the experiment, observers only adapted to the red- gray grating. Observers were then shown quasi-successive presentations of eight displays separated by a blank interval of $2s$ of mean luminance. The test sequence consisted of four rivalrous test patterns and their corresponding four non-rivalrous ones (see Figure 3.23, Figure 3.24, Figure 3.25, and Figure 3.26). The order of presentation of the test patterns was randomized. During the test sequence observers were asked to describe the perceived color of the display as either pink (red) or (pale) green. For both the simple (red color only) and the dual induction procedure (both colors), observers gave color aftereffect descriptions for the test gratings that were in overall good agreement with the orientation-specific induction colors (see Figure 3.30).

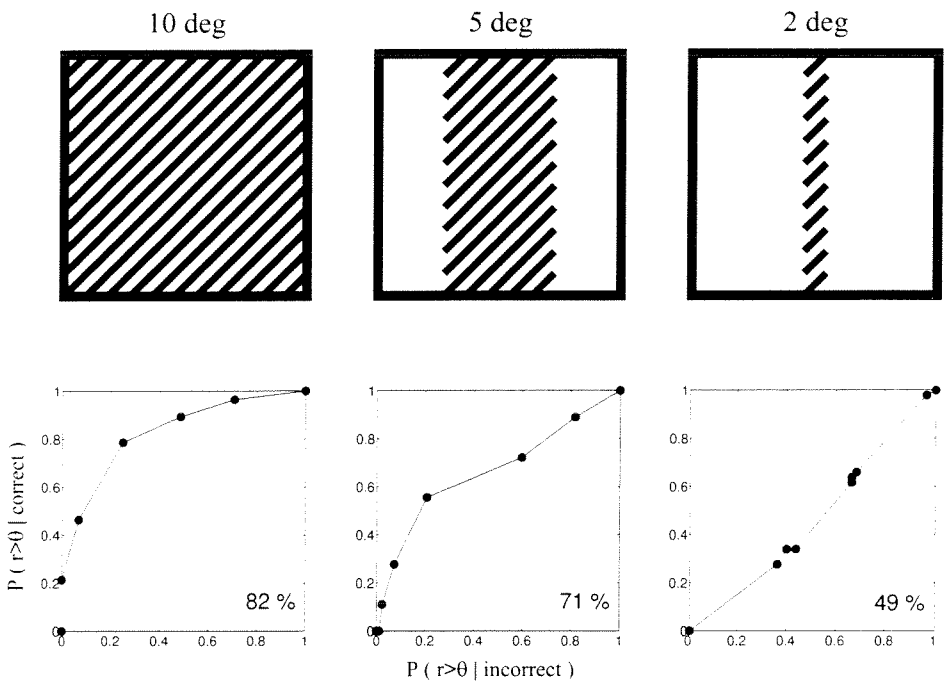

Figure 3.29: Psychophysical display (schematic) and receiver- operating characteristics (ROCs) for two subject (CK, EW; 1,800 trials; $60ms$). Three display widths were investigated: 10° (full-size display), 5° and 2° (see Figure 3.22). Binocular fusion of orthogonally oriented elements conceals display orientation from visual awareness only for a very small "aperture" (1° width) but does not prevent its discrimination. For larger apertures (5° and 10° widths) a strong correlation between performance and awareness was observed. (Here, the ROC is defined as the conditional probability of a confidence rating $r > \theta$, $\theta = 0, 1, \ldots, 10$, given that the response is correct, $P_{(r>\theta \mid correct)}$, plotted against the conditional probability of $r > \theta$ given that the response is incorrect, $P_{(r>\theta \mid incorrect)}$, where $P_{(r>\theta \mid correct)} = \sum_{r>\theta} c_r / \sum_r c_r$ and $P_{(r>\theta \mid incorrect)} = \sum_{r>\theta} i_r / \sum_r i_r$.)

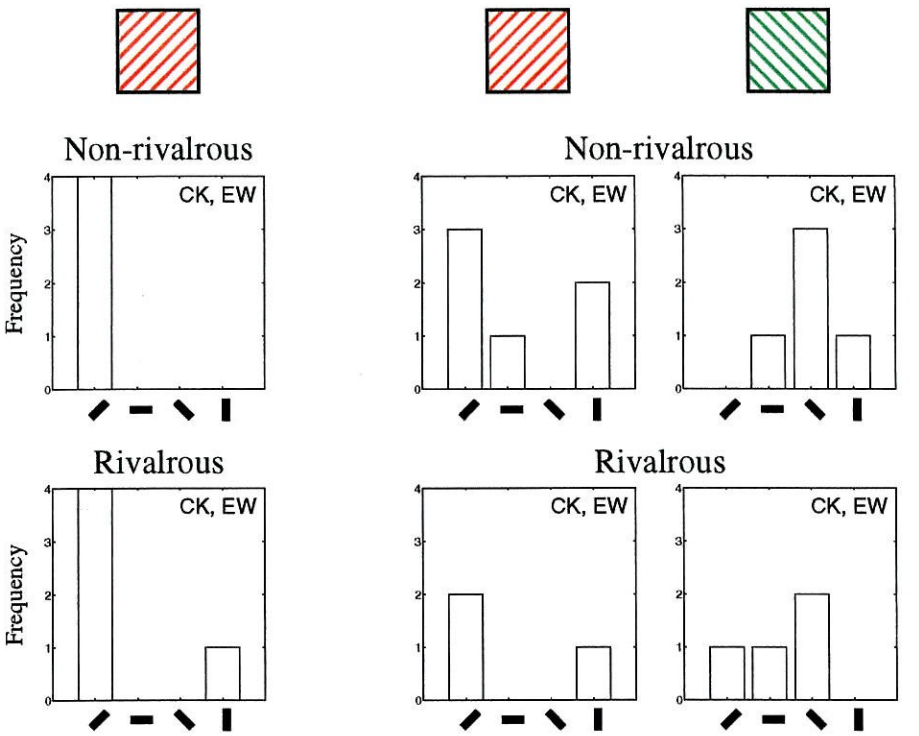

Figure 3.30: Data for two observers (CK, EW; 16 trials). In two experiments observers adapted to either the red grating (see Figure 3.27) or to the red and the green grating (see Figure 3.27 and Figure 3.28), respectively. After the induction phase, observers were shown quasi-successive presentations of eight displays separated by a blank interval of $2s$ of mean luminance. The test sequence consisted of the four rivalrous test patterns (not shown here) and the corresponding four non-rivalrous patterns (see Figure 3.23, Figure 3.24, Figure 3.25, and Figure 3.26). The order of presentation of the test patterns was randomized. Left side shows results for the first experiment using only the red grating as an inducer. Right side show results for the second experiment using both red and green gratings as inducers. The horizontal axes represent the four principal orientations of the test patterns ($\pi/4$, $\pi/2$,$3\pi/4$, and 0). Vertical axes are absolute frequency of responses "red" (only response option in first experiment) or "green". Note that observers were not forced to respond in each trial.

3.3.4 Discussion

The McCollough effect has been demonstrated in a patient (P.B.) who shows no evidence of orientation processing either in perceptual discrimination or in visuomotor control (Humphrey *et al.*, 1995). The fact that patient P.B. experiences the effect, though he is unable to make any (even behaviorally relevant) judgments pertaining to orientation discrimination, is taken to imply an early locus (presumably cells in primary visual cortex) for the mechanisms underlying the effect. Blob cells would have to interact with other cells in striate cortex that are somewhat sensitive to both orientation and wavelength. Another possible mechanisms was suggested by Michael (1978) in terms of adaptation of striate cortical neurons that code simultaneously for both orientation and color.

3.3.5 Conclusion

In our unecological displays an orientation contrast can escape visual awareness but is detected at much above-chance level for some specific stimulus conditions. Exploiting these conditions - that minimize perceptual grouping - we induce the McCollough (retinotopic, no interocular transfer) effect in normals who have no visual awareness of the display orientation but can reliably report the orientation-contingent aftereffect color. In that sense, our situation resembles a clinical case of cortical (orientation) blindness with color discrimination (Humphrey *et al.*, 1995).

Chapter 4 Visual discrimination without visual awareness

4.1 Unconscious visual shape discrimination and top-down influences in blindsight

4.1.1 Background

We have recently (see Chapter 3) reported a dramatic dissociation between visual localization performance and visual awareness of the target location in "conflicting" displays (Kolb & Braun, 1995). In this chapter we demonstrate complex visual pattern discrimination in the absence of visual awareness (Kolb *et al.*, 1996). Under certain stimulus conditions ("artificial blindsight") and in forced-choice situations, normal observers are able to reliably report the location of a figure-ground target without being consciously aware of it. Naturally, two questions arise. First, does rivalrous (unecological) presentation bar only "simple" visual entities/events (*e.g.*, the occurrence of one square in one of four corners on the screen) from being consciously perceived, or does the paradigm extend to "complex" visual forms (perceptual grouping)? Second, is artificial blindsight confined to forced-choice situations where the response possibilities are limited in space and time? Ultimately, both questions address the nature of the neural processing underlying non-pathological blindsight.

There is a thin line between complex pattern matching (symbolic reasoning) and the cognitive interpretation of that pattern (semantic reasoning), where interpretation usually concerns distinctions between familiar/unfamiliar and/or meaning-

ful/meaningless. Familiar or meaningful patterns are also said to possess "semantic value". Performance in perceptual matching tasks (speed of visual discrimination) is greatly influenced by the semantic value of the patterns in question (Mozer, 1991). For example, upon short presentation the visual patterns "impediment" and "pertinence" are more easily distinguishable than, say, "tinmepmeid" and "epcenretni" - if those were embedded in patterns alike. It is precisely due to that grouping of letters into words that we find *reading* a comparably effortless perceptual task (even in the face of occasional cognitive frustration). Note that this example is *not* supposed to reflect the debate between *early* and *late* selection theorists of visual attention. Early-selection models typically propose that selection is based on low-level stimulus features and occurs before stimulus identification (Broadbent, 1958; Treisman, 1969). In contrast, late-selection theories hold that selection occurs late in the process and is based on high-level features such as stimulus identity (Norman, 1968; Posner, 1978; Shiffrin & Schneider, 1977). In an orthogonal fashion, as the early- *vs* late-selection dichotomy has failed to account for the abundance of attentional data, a clear distinction between symbolic and semantic processing has yet to elucidate the numerous examples of cognitive influences on early perception. Hence we are curious to learn whether the low-level phenomenon of artificial blindsight (Braun & Kolb, 1996) is subject to top-down influences such as semantic processing.

If no such higher-level capacities were to be documented during blindsight, *e.g.*, when normal observers tried to distinguish between the patterns "impediment" and "pertinence" based on their semantic content alone, we would be tempted to relegate unconscious perceptual grouping to sub-cognitive mechanisms, such as "strictly" symbolic template matching. If that it is indeed the case, the next step is to investigate the spatio-temporal characteristics of the matching process, *i.e.*, how does it depend on the complexity or number of the possible matches?

4.1.2 Materials and methods

Two 40×40 arrays of Gabor elements (orientation $\pm\pi/4$, period $0.25°$, $\sigma = 0.125°$, phase $\pm\pi/2$) are presented dichoptically. Fore- and background elements have orthogonal orientation. With the exception of Experiment 1, foreground elements are arranged to form four alphabetic letter shapes (size 8×8 elements each) along the horizontal midline. The left and right eye view orthogonal elements at every array location. In Experiment 1 only one target letter could appear in one out of eight possible locations on an octahedral grid (see Figure 4.1, A and B). When left and right eye views are superimposed, the array subjectively appears uniform with no indication of the letter shapes whatsoever (presentation times of $\approx 150ms$ are too short for one eye to dominate the other).

4.1.3 Results

Experiment 1

After brief presentation ($150ms$), the observer identifies the target letter in a 4-alternative forced-choice procedure (4AFC) and subsequently rates his confidence on a scale of 1 to 10 (see Figure 4.1). Possible answers in the 4AFC task are "T", "L", "F", and "H". Discrimination performance is far above chance ($(44 \pm 1\%)$, whereas the receiver-operating characteristic is essentially straight, showing failed awareness of the target (see Figure 4.1, D). Note that the extent of spatial variability is not to be reported in this task.

Experiment 2

Observers discriminate a sequence of four identical letters (4AFC) and rate their confidence (scale of 1 to 10) (see Figure 4.2). Receiver-operating characteristics for three observers were obtained over a range of four different luminance contrast conditions

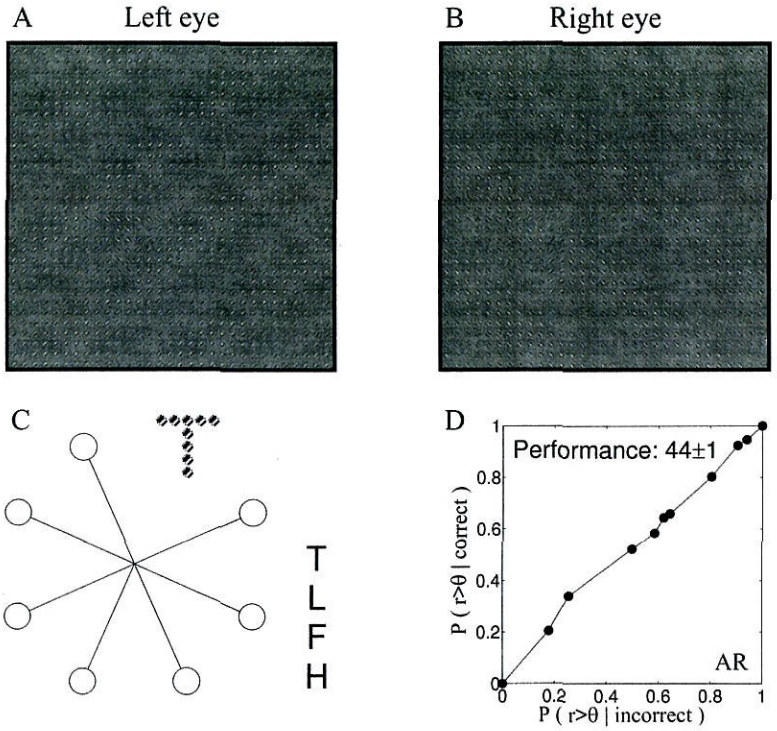

Figure 4.1: Illustration of stimulus used to investigate unconscious recognition of a single letter that randomly occurred at one of eight possible locations and receiver-operating characteristic (ROC) for one subject (AR; 300 trials; $150ms$). Both eyes view a 40×40 array of oriented elements (2-D Gabor functions with polar orientation $\pm\pi/4$, period $0.248°$, $\sigma = 0.124°$, phase $\pm\pi/2$). Elements that form a particular letter are oriented orthogonally with respect to the background (size 8×8 Gabor elements) at one out of eight positions in the display (C). When presented dichoptically (A) and (B) will form a rivalrous display (corresponding left and right elements have orthogonal orientation) with one concealed target letter, *e.g.*, the letter "T" (see Figure 3.8). After brief presentation ($150ms$), the observer identifies the target letter in a 4-alternative forced-choice procedure (4AFC). (C) Possible answers are "T", "L", "F", and "H". The target randomly occurs at one of eight locations (circles). (D) ROC for rivalrous trials. The ROC is essentially straight, showing failed awareness of the target. (Here, the ROC is defined as the conditional probability of a confidence rating $r > \theta$, $\theta = 0, 1, \ldots, 10$, given that the response is correct, $P_{(r>\theta \mid correct)}$, plotted against the conditional probability of $r > \theta$ given that the response is incorrect, $P_{(r>\theta \mid incorrect)}$, where $P_{(r>\theta \mid correct)} = \sum_{r>\theta} c_r / \sum_r c_r$ and $P_{(r>\theta \mid incorrect)} = \sum_{r>\theta} i_r / \sum_r i_r$.)

(100%, 50%, 20%, and 10%, as indicated by top row of schematic stimulus conditions) (see Figure 4.3). ROCs for non-rivalrous (upper row of graphs) and rivalrous (lower row of graphs) trials (individual observers as identified by labeling). The ROC of rivalrous trials is essentially straight, showing failed awareness of the target, while the ROC of non-rivalrous trials is highly curved, showing normal awareness of the target even at near- chance performance levels. Chance is 25%. Note that not all possible conditions were investigated. Non- rivalrous displays of full (100%) luminance contrast yielded virtually perfect results, whereas performance virtually diminished for rivalrous displays of luminance contrasts equal or lower than 20%.

Experiment 3

The experimental protocol was identical to the one in Experiment 2, but in Experiment 3 each trial was preceded by a normally visible primer letter (50% incorrect, 50% correct) (see Figure 4.4, A and B). Incorrect and correct primers are randomly interleaved in a block of 100 trials. A correct prime significantly increases performance, whereas and incorrect prime reduces it essentially to chance (see Figure 4.5).

Experiment 4

Observers discriminate a sequence of four letters forming a word (4AFC) and rate their confidence (scale of 1 to 10). When presented dichoptically (A) and (B) in Figure 4.6 will form a rivalrous display (corresponding left and right elements have orthogonal orientation) with four concealed target letters, *e.g.*, the word "math". Words in each block of possible responses are matched in the sense that both, first and last letters are identical, respectively (*e.g.*, "love", "lake", "lime", and "late"). Data are shown for three observers for stimulus presentation times of $1s$, $2s$, $3s$, and $5s$ (see Figure 4.7). It is most important to note that word discrimination based on semantic information alone was practically impossible (see Figure 4.8).

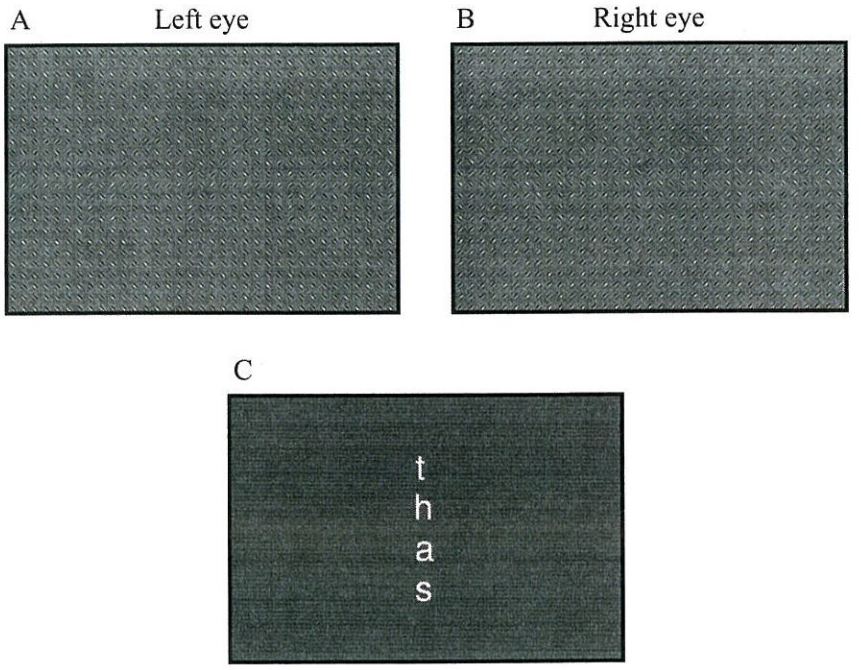

Figure 4.2: Illustration of stimulus used to investigate unconscious recognition of a four-letter chain (all letters are the same). Both eyes view a 40×40 array of oriented elements (2-D Gabor functions with polar orientation $\pm\pi/4$, period $0.248°$, $\sigma = 0.124°$, phase $\pm\pi/2$). Elements that form a particular letter are oriented orthogonally with respect to the background (size 8×8 Gabor elements) at four display positions along the horizontal midline. When presented dichoptically (A) and (B) will form a rivalrous display (corresponding left and right elements have orthogonal orientation) with four concealed target letters, *e.g.*, the chain "AAAA" (see Figure 3.8). After brief presentation ($\approx 150ms$), observers identify the letter comprising the chain in a 4-alternative forced-choice procedure (4AFC). (C) Note that the four alternatives are given in lower-case (text font) letters.

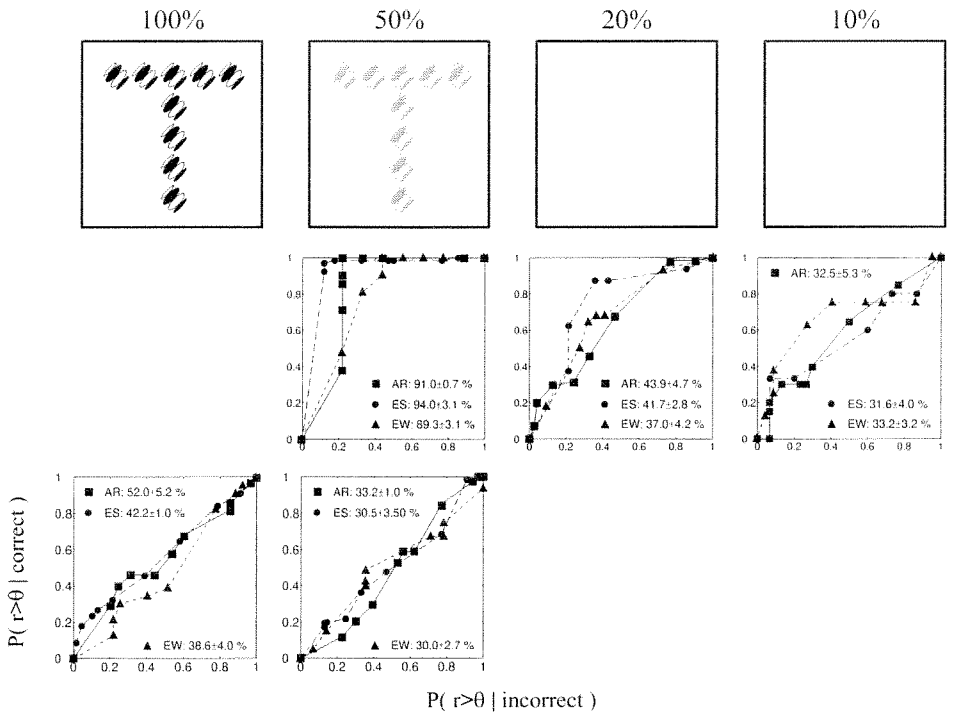

Figure 4.3: Receiver-operating characteristics for three observers (AR, ES, EW; 4,500 trials; $150ms$) obtained over a range of four different luminance contrast conditions (100%, 50%, 20%, and 10%, as indicated by top row of schematic stimulus conditions). ROCs for non-rivalrous (upper row of graphs) and rivalrous (lower row of graphs) trials (individual observers as identified by labeling). The ROC of rivalrous trials is essentially straight, showing failed awareness of the target, while the ROC of non-rivalrous trials is highly curved, showing normal awareness of the target even at near-chance performance levels. Chance is 25%. Note that not all possible conditions were investigated. Virtually perfect results were obtained in non-rivalrous displays of full (100%) luminance contrast, whereas performance virtually diminished for rivalrous displays of luminance contrasts equal or lower than 20%. (Here, the ROC is defined as the conditional probability of a confidence rating $r > \theta$, $\theta = 0, 1, \ldots, 10$, given that the response is correct, $P_{(r>\theta \mid correct)}$, plotted against the conditional probability of $r > \theta$ given that the response is incorrect, $P_{(r>\theta \mid incorrect)}$, where $P_{(r>\theta \mid correct)} = \sum_{r>\theta} c_r / \sum_r c_r$ and $P_{(r>\theta \mid incorrect)} = \sum_{r>\theta} i_r / \sum_r i_r$.)

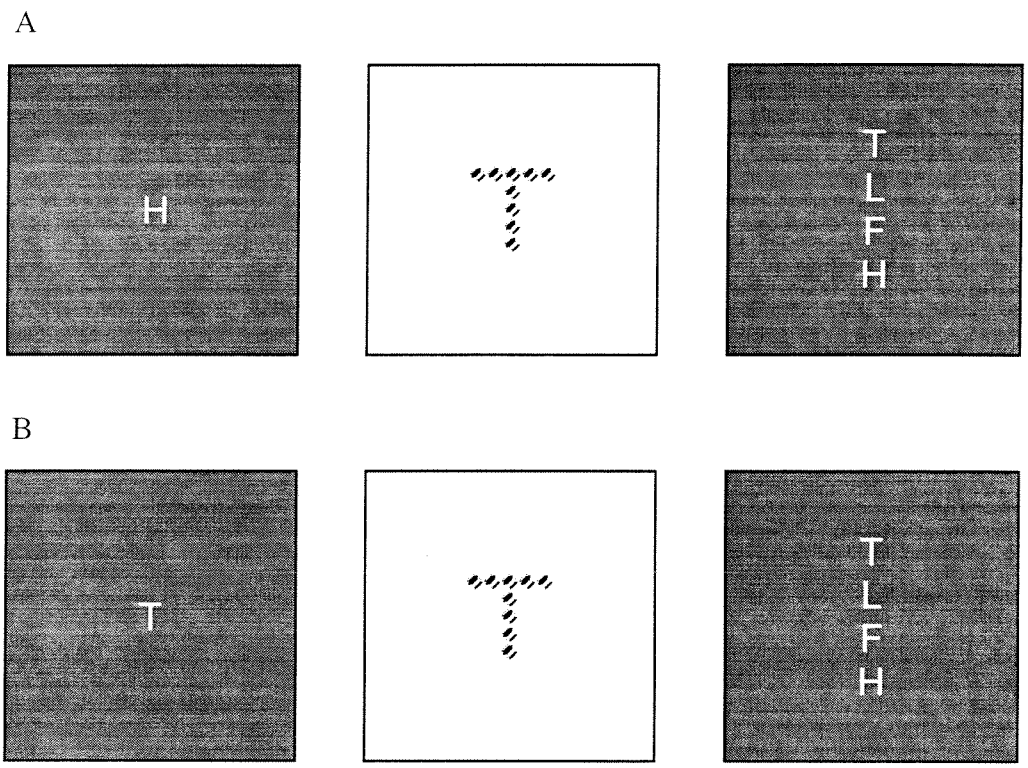

Figure 4.4: Psychophysical displays (schematic) illustrating incorrect (A) and correct (B) priming. Stimulus and procedure are similar to Figure 4.2; in addition, the stimulus display is preceded by a letter display in upper-case text font ("primer"). The primer has a $50-50$ chance of matching the letter comprising the following stimulus chain. Incorrect and correct primers are randomly interleaved in a block of 100 trials.

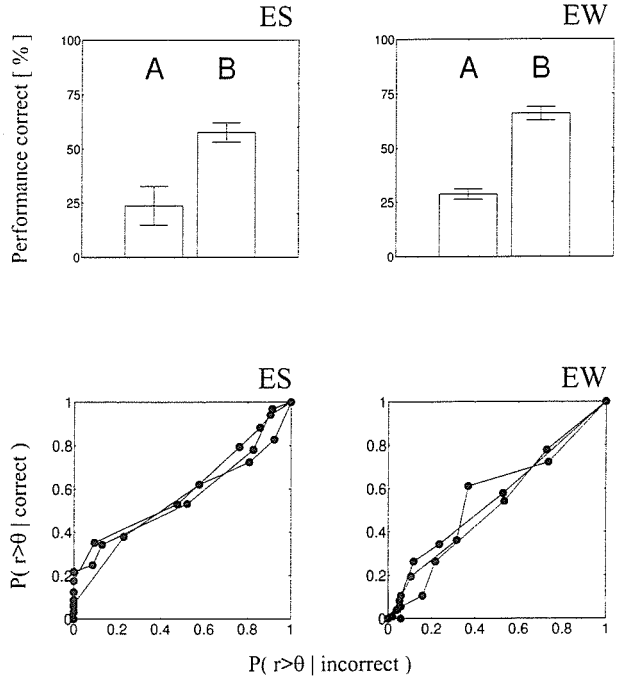

Figure 4.5: Data and receiver-operating characteristics (ROCs) for two observers (ES, EW; 1,000 trials). The left histogram bars in the upper-row graphs represent performance when the letter chain if incorrectly primed (see Figure 4.4, A). The right histogram bars in the upper-row graphs represent performance when the letter chain if correctly primed (Figure 4.4, B). Lower-row graphs contain ROCs for conditions where the target is correctly primed (individual observers). When the letter chain is incorrectly primed, discrimination is virtually at chance (25%). Furthermore, when the letter chain is preceded by the matching letter (correct priming), the blindsight performance (straight ROCs) is significantly higher than in the absence of priming (see Figure 4.3). (Here, the ROC is defined as the conditional probability of a confidence rating $r > \theta$, $\theta = 0, 1, \ldots, 10$, given that the response is correct, $P_{(r>\theta \mid \mathit{correct})}$, plotted against the conditional probability of $r > \theta$ given that the response is incorrect, $P_{(r>\theta \mid \mathit{incorrect})}$, where $P_{(r>\theta \mid \mathit{correct})} = \sum_{r>\theta} c_r / \sum_r c_r$ and $P_{(r>\theta \mid \mathit{incorrect})} = \sum_{r>\theta} i_r / \sum_r i_r$.)

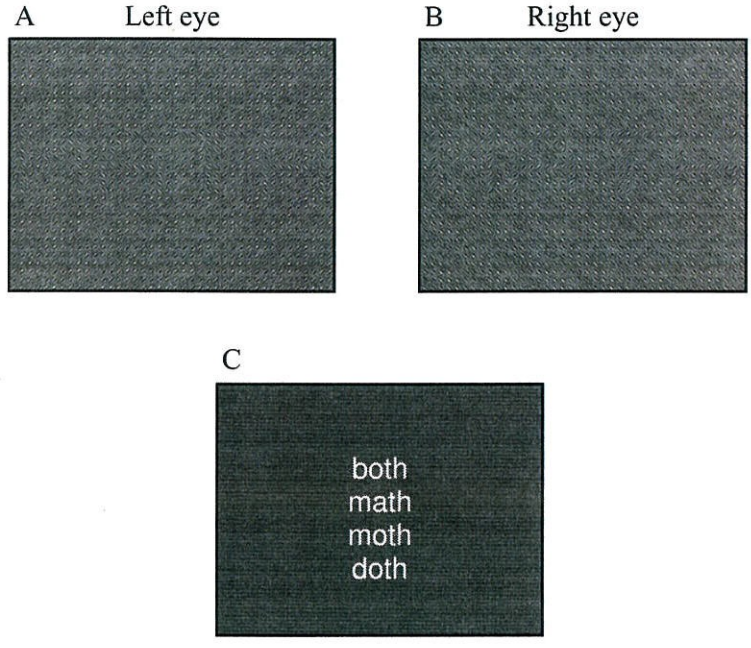

Figure 4.6: Illustration of stimulus used to investigate unconscious recognition of four-letter words. Both eyes view a 30×40 array of oriented elements (2-D Gabor functions with polar orientation $\pm\pi/4$, period $0.248°$, $\sigma = 0.124°$, phase $\pm\pi/2$). Elements that form a particular letter are oriented orthogonally with respect to the background (size 8×8 Gabor elements) at four display positions along the horizontal midline. When presented dichoptically (A) and (B) will form a rivalrous display (corresponding left and right elements have orthogonal orientation) with four concealed target letters, *e.g.*, the word "math" (see Figure 3.8). After a brief presentation, ranging from $1s$ to $5s$, observers identify the word in a 4-alternative forced-choice (4AFC) procedure. (C) Note that the four alternatives are given in lower-case (text font) letters.

babe	dart	fist	gaze	home	love	mile	stir	wire
bore	debt	flat	glue	hale	lake	mine	scar	wise
blue	dust	feat	gate	hose	lime	mace	sour	wave
bite	daft	foot	glee	hide	late	mute	slur	wale

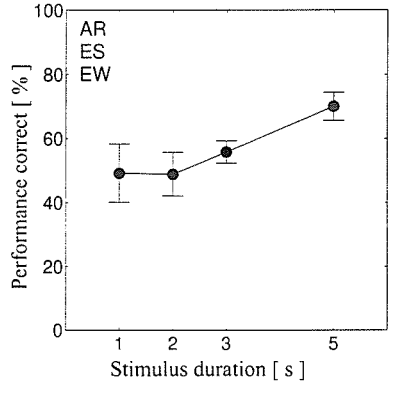

Figure 4.7: Examples of possible matched word answers in the 4- alternative forced-choice (4AFC). Words in each block of possible responses are matched in the sense that both, first and last letters are identical, respectively (*e.g.*, "love", "lake", "lime", and "late"). Data are shown for three observers (AR, ES, EW; 4,800 trials) for stimulus presentation times of $1s$, $2s$, $3s$, and $5s$.

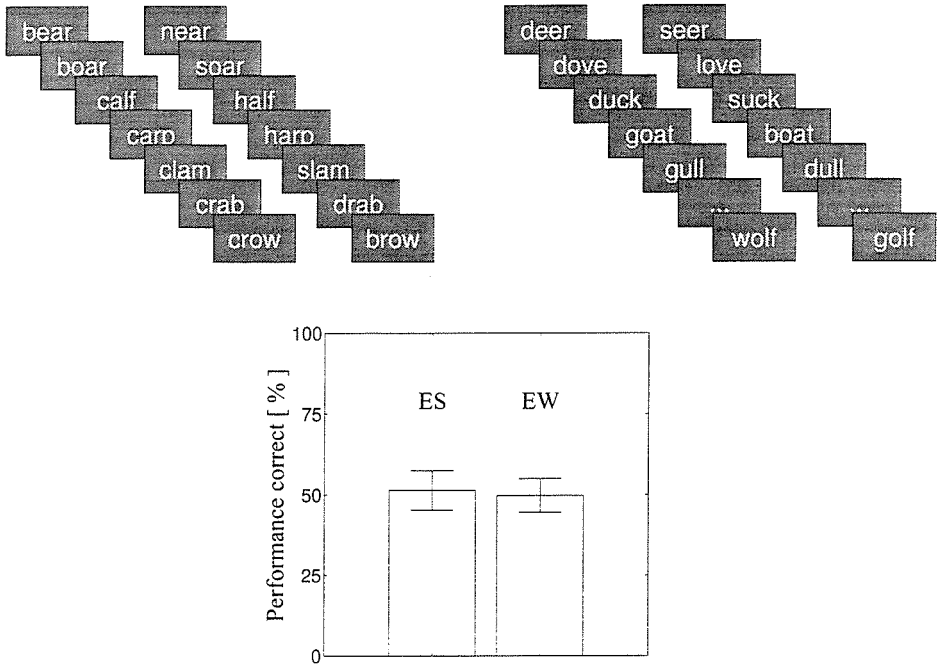

Figure 4.8: Psychophysical display (schematic) and data for two observers (ES, EW; 1,000 trials). Both eyes view two quasi-successive displays (separated by $200ms$ interval of mean luminance) of 30×40 array of oriented elements (2-D Gabor functions with polar orientation $\pm\pi/4$, period $0.248°$, $\sigma = 0.124°$, phase $\pm\pi/2$). Elements that form a particular letter are oriented orthogonally with respect to the background (size 8×8 Gabor elements) at four display positions. When presented dichoptically (A) and (B) will form a rivalrous display (corresponding left and right elements have orthogonal orientation) with four concealed target letters, *e.g.*, the word "DUCK". One of the two displays contains an animal word (*e.g.* duck); the other contains a matched non-animal word (*e.g.* suck). All four-letter animal and non-animal words have the consonant in the same place. Observers identify the animal word in a 2- alternative forced-choice procedure (2AFC). Discrimination of animals from non-animal words is virtually at chance (50%).

Experiment 5

Observers are visually or auditorily (not shown here) presented with a target word, view a sequence of ten "conflicting" displays and *voluntarily* identify the one that conceals the target word (see Figure 4.9). Spontaneous identification of a subjectively non-apparent word was significantly above chance.

4.1.4 Discussion

Normal observers discriminate a letter sequence in forced and non-forced situation and rate their confidence (scale of 1 to 10). In both cases, discrimination is performed well above chance without visual awareness (no correlation between confidence and performance). The fact that artificial blindsight is not limited to forced-choice situations allows us to safely attribute the lack of sensory awareness to the level of (voluntary) perception rather than (involuntary) response. The outcome of Experiment 5 harvests a lot of sympathy for the "conjunction" theory of attention and awareness (James, 1890), where sensory information is thought to be steered towards conscious perception if it enters short-term memory for a sufficient amount of time to be voluntarily reported. While visually guided attention is thought to operate from the bottom up, we maintain that visually induced behavior without awareness is directed from the top down (template matching) without significant semantic influences.

In addition, we observed a curious relationship between the spatial complexity of the feature grouping and the temporal extent of blindsight (*i.e.*, the time it took before binocular rivalry revealed the true nature of the dichoptic stimulus). It appears, the more complex the pattern the longer it is barred from visual awareness, suggesting that the proposed template matching is also modulated by low-level processes that govern binocular rivalry (as if those areas had "a mind of their own").

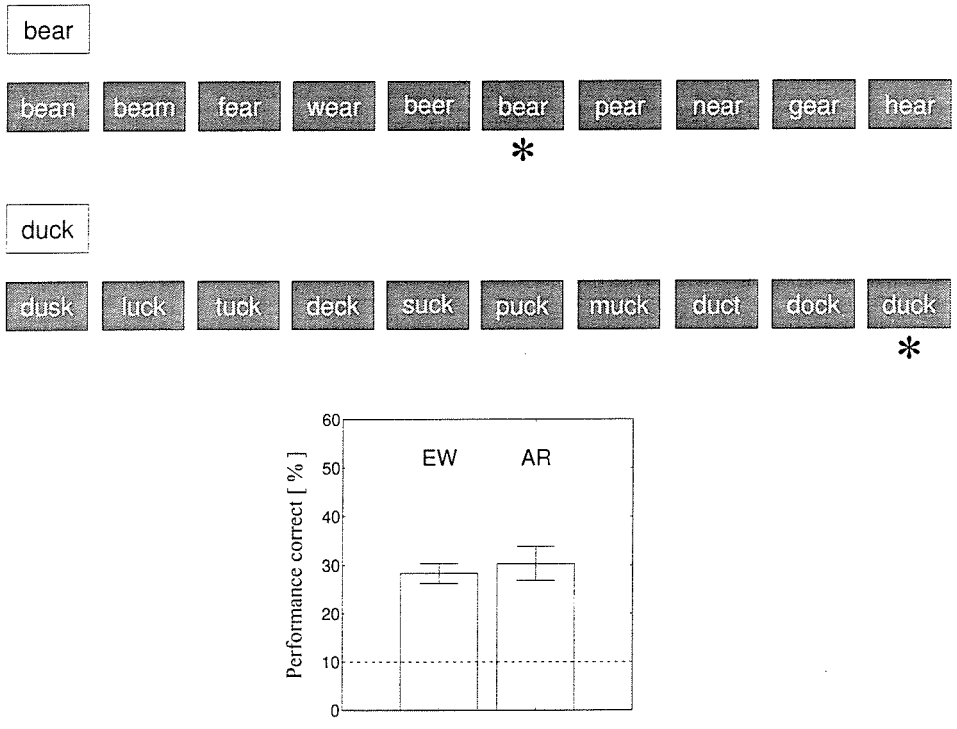

Figure 4.9: Psychophysical display (schematic) and data for two observers (EW, AR; 1,000 trials). An animal word appears on the screen in lower-case text font (*e.g.* bear) for $2s$ and is followed by a series of ten quasi-successive displays (displays of $200ms$ are separated by $2s$ intervals of mean luminance) that are shown to both eyes and each contains a 30×40 array of oriented elements (2-D Gabor functions with polar orientation $\pm\pi/4$, period $0.248°$, $\sigma = 0.124°$, phase $\pm\pi/2$). Elements that form a particular letter are oriented orthogonally with respect to the background (size 8×8 Gabor elements) at four display positions. All displays are rivalrous (corresponding left and right elements have orthogonal orientation) with four concealed target letters, *e.g.*, the word "BEAR". Only one of the ten displays contains the animal word in question; the other nine displays contain matched non-animal words (*e.g.*, bean, beam, fear, wear etc.). All four-letter animal and non-animal words have the consonant in the same place. Observers voluntarily indicate the occurrence of the animal word in the series of remaining non-animal words. Note that observers are not forced to respond in each trial. The graph contains data for observers EW and AR. The broken line indicates chance level (at 10%).

4.1.5 Conclusion

Blindsight in normal observers extends to a range of complex patterns including letters and words. Visual patterns forming words can not be discriminated based on semantic information alone. Unconscious shape discrimination appears to work top-down in the style of simple template matching but is influenced by (hard-wired) low-level processes that govern binocular rivalry. Rivalrous trials preceded by a phenomenally visible valid primer letter give rise to a significant improvement in task performance, whereas trials preceded by a phenomenally visible invalid primer are performed at chance level. Priming is thought to create expectations that are stored in short-term memory to elevate neural activity in perceptual circuits, corresponding to shape or identity of objects. The fact that performance diminishes to chance level is consistent with the view that blindsight represents a pattern matching process in short term memory. Blindsight in normal observers is not limited to forced-choice situations.

In conclusion, we have demonstrated an ability in normal observers to discriminate simple and complex patterns without visual awareness of the pattern shape. This poses a general problem for perceptual grouping in the absence of awareness. The very lack of visual awareness was determined both by (subjective) introspection and an objective method that correlates task performance and observer confidence. Although strong priming effects allude to a top-down pattern-matching mechanism in artificial blindsight - together with the finding that blindsight can occur in non-forced choice situations - failed semantic discernability of rivalrous displays speaks against high-level (cognitive) processing.

Chapter 5 Utrocular perception

5.1 Eye-of-origin unmasked

5.1.1 Background

Humans naturally exploit eye-of-origin information in stereopsis, but may not ordinarily be aware of the eye to which a visual stimulus is presented. Since eye-of-origin is present only in early visual cortical areas, utrocular ("which eye") identification would imply that information in these areas can be intentionally accessed. We report that most observers can distinguish eye-of-origin when presented with a class of dichoptic (unmatched binocular) stimuli expected to excite distinct monocular populations whilst producing little binocular activation. Observers were unsuccessful in utrocular identification with other dichoptic stimuli, a difference that may be attributed to greater binocular activation with the latter class of stimuli. These results imply that humans can exploit information available only in the initial stages of cortical processing. The presence of long feedback connections from higher cortical areas to V1 and V2 suggests a mechanism for biasing the responses of chains of neurons to permit utrocular identification despite the absence of explicit ocularity at the top of the chain.

At higher cortical processing stages concerned with shape description and spatial relations of objects, most local image features are incidental, and therefore are no longer represented explicitly. Nevertheless, the fact that one can discriminate minute details of a visual scene implies access to computations early on in visual cortex (Westheimer, 1981). How can humans use both information in local, primitive

measurements as well as highly abstract representations depending on their current needs? The notion of distributed visual representation implies mappings that permit reference to certain aspects of the data at the expense of others (Marr, 1982). The representation of eye-of-origin is distributed across primary visual cortex (V1) in neurons which are excitable exclusively or dominantly through one eye (Hubel & Wiesel, 1968; Hitchcock & Hickey, 1980; Horton & Hedley-White, 1984). In contrast, most neurons beyond V2 receive approximately equal excitation through both eyes (Zeki, 1978; Burkhalter & Van Essen; Maunsell & VanEssen, 1983). To study the ability of humans to utilize information present only in early visual cortex, we tested human performance in utrocular (which eye) identification with dichoptically viewed textured patterns (Kolb & Braun, 1995). In our paradigm two types of targets are used. They are distinctive with respect to the degree of perceived coherence, and in their effect on cortical neurons in primary and extrastriate cortex. We tested the ability of observers to identify targets which differed from distractors in motion (moving *vs* flickering, moving *vs* stationary), in direction of motion, or in (isoluminant) color. Observers were successful at utrocular identification under all circumstances except when the distractor involved flicker.

5.1.2 Materials and methods

Observers dichoptically viewed low density texture patterns composed of randomly positioned limited- lifetime dots. This arrangement obviates a number of potential problems, by assuming that (i) equal luminance energy was presented to the two eyes, (ii) stimuli did not have definite edges, thus preventing fixation disparity from being a discrimination cue, and, (iii) the low density and brief presentation time of stimuli precluded binocular rivalry. In the first experiment, observers viewed a target consisting of either coherent unbalanced or locally balanced motion (Qian *et al.*, 1994a). The dichoptic distractor ("foil") was either a flickering noise pattern (FN)

or a stationary noise pattern (SN) (see Figure 5.1). Observers were required to report the eye-of-origin of the target stimulus in a two-alternative forced choice task.

5.1.3 Results

Experiment 1

Figure 5.2 shows the results for four observers (two naive). The results, averaged across observers, are shown in Figure 5.2, A and the logarithm of the significance level in a one-tailed χ^2 test is shown in Figure 5.2, C for all observers (and Figure 5.4). Data for each individual observer are shown in Figure 5.3. In the two conditions with flickering noise as a foil, utrocular identification was poor. No observer performed above chance when the target motion was locally balanced. With unbalanced motion as target, one observer performed significantly above chance, and one observer gave responses that were significantly anticorrelated with correct target identification. This signified utrocular discrimination but not identification. In contrast, with stationary noise as foil, three of four observers were significantly above chance for both locally balanced and coherent unbalanced motion targets. Also note that their significance levels were drastically different than with flicker noise as foil (Figure 5.2, C). There was, however, little overall difference between performance in conditions with coherent unbalanced motion as target and conditions with locally balanced motion as target. The observer exhibiting anticorrelation in the coherent unbalanced case performed at high levels in conditions with stationary noise patterns as foil. One observer did not perform above chance in any of the four conditions. From these results we conclude that: first, observers can identify the eye of origin of dynamic random-dot textures; second, the putative suppression of area MT has little or no effect on utrocular identification; and third, flicker noise with the same spatiotemporal frequency characteristics as the target stimulus abolishes utrocular performance.

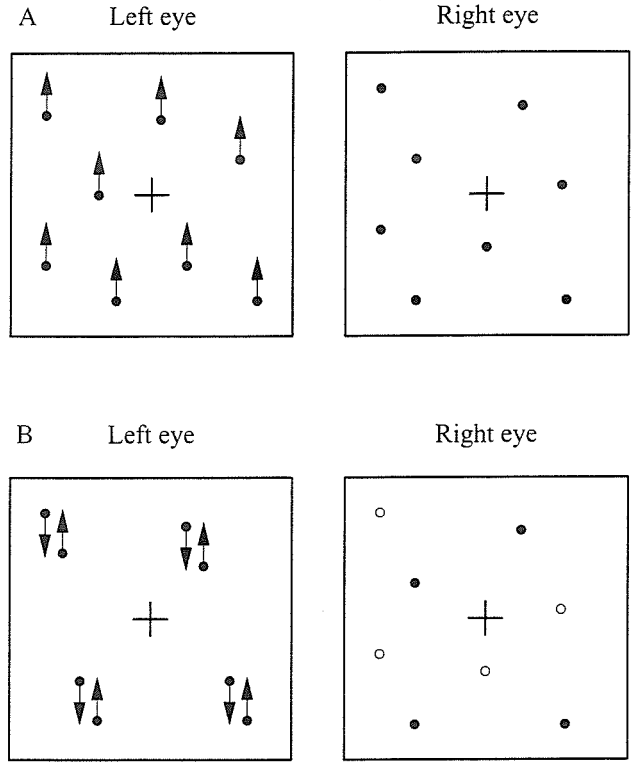

Figure 5.1: Each panel illustrates iconically one of the four types of stimuli used in this experiment. (A) Left eye. Limited lifetime unidirectional dots (CM) are born at random locations, move in a direction shared by all dots, and are replotted to a new random location after a fixed number of frames. Right eye. Static dots (SF) have random locations and last for the duration of the display. (B) Left eye. Limited lifetime, locally balanced motion (LBM) stimulus with a common axis of motion. Dots are born in pairs at a fixed separation, move past each other on an axis shared by all dot pairs, and are replotted at a new random location after a fixed number of frames. Right eye. Limited lifetime flickering dots (FF) are born at random locations, and remain visible for a fixed number of frames before being replotted to a new random location. CM appears to be a coherent translating sheet, while LBM elicits no such percept. CM excites neurons in both V1 and the middle temporal area (MT) of macaques, while LBM excites the former and largely suppresses the latter. Stimuli were presented dichoptically via liquid crystal shutter glasses on an SGI Indigo 2 (1024×1024 pixels) with 30 frames per *sec* for each eye. Observers viewed displays subtending $20 \times 10°$ at a viewing distance of $57cm$. Mean dot density and lifetime were equal in all cases. Dot density was $10\,\mathrm{deg}^{-2}$, dot direction was horizontal or vertical, dot velocity was $2°/s$, and dot life-time was $50ms$.

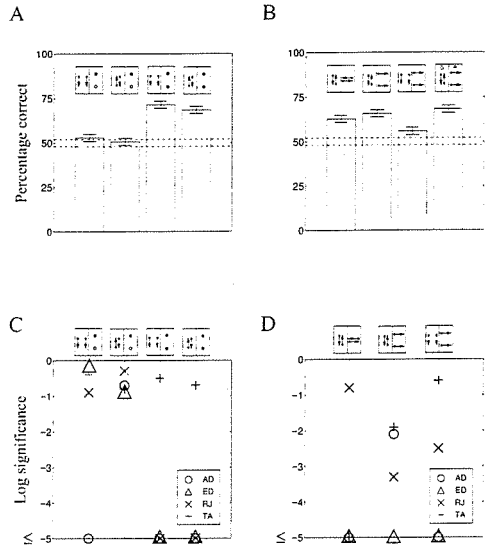

Figure 5.2: The top row shows results averaged across observers and the errorbars illustrate 95% confidence intervals. The dashed lines show 95% confidence intervals based on random guessing in 500 trials (the minimum performed by all observers in each condition). The bottom row shows the logarithm (base 10) of the significance level in a one-tailed χ^2 test of significance of deviation above chance for the individual observers in each condition. (A) and (C) Results for experiments in which the target was either vertical LBM or CM (up or down in different trials), and the foil either FF or SF for four observers (two naive). Column 1. CM *vs* FF. One of four observers was above chance, and a second observer (ED - indicated at zero) was significantly above chance ($\chi^2, df = 1, p < 0.001$) but with anticorrelated responses. This observer was performing discrimination but not identification. Column 2. LBM *vs* FF. No observer was above chance. Utrocular identification was difficult or impossible with flickering distractors. Column 3. CM *vs* SF. Three of four observers were significantly above chance. Column 4. LBM *vs* SF. Three of four observers were significantly above chance. Observers were not consistently better at utrocular identification with the MT-suppressing stimulus than with the MT-exciting stimulus. (B) and (D) The results for four observers (five in the fourth column) for experimental conditions in which the target and foil were orthogonal motion stimuli. Each observer performed at least 500 trials per condition. From left to right the conditions are: LBM horizontal *vs* LBM vertical, LBM horizontal *vs* CM vertical, CM horizontal *vs* CM vertical, red vertical CM *vs* green horizontal LBM with the red/green balance randomly perturbed around isoluminance on each trial. The target was always the horizontally-moving stimulus. In the first three columns three of four observers were significantly above chance and in the isoluminant color motion condition four of five observers were significantly above chance ($\chi^2, df = 1, p < 0.01$). The fourth column is not shown in (D) because different observers participated.

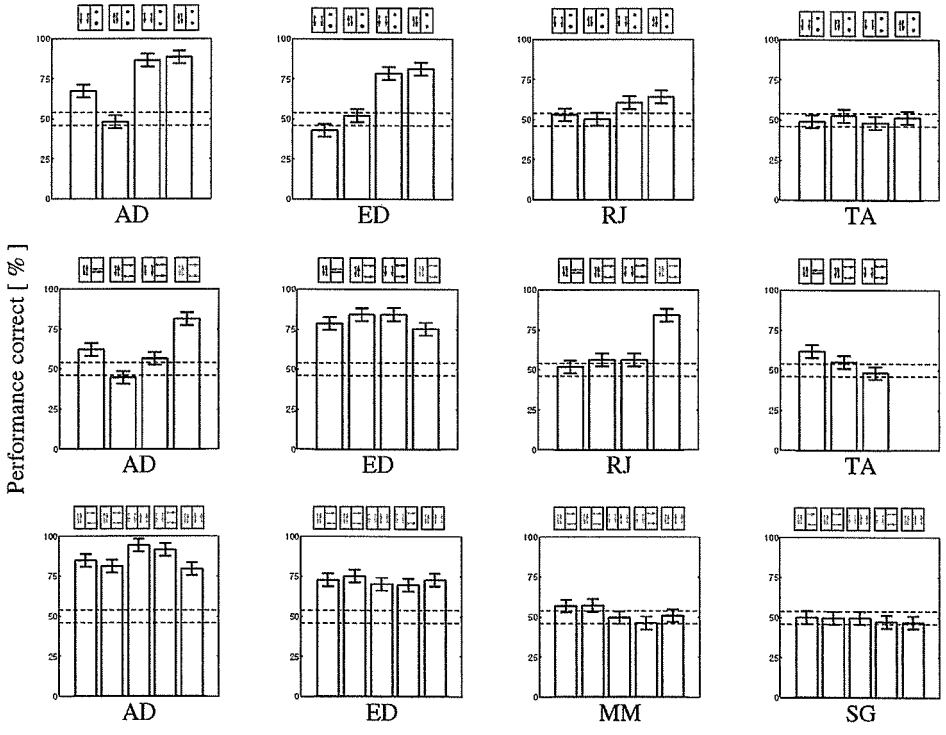

Figure 5.3: Utrocular identification data for six observers (AD, ED, RJ, TA, MM, SG; 25,500 trials). Stimulus conditions are indicated by pictograms on top of graphs. Errorbars illustrate standard deviation (individual). The dashed lines show 95% confidence intervals based on random guessing in 500 trials (the minimum performed by all observers in each condition).

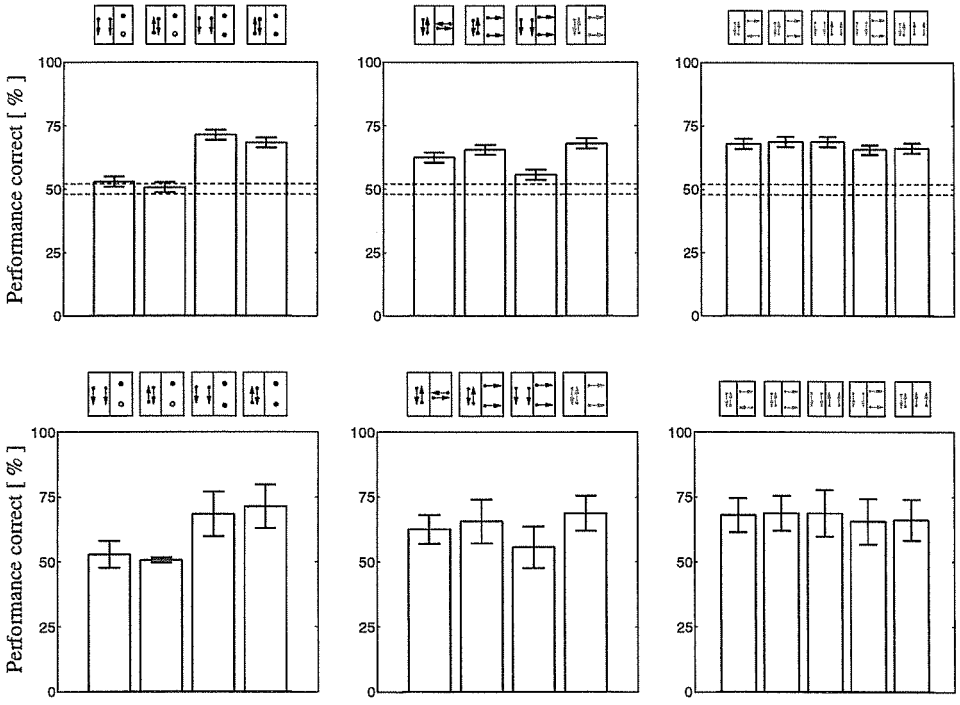

Figure 5.4: Utrocular identification data for six observers (AD, ED, RJ, TA, MM, SG; 25,500 trials). Histogram bars represent averaged data across all relevant observers (see Figure 5.3). Stimulus conditions are indicated by pictograms on top of graphs. Top-row graphs contain results averaged across observers and the errorbars illustrate 95% confidence intervals based on random guessing in 500 trials (the minimum performed by all observers in each condition). Bottom-row graphs contain results averaged across observers and the errorbars illustrate standard deviation between observers.

Perceptually, the stationary dots were clearly visible while the flickering dots had low visibility. Two phenomena may be relevant to the difference in visibility of static and flickering foils: binocular suppression and binocular activation. It is well known that motion is dominant over stasis in binocular rivalry (Fox, 1991). This is inconsistent with the greater visibility of stationary distractors in our experiments. On the other hand, it is possible that dichoptic motion and flicker patterns with common spatiotemporal frequency characteristics cause substantial activation of binocular neurons in V1.

Experiment 2

To address the issue of monocular *vs* binocular activity, we performed a second set of experiments designed to equally activate distinct groups of monocular neurons in area V1 while minimizing activation of binocular neurons. Observers dichoptically viewed stimuli with orthogonal directions of motion in the two eyes. In different conditions, the stimuli were coherent unbalanced or locally balanced moving textures in either eye, a combination of the two, or coherent unbalanced or locally balanced dynamic textures with isoluminant green dots in one eye ("target") and red dots in the other ("foil"). Figure 5.2, B and D show the results of the experiment. Three of four observers performed significantly above chance in all conditions. In the condition illustrated in the second column, one observer gave responses anticorrelated to the target ($\chi^2, df = 1, p < 0.01$), thus performing utrocular discrimination but not identification.

Two observers had a somewhat higher percentage correct when targets were locally balanced, and two of four observers showed the opposite trend. Therefore, despite the average difference shown in Figure 5.2, B, we conclude that the even split among observers implies there is no consistent difference between conditions in which area MT is active or putatively suppressed. We conclude that the degree of activation of area MT is not a significant factor in utrocular identification. Sketches of the

conjectured activity in V1 for the conditions involving flickering, and distractors of orthogonal orientation are shown in Figure 5.6, B. Sketches of the conjectured activity levels in both area V1 and MT for all conditions are depicted in Figure 5.5.

Experiment 3

In a third series of experiments, observers dichoptically viewed isoluminant green and red textures (Cavanagh & Anstis, 1991). The results of one experimental condition is shown in Figure 5.2, B. Performance was well above chance studied for four of five observers in this condition, and for at least three of five observers in all the conditions examined. It is known that the cytochrome oxidase blobs in V1 of Old World primates contain many monocular, color-opponent neurons (Livingstone & Hubel, 1984). These cells, and possibly their targets in area V2, may provide a basis for utrocular identification in the isoluminant color experiments.

In most of the experiments observers reported being only moderately confident of their ability to perform the task. It is tempting to assume that observers performing at 75-95% correct were indeed *aware* of stimulus eye-of-origin, but the variability among observers counsels strong caution (Kolb & Braun, 1995). How observers achieve utrocular identification poses a problem. A mechanism for enhancing the difference between activities in monocular populations in area V1 is illustrated in Figure 5.6, C. A bias signal (broken line) originating in higher visual cortical areas, and terminating on specific sets of neurons in V1 could produce a differential response magnitude when the horizontal target is in one eye rather than the other. Observers could then base a judgment upon that difference in amplitude at a later cortical stage without explicit awareness of eye-of- origin (Crick & Koch, 1995).

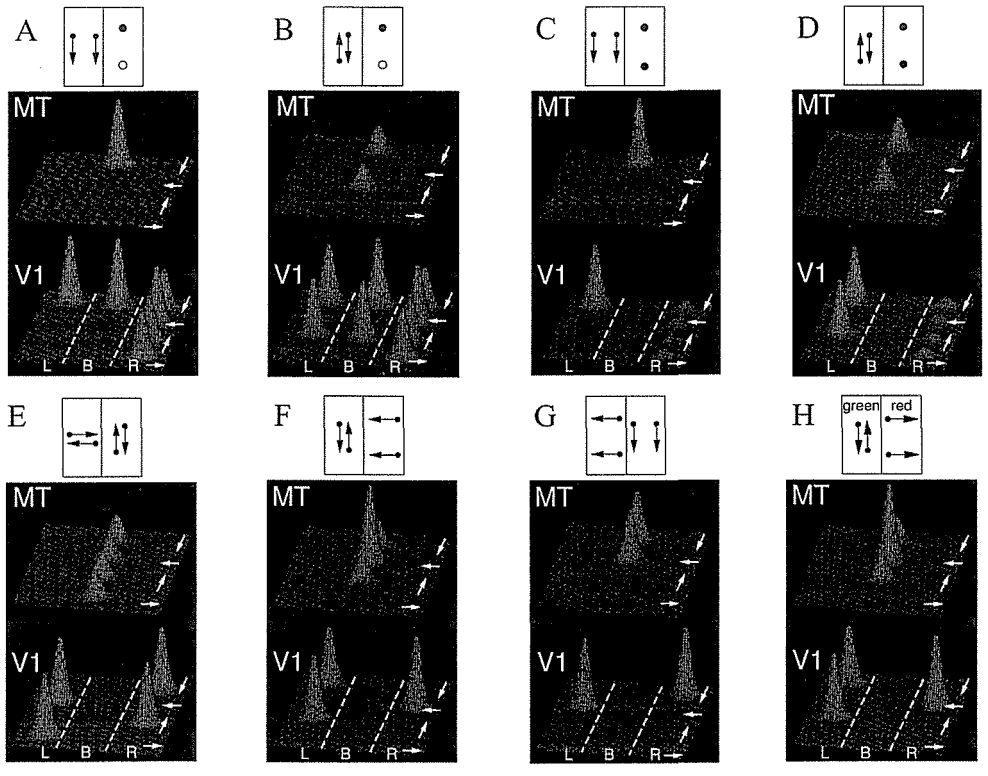

Figure 5.5: A schematic account of the pattern of results of the present experiments. Sketches of the conjectured activity in cortical visual areas V1 and MT for conditions involving stationary, flickering, and distractors of orthogonal orientation (locally and globally balanced). The various conditions are iconically depicted on top of activation plots. (A) and (B) When the flickering noise pattern is the distractor (foil) there is significant activation of binocular units in V1, making utrocular extraction difficult. (C) and (D) The stationary noise distractor causes little or no binocular activation. Similarly, in (E-H) there is little binocular activation with orthogonal directions of motion in the two eyes. Note there is no consistent difference in the data between conditions in which area MT is active or putatively suppressed (see Figure 5.2). Evidently, the degree of activation of area MT is not a significant factor in utrocular identification.

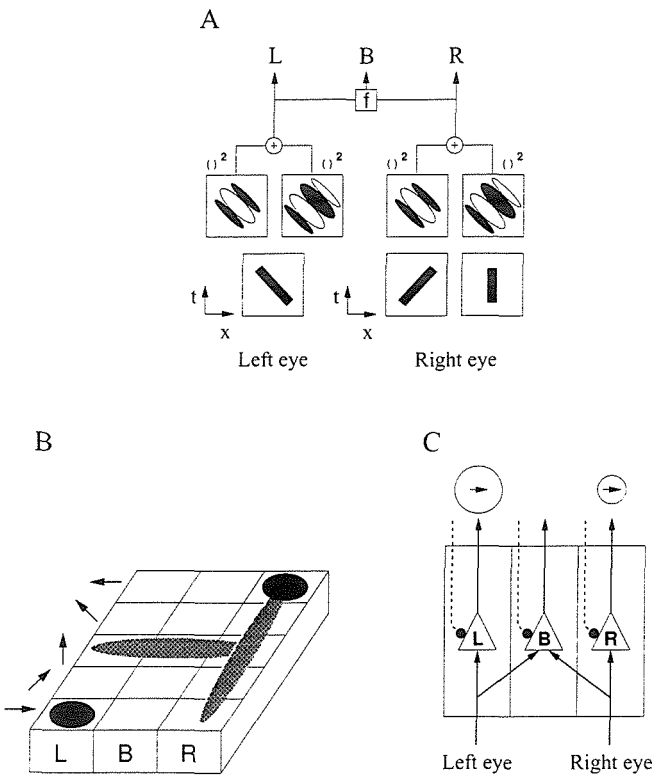

Figure 5.6: (A) Illustration of monocular and binocular motion energy detectors and limited lifetime moving and flickering stimuli. We assume that there is an expansive (supralinear) nonlinearity in the binocular combination. Note that a flickering dot is more effective than a dot moving opposite to the preferred direction. Consequently, following suitable normalization, dichoptic combination of vertical motion in the left eye with flicker in the right eye, would be expected to produce a diffuse pattern of activation in V1 as shown in (B). In contrast, dichoptic presentation of orthogonal dot motion, or opposite motion as shown here for graphical purposes is expected to lead to distinctly less binocular activation, and more circumscribed and distinctive monocular activation in V1. (C) A schematic illustration of our hypothesis to explain above-chance performance in utrocular identification. Feedback connections are used to provide a differential bias signal onto left eye *vs* right eye neurons. For example if the target is vertical and the foil horizontal, positive bias applied to left eye vertical neurons or negative bias applied to left eye horizontal neurons or both, leads to enhanced response when vertical is in the left eye compared to when it is in the right. Reversing these biases for right eye neurons further increases the difference in response magnitudes. Consequently, eye-of-origin can be determined from the relative responses of horizontal and vertical populations that do not in themselves conserve eye-of-origin.

5.1.4 Discussion

The fact that observers showed differential performance across conditions implied that there was no general artifact of the display that could be exploited. Ono and Barbeito (1985) found that previous reports of eye-of-origin discrimination could be attributed to either fixation disparity, or a "feeling in the eye" associated with a difference in stimulus energy in the two eyes. These cues were shown to provide a means of performing utrocular discrimination but not identification. In the present experiments, the use of large, low density random fields with amorphous borders made small fixation disparities uninformative. Because equally energetic stimuli were presented to both eyes in our experiments, observers did not experience the asymmetric "feeling in the eye". We emphasize that if these cues could be exploited in one condition they should be exploited in all. Moreover, absence of feedback about performance prevented observers from learning to bridge the gap between discrimination and identification.

5.1.5 Conclusion

Eye-of-origin plays different roles in animals with eyes arranged for panoramic versus full binocular vision. For the former, eye-of-origin is an integral aspect of visual direction, while for the latter, primarily carnivores and primates, eye-of-origin is likely to play multiple roles in stereopsis. These include disparity sign for binocular excitatory neurons, and representation of occluding flanks in da Vinci stereopsis (Nakayama & Shimojo, 1990). In all cases, however, utrocular information is an essential part of the input but not the output of binocular surface representation. We suggest that the fact that humans are not vividly aware of eye-of-origin is because it is not the output of natural computation. We conclude that utrocular identification is possible under conditions where monocular neurons are differentially activated with respect

to binocular neurons in early visual cortex.

Chapter 6 Perception of dichoptic motion coherency

6.1 Dichoptic integration of motion signals

6.1.1 Background

In the last decade or so, the question of how "first-stage" motion signals may be implemented in a second stage of processing has received an overwhelming amount of attention (Fennema & Thompson, 1979; Marr & Ullman, 1981; Horn & Schunck, 1981; Adelson & Movshon, 1982; Albright, 1984; Hildreth, 1984; Nagel & Enkelmann, 1986; Sereno, 1987; Yuille & Grzywacz, 1988; Sereno, 1989; Bülthoff *et al.*, 1989; Wang *et al.*, 1989). In a now classic series of experiments, Adelson and Movshon (1982) employed masking and adaptation techniques to determine whether the mechanisms responsible for extracting 2-D motion information represent a distinct and possibly later processing stage than the mechanisms subserving 1-D pattern detection, (Movshon *et al.*, 1985). In their experiment stimulus conditions were such that separate detection and coherence thresholds were obtained for overlapping moving gratings of different spatial frequency (1.5 and 2.0 cycles /°, at an angle of 120°, with a fixed contrast of 30% for the low frequency grating). Detection and coherence thresholds were similar when angle, spatial frequency, and contrast were the same. Detection and coherence thresholds were determined by increasing the contrast of the second (higher frequency) grating from 0% and measuring the probability that the observer (i) detected the grating or (ii) judged that the two gratings moved coherently, *i.e.*, were perceived as belonging to a single rigidly moving plaid pattern. Adelson and

Movshon (1982) defined threshold as the contrast of the weaker grating that produced a 50% probability of eliciting either a detection or a coherence judgment. Under these conditions, coherence thresholds were always higher than detection, implying a range of stimulus contrasts for which gratings were visible but did not cohere. They then performed a masking experiment using 1-D dynamic noise (randomly moving patterns of stripes having the same orientation but different widths) to determine that motion coherence indeed depends on the outputs of oriented analyzers, in other words, coherence thresholds increase when the noisy grating is oriented parallel (within 20°) to the individual grating components but not at other orientations (including orientation perpendicular to the pattern direction).

To determine whether there were indeed two distinct stages of motion processing, Adelson and Movshon (1982) using adaptation techniques showed in a second set of experiments that the first stage could be identified by orientation-dependent effects), whereas the second stage could be revealed by coherence- dependent effects. Based on various orientation-specific adaptation effects (Sekuler & Ganz, 1963; Sharpe & Tolhurst, 1973), they argued that adaptation to component motion should affect detection thresholds, whereas adaptation to pattern motion should effect coherence thresholds. There were two different stimuli in this experiment, both moving rightward with constant speed: a single vertical grating and a 120° plaid (component gratings were oriented plus and minus 60° from the vertical). There were four different test-adapt combinations, each stimulus type being used as the adaptation stimulus then tested with both stimulus types. For each test-adapt combination, contrast thresholds for the test stimulus were measured in both the adapted and unadapted direction (*i.e.*, left and right directions of motion). A large elevation of detection thresholds for the test plaid was observed as a result of adaptation to a similar pattern, indicating that the 1-D motion of the oriented components rather than the 2-D motion of the plaid caused the observed adaptation effects on detection thresholds. In contrast, when a

rightward-moving grating was used as the adaptation pattern and the test pattern was a rightward- moving or leftward-moving plaid (a condition which produced no changes in the detectability of the plaid) there was a large elevation of the coherence threshold for the plaid moving in the adapted direction.

If MT neurons are indeed the neural substrate of motion coherency, as a multitude of studies have suggested, one might expect their directional tuning curves to reflect the dominant percept, that is - responses to movement in the component directions being greatest when only non-coherent component motion is perceived and responses to movement being in the pattern direction being greatest when only pattern motion is perceived. Physiologically, MT neurons are distinguished by a high degree of selectivity for aspects of motion, including direction and speed, with little selectivity for color or form (Albright, 1984; Baker *et al.*, 1981; Felleman & Kaas, 1984; Maunsell & Van Essen, 1983; Rodman & Albright, 1987; Zeki, 1974). Using similar stimuli as Adelson and Movshon (1982), Albright (1992) found neural correlates of perceptual motion signal integration in area MT of the rhesus monkey. When presented with perceptually coherent plaid patterns, the investigated MT cells responded more strongly when the pattern moved in the preferred direction ("pattern response") than when either of the components moved in the same direction ("component response"). This type of directional tuning appears to be characteristic of pattern neurons (Movshon *et al.*, 1985; Rodman & Albright, 1989) and reflects integration of the motion signals deriving from the two gratings. Albright (1992) also found that when presented the perceptually non-coherent plaid, pattern responses in MT cells dropped substantially, while component responses increased drastically, in other words, the cells became increasingly component-like when the stimulus was configured to render non-coherent component motion as the dominant percept.

In addition to the single-cell physiology, lesion studies confirm the role of area MT in computing 2-D velocities of moving stimuli. Lesions in area MT produced by

ibotenic acid injections produce deficits in discriminating directions of motion and executing pursuit eye movements (Newsome & Pare, 1986; Newsome *et al.*, 1985). MT lesions are known to also cause deficits in discriminating the 3-D shape of moving dot patterns (Siegel & Andersen, 1986; Andersen & Siegel, 1988). Note that pursuit eye movements and the computation of structure from motion cues depend on the extraction of fairly accurate 2-D velocity information. Several other studies provide evidence for two stages of motion analysis (Ferrera & Wilson, 1987; Welch, 1989; Wiesenfelder & Blake, 1990). For example, Welch (1989) found that speed discrimination for plaids was determined by the speed of the component gratings. Also speed discrimination for the nodes of a plaid pattern (*i.e.*, the intersection of component gratings), represented as a grid of thick dots, was different than speed discrimination for the plaid itself, indicating that the visual system does not track the nodes of a plaid to determine its constituent pattern motion. However, this finding may also be attributed to the fact that lower contrast gratings appear to move slower than higher contrast gratings when viewed side by side (Thompson, 1982). In a similar vein, other studies suggest that the perceived direction of plaid motion may be shifted by manipulating the perceived speed of the plaid's grating through adaptation (Derrington & Suero, 1991).

Taken together, the experiments by Adelson and Movshon (1982) and the physiological studies by Albright (1984) and others, imply the existence of two separate stages of motion processing: one stage responsible for the analysis of 2-D component motion and the other responsible for the analysis of 2-D pattern motion. However, the process of motion integration - the focus of this chapter - may depend on both the velocity estimates of discrete features such as "terminators" as well as component motion at contours. The perceived direction of a contour viewed through an aperture, for example, is influenced by the aperture's shape (Wallach, 1976), and the status of the terminators at the aperture's edge as intrinsic or extrinsic to the contour (Shi-

mojo *et al.*, 1989). Other studies have stressed the influence of terminators on figural rigidity (Nakayama & Silverman, 1988) and motion integration across contours seen through apertures (Schiffrar & Lorenceau, 1991).

Within the geniculostriate subsystem of the nonhuman primate brain, visual motion detection is first accomplished by single neurons in sriate cortex. Cells at this stage have small receptive fields and strong orientation tuning (Hubel & Wiesel, 1968). Hence V1 neurons can provide information only about the local 1-D motion of image features. The activity of any individual neuron is thus ambiguous with regard to the true motion of a 2-D pattern (Movshon *et al.*, 1985). In principle, multiple 1-D ("component") motion measurements made along different axes can disambiguate the motion of 2-D pattern in the retinal image. This disambiguation is achieved by a process where the 2-D pattern motion is determined to be the single direction and speed compatible with the motions of all 1-D components that make up the pattern (Fennema & Thompson, 1979; Adelson & Movshon, 1982; Albright, 1984). Since physiological evidence suggests that something similar to this "intersection of constraint-lines" solution is implemented within the primate visual system *via* integration of first-stage measurements, we briefly discuss earlier outlines of this approach to modeling the processes underlying motion integration.

Researchers in computer vision have frequently used multiple-motion constraints in velocity space to obtain pattern velocity (Adelson & Movshon, 1982; Albright, 1984; Fennema & Thompson, 1979; Marr & Ullman, 1981). Prominently, Marr and Ullman (1981) noted that a local estimate of velocity at a single line segment can specify the true velocity only within a range of 180°; multiple local estimates of velocity are needed to narrow down the range of possible velocities. Fennema and Thompson (1979) and Adelson and Movshon (1982) have coined the term "constraint-lines" that define a family of possible object motions for each component motion vector, intersecting in velocity space to determine the motion of a translating object.

Their models have primarily addressed rigid planar-translational motion. Fennema and Thompson (1979) assumed that the image consists of distinct regions of uniform motion for which they determined the translational velocities using a modified Hough-transform algorithm. Approaching the issue from a different angle, Adelson and Movshon (1982) assumed that a 2-D pattern motion analyzer could determine the true translational motion of an image patch if its receptive field included 1- D motion analyzers whose velocity preferences lay along a circle in velocity space. Furthermore, they reasoned that if a system of such analyzers is to signal one direction of motion, the second-stage (pattern) motion analyzer should combine the outputs of the 1-D motion analyzer with an operation similar to a logical AND gate.

Exactly these assumptions about motion-based segmentation (besides others not mentioned here) belie the dauntingly complex problem of motion integration. Although MT neurons that are selective for translational motion are often "shown" portions of smoothly varying velocity fields, they cannot "assume" that velocity is given as locally uniform. Rather, they simply take whatever input they are represented with - for example, velocity distributions that are smoothly varying or bimodal - and generate an output. In the case of a smoothly varying velocity field, individual neurons may analyze a portion of this vector field and integrate this information to yield an estimate of velocity. But the overall integration of image velocities will be coded in a distributed manner by a set of neurons with different velocity preferences that may "see" the same patch of space. The problem here is to formulate exactly how the final velocity estimate is related to the real velocity field.

Apparently, there are two conflicting demands that must be met in computing the optical flow field. First, signals from neighboring regions of the visual field need to be spatially integrated; and second, sensitivity to small velocity differences across space should be preserved for segmentation of regions corresponding to different objects (Braddick, 1993). Without a doubt, segmentation is an essential process in the

analysis of visual information. Early visual representations, for example in striate cortex, encode properties of the light distribution in each image location as an undifferentiated array of signals. However, at some point in the visual hierarchy, this kind of *local* representation must be converted into one that can explicitly represent *global* aspects of the image, such as the fact that some visual features belong to a common object or lie on one surface, while other features, which might enjoy equal spatial proximity in the image, ought to be processed independently because they belong to distinct objects.

Image segmentation can be based on differences in many visual properties, including brightness, color, texture, and disparity, but differences in motion ("motion contrast") are particularly operative. It has often been suggested that a functional two-way relationship must hold between motion processing and image segmentation, based on the observation that the processes that resolve the ambiguity of local motion measurements (*e.g.*, by minimizing variation) are only effective within the region representing a coherent object (Adelson & Movshon, 1982; Braddick, 1993). If two nearby points belong to separate surfaces, their motions may actually be quite different from each other. Any interactions that integrate and smooth local motion signals would therefore work best if they could be prevented from propagating across the surface boundaries, and such boundaries are defined in part by motion discontinuities (Braddick, 1993). Indeed the functional requirements for interactions between local motion detectors would hence appear as contradictory. To achieve the best estimation of the velocity field, the visual system needs smoothing or integrative interactions that would *nolens volens* reduce the difference between local motion signals across an edge or surface boundary.

We would therefore expect smoothing effects to impair perceptual sensitivity to local motion differences. Indeed psychophysical experiments yield clear evidence for both segmentation and smoothing effects. Extensive work with random-dot kine-

matograms has revealed the fine precision of motion-defined shape processing (Julesz, 1971; Anstis, 1970; Braddick, 1974; Regan & Hong, 1990; Regan, 1986). Additional evidence shows that a motion-defined grating can be detected when each strip is four minutes of arc wide, indicating that motion contrast can be registered between visual locations at very few minutes of arc apart (Nakayama *et al.*, 1985). The notion of a segmentation process underlying this differencing ability is further supported by a perceptual phenomenon known as "induced motion", where a surround moving in one direction induces a perception of the opposite motion in a neighboring region (Duncker, 1929; Loomis & Nakayama, 1973; Tynan & Sekuler, 1975).

The opposite perceptual effect, known as "motion capture" occurs if an outline shape is moved over a screen displaying dynamic visual noise (flicker). Subsequently, the noisy dots within the outline are captured by its motion and appear to move coherently along with it (MacKay, 1961). Also the motion of a low-frequency grating or a subjective contour may induce motion capture (Ramachandran, 1985; Ramachandran & Inada, 1985). Chang and Julesz (1984) have studied a case of motion capture, where they used a test pattern of ambiguously moving dots (ambiguous with respect to the direction of motion). In every other frame of their presentation, a dot had a displaced partner both to the right and to the left. If dots in a flanking region were moving ambiguously, this would strongly bias the perception of the ambiguous region to be perceived in the same direction of motion. Chang and Julesz (1984) argued that this phenomenon reflected the operation of a cooperative network, in which neighboring detectors for the same direction of motion enhance each other's responses.

Thus there is psychophysical evidence for both differencing and smoothing processes. The question arises how the sharp localization of motion discontinuities and the existence of perceptual contrast effects (segmentation) be reconciled with the computational need and empirical evidence for smoothing, cooperative processes (in-

tegration) (Braddick, 1993)? A prominent idea in computational theories of motion integration, fueled by substantial evidence from physiology, is that fine-grained, coarse-grained and intermediate visual maps exist concurrently to compare different "motion receptive fields" (Braddick *et al.*, 1978; De Valois & De Valois, 1988; Burt & Adelson, 1983). In a multiple-map scenario like this, the joint upshot would be that large motion receptive fields could derive the smoothed velocity signal averaged over extended areas (integration), while much smaller receptive fields with strong inhibitory surrounds could generate signals at motion discontinuities (segmentation).

MT cells have larger receptive fields than V1 cells (about 10 times larger in diameter) that range from less than 5° in the fovea to as much as 30° in the far periphery. Receptive field size also increases more rapidly with increasing eccentricity in MT than in V1 (Albright & Desimone, 1987; Gattass & Gross, 1981). By way of comparison, for the central 10° of visual space in area V1, mean receptive field size increases from approximately 10 minutes of arc in diameter (at 0° eccentricity) to roughly 30 minutes of arc (at 5° eccentricity) to several degrees at large eccentricity (Dow *et al.*, 1981). In addition, compared to V1, MT cells have a wider range and higher cut-off of preferred speeds: 2 to 256°/s for MT neurons and 1 to 32°/s for V1 neurons (Van Essen, 1985). Speed discrimination abilities, measured psychophysically, are in better correspondence with MT than V1 data: human sensitivity to speed of visual motion is best between 4 to 64°/s (McKee, 1981; Orban *et al.*, 1984).

Thus it seems that MT cells would be best equipped to integrate velocities across larger areas while V1 cells could signal local motion discontinuities. In this chapter we provide psychophysical evidence for such an anatomical distinction between segmentation (V1) and integration (MT) processes. In our paradigm experiment we can generate situations where integration of motion signals fails due to putative MT suppression, and directional segmentation cues are pitted against spatial segmentation cues at the monocular (in all likelihood V1) level (see Fgure 6.1).

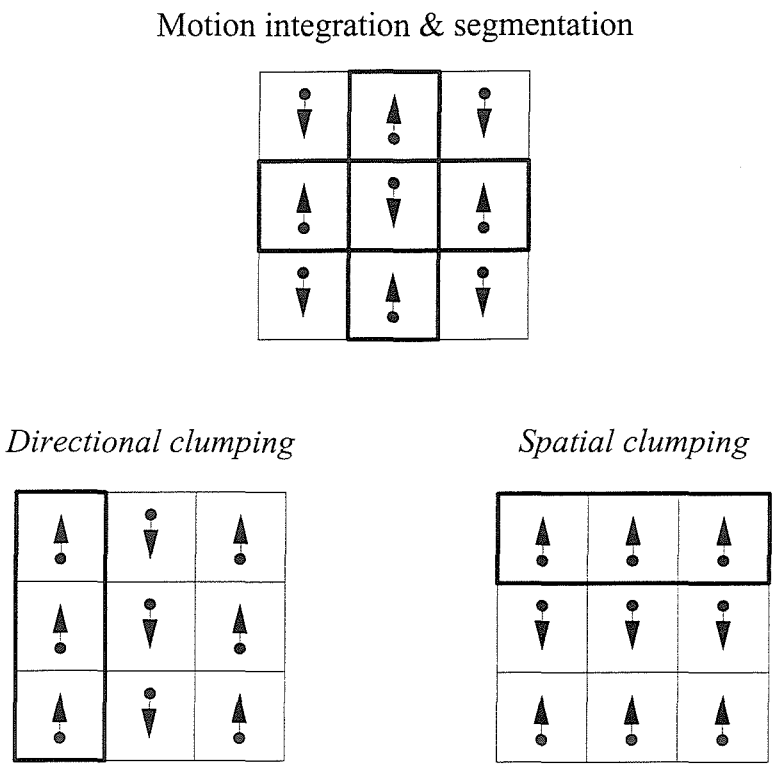

Figure 6.1: Hypothetical mechanisms underlying motion integration and segmentation. Generally, there are two conflicting demands that must be met in computing multiple motions, such as motion transparency (top schema). First, motion signals from neighboring regions must be spatially integrated (aperture problem, noise reduction); second, sensitivity to small velocity differences across space must be preserved for segmentation of regions corresponding to separate objects. Early visual processes (probably including V1) appear to represent the image as an undifferentiated array of signals that encode properties of light intensities at local image regions, but at some point in the cortical hierarchy an explicit representation should code for visual features as belonging to one object (*e.g.*, a surface) rather than another. Psychophysical evidence points to both integration (smoothing) and segmentation (effects of differentiating) mechanisms, but is not clear how both, local smoothing of the image and sharp localization of motion discontinuities, can be accommodated in one conceptual (computational) framework. We hypothesize the computational stage concerned with integration of motion signals may be identified as area MT, whereas image segmentation could occur as early as area V1. To test this hypothesis, we distinguish between instances of surface integration based on directional *vs* spatial information (clumping).

6.1.2 Materials and methods

Moving dots (size 0.01°, life-time $50ms$, velocity $2°/s$, density $10\,\mathrm{deg}^{-2}$) populated both displays. In spite of the short lifetime of dots, dot density remained constant because every dot that "died" was instantly "reborn" elsewhere in the display. Dots moved in one of two directions: either up or down along the vertical. Two dynamic dot textures were involved: globally balanced motion ("GB") and locally balanced motion ("LB"). The GB-texture consisted of two spatially *uncorrelated* sets of dots with two equal and opposite velocities, respectively, perceived as two surfaces sliding coherently over each other ("motion transparency"). The LB-texture consisted of two spatially *correlated* sets of dots with two equal and opposite velocities, respectively, perceived as incoherent flicker rather than coherent motion (Qian *et al.*, 1994a). Spatially correlated dots were "born" in pairs at a fixed separation of approximately 0.2° and moved towards (and past) each other for the duration of their lifetime. Dots populated two displays of equal size ($10 \times 10°$) that were quasi-simultaneously presented to both eyes (left-eye and right-eye display) (see Figure 6.2 and Figure 6.3). Left and right eyes were stimulated dichoptically with the help of liquid crystal shutters. For each display (monocular only) the ratio of equal and opposite velocities could be manipulated ranging from 0% (*e.g.*, all dots in the left-eye display moving upwards) to 100% (*e.g.*, all dots in the right-eye display moving downwards). For example, the third pictogram on top of the data-graph in Figure 6.3 represents an "intraocular coherence" index of 80% (20%), meaning that 80% of all dots in the left eye (red arrows) move upwards (and 20% of them downwards) and that 20% of all dots in the right eye (green arrows) move upwards (and 80% of them downwards). Each presentation constituted a trial. Data were collected in blocks of 200 trials. Note that for each dot in the left-eye display there was a corresponding (spatially uncorrelated) dot in the right-eye display moving in the opposite direction. Displays were generated by an SGI Indigo 2 on a high-resolution color monitor (SGI). The resolution was 1024×1024 pixels and the

frame rate $60Hz$, permitting presentation times to be varied in steps of $16.6ms$. No chin-rest was used.

6.1.3 Results

Experiment 1

Observers were shown in pseudo-random order globally balanced displays with either one of eleven possible intraocular coherence indices. During each trial, observers fixated a cross-shaped mark at display center. Instructions encouraged observers to react as quickly as possible once the percept of motion-transparency was obtained (see Figure 6.2). Reaction times varied between approximately 1 and 3 s. There was no significant trend between conditions (different intraocular coherence indices), implying successful motion integration at a binocular (presumably MT) level regardless of monocular segmentation cues.

Experiment 2

Observers were shown in pseudo-random order locally balanced displays with either one of eleven possible intraocular coherence indices. During each trial, observers fixated a cross-shaped mark at display center. Instructions encouraged observers to react as quickly as possible once the percept of motion-transparency was obtained (see Figure 6.3). Reaction times varied between approximately 1 and 11 s, depending on which intraocular coherence index was used. At the one extreme, for intraocular coherence indices of 100-0 and 0-100 (*i.e.*, unidirectional monocular motion cues) reaction time latency was drastically increased ($9.5 \pm 4.2s$ and $9.1 \pm 4.1s$, respectively). At the other extreme, reaction time for interocular coherence (corresponding to intraocular coherence of $50 - 50$) was comparable to reaction times obtained in the previous experiment ($1.1 \pm 0.5s$). Interestingly, when a color scheme was applied

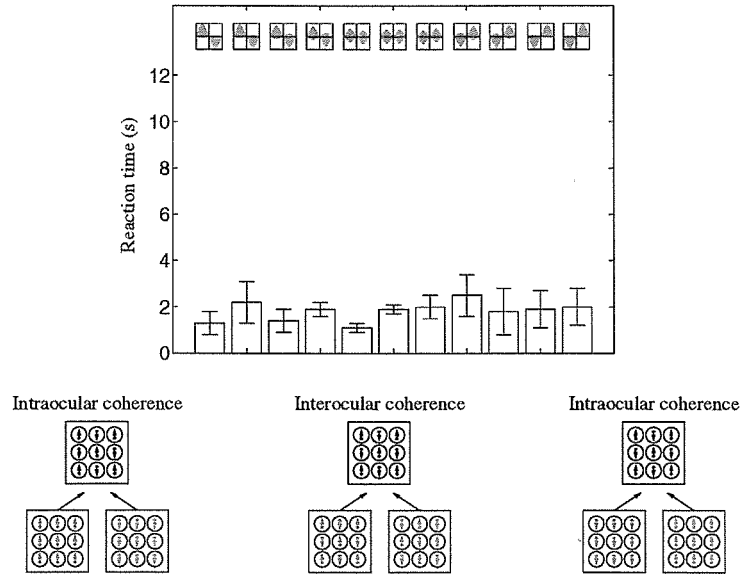

Figure 6.2: Psychophysical displays (schematic) and data for three observers (DE, CK, SK; 900 trials). Moving dots (size 0.01°, life-time $50ms$, velocity $2°/s$, density $10\,\mathrm{deg}^{-2}$) populated two displays of equal size ($10 \times 10°$) that were simultaneously presented to both eyes (left-eye and right-eye display). Left and right eyes were stimulated dichoptically with the help of liquid crystal shutters. In spite of the short lifetime of dots, dot density remained constant because every dot that "died" was instantly "reborn" elsewhere in the display. Under binocular fusion left-eye and right-eye display formed a globally balanced texture, that is two spatially *uncorrelated* sets of dots with equal and opposite velocities along the vertical axis. For each display (monocular only) the ratio of equal and opposite velocities could be manipulated ranging from 0% (*e.g.*, all dots in the left-eye display moving upwards) to 100% (*e.g.*, all dots in the right-eye display moving downwards). During each trial, observers fixated a cross-shaped mark at display center (not shown here). Observers were shown in pseudo-random order displays with either one of eleven possible intraocular coherence indices (100−0, 90−10, 80−20, ..., 50−50, ..., 20−80, 10−90, 0−100). By pressing a key observers indicated whence they were able to see "two clearly distinct surfaces sliding across each other". Reaction time was measured from stimulus onset until the key press and is plotted for each intraocular coherence index as the mean of all observers and the standard deviation between observers (errorbar) Bottom row, three schematic depictions of displays with different intraocular coherence indices. Left $100 - 0$, middle $50 - 50$ (*interocular coherence*), and right $0 - 100$.

to label left- and right-eye displays independently to control for binocular rivalry, observers reported seeing both colors and perceiving two transparent surfaces sliding across each other.

6.1.4 Discussion

Adelson and Movshon (1982) employed plaid patterns to examine the mechanisms concerned with perceptual motion integration. They found that when the component gratings differed significantly in spatial frequency or luminance contrast, human observers reported perceptual non-coherency, indicating that the motions of the component gratings were not integrated by the second processing stage. If this finding was indicative of the existence of two separate channels subserving motion integration, one would predict second-stage "pattern neurons" to receive input from first-stage "component neurons" having a limited range of spatial frequency (or contrast) tuning preferences. Coherent motion would hence result only when the component gratings were similar enough to stimulate neurons within the same channel. Adelson and Movshon (1984) also found that motion coherency was less likely to occur when the component gratings were placed in different depth planes.

We investigated perception of motion coherency in situations where area MT was active and putatively suppressed (for related experiments in non-human primates see Qian & Andersen, 1994). When MT was active, we found that pattern motion (surface transparency) occurred even with component motions presented to different eyes. There was no noticeable difference between directional or spatial "clumping" of the component motions. On the other hand, when MT was functionally inactivated, a striking difference was observed for dichoptic integration based on directional versus spatial segmentation cues. Long reaction time latencies were found in cases where only directional cues were available at the monocular level, implying both failed integration and segmentation. The fact that surface transparency occurred at all after

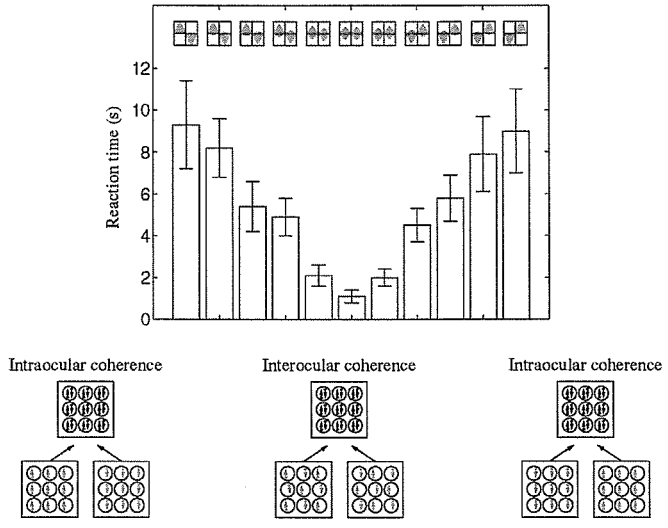

Figure 6.3: Psychophysical display (schematic) and data for three observers (DE, CK, SK; 900 trials). Moving dots (size 0.01°, life-time $50ms$, velocity $2°/s$, density $10\,\mathrm{deg}^{-2}$) populated two displays of equal size ($10 \times 10°$) that were quasi-simultaneously presented to both eyes (left-eye and right-eye display). Left and right eyes were stimulated dichoptically with the help of polarizing goggles. In spite of the short lifetime of dots, dot density remained constant because every dot that "died" was instantly "reborn" elsewhere in the display. Under binocular fusion left-eye and right-eye display formed a locally balanced texture, that is two spatially *correlated* sets of dots with two equal and opposite velocities, respectively, perceived as incoherent flicker rather than coherent motion (Qian *et al.*, 1994). Spatially correlated dots were "born" in pairs at a fixed separation of approximately 0.2° and moved towards (and past) each other for the duration of their lifetime. For each display (monocular only) the ratio of equal and opposite velocities could be manipulated ranging from 0% (*e.g.*, all dots in the left-eye display moving upwards) to 100% (*e.g.*, all dots in the right-eye display moving downwards). During each trial, observers fixated a cross-shaped mark at display center (not shown here). Observers were shown in pseudo-random order displays with either one of eleven possible intraocular coherence indices ($100-0$, $90-10$, $80-20$, ..., $0-50$, ..., $20-80$, $10-90$, $0-100$). By pressing a key observers indicated whence they were able to see "two clearly distinct surfaces sliding across each other". Reaction time was measured from stimulus onset until the key press and is plotted for each intraocular coherence index as the mean of all observers and the standard deviation between observers (errorbar). Bottom row, three schematic depictions of displays with different intraocular coherence indices. Left $100-0$, middle $50-50$ (*interocular coherence*), and right $0-100$.

some viewing time is suggestive of transiently strengthened lateral interactions between striate cortical neurons ("short-term plasticity") (Braun, 1995). In the case of interocular coherence, where both spatial and directional segmentation cues were present at the monocular level, motion transparency was immediately perceived, implying again the existence of a low-level stage (possibly V1) concerned with image segmentation.

Further evidence for the conception of image segmentation as prior to motion integration is provided by Stoner and Albright (1994). Their work points to a conception of motion processing in which the first stage has access to a wide spectrum of form cues and the second stage is gated by image segmentation processes normally thought to lie outside the domain of the motion system. Other psychophysical evidence points to an early representation of surface "relationships" (Ramachandran & Cavanagh, 1985; Nakayama *et al.*, 1990; Shimojo *et al.*, 1989). This is consistent with the demonstration that neurons in area V2 respond to subjective contours (von der Heydt *et al.*, 1984; von der Heydt & Peterhans, 1989) and are thus candidates for detecting surface occlusion and transparency (Nakayama & Shimojo, 1992). Projections between area V2 and area MT (as well as between V2 and V1) are abundant and diffuse and could support the segmentation-gated integration proposed by Stoner and Albright (1993).

In a recent study Nawrot and Sekuler (1990) addressed the issue of stimulus conditions "in-between" motion contrast and motion capture. They measured the threshold for detecting the motion of a small percentage of coherently moving dots, in a pattern where most of the dots were moving randomly. Such test regions were situated in-between "inducing regions" whose direction of movement was unambiguous. When the test regions were wide, motion was easier to detect if the motion in the inducing regions was in the opposite directions, indicating motion contrast. For narrow test stripes, detection of motion in the same direction as the inducing regions

was facilitated, indicating motion capture. Nawrot and Sekuler (1990) suggested, therefore, that interactions between motion detectors acted to summate similar motions over short-spatial ranges, but had a differential effect over longer distances. This is consistent with the idea of motion-receptive fields with summation over a central region and opponent surrounds.

In this respect, another interesting property of MT cells is the presence of large surround interactions. The response to an optimally moving stimulus within a cell's classical (excitatory) receptive field can be influenced by motion well outside its receptive field (Allman *et al.*, 1985; Tanaka *et al.*, 1986). The existence of surround interaction becomes apparent only with simultaneous stimulation of the classical receptive field and the surround (no direct response is elicited from the surround alone). More than 90% of MT neurons have large silent surrounds whose areas are fifty to a hundred times the area of the classical receptive field. In area MT, the surrounds commonly have direction- and speed-specific influences that are antagonistic to the classical receptive field's response. Allman *et al.* (1985) tested these effects by exciting an MT neuron's classical receptive field with random dots moving in the cell's preferred direction and speed, then varied the direction of a surrounding field of random dots. They found that 44% of cells tested had directionally selective surrounds with maximum suppression for background movements in the preferred direction of the center, and often some facilitation for background motion in the opposite direction. Another 30% were suppressed by all directions of coherent background motion. Similar antagonistic effects were found when the speed of the background random dots was varied. Hence the antagonistic center-surround organization allows comparisons to be made between local and surrounding motion measurements - comparisons that may play a role in motion discontinuity detection.

6.1.5 Conclusion

One of the universal features of the cortical architecture of sensory systems in non-human primates is the presence of multiple topographic maps projecting to each other. Proceeding from lower- to higher-order maps, receptive field sizes become larger due to the somewhat divergent projections from lower to higher areas together with the generally larger physical size of lower *vs* higher cortical areas. The increase in receptive field size implies that a higher-level neuron integrates signals from many lower-level neurons with adjacent, spatially restricted receptive fields, transforming spatially localized data into global representations. Neurophysiological evidence from recording studies suggest that area MT provides a particularly convincing example of functional specialization in primate extrastriate visual cortex. Most MT neurons are selective for both direction and speed of stimulus motion (Maunsell & Van Essen, 1983; Albright, 1984; Rodman & Albright, 1987). Moreover, lesions of area MT disrupt psychophysical thresholds for detection and discrimination of visual motion (Newsome & Pare, 1986; Siegel & Andersen, 1986).

Reliable motion perception requires processes that integrate visual motion signals from neighboring locations in the visual field, which should have the effect of smoothing out spatial variations in velocity. However, motion processing should also afford sensitivity to local velocity differences, so that moving objects appear sharply distinct from their background and specific differential properties of optical flow associated with the observer's motion can be detected. We suggest that the first stage of motion analysis is also concerned with detecting motion discontinuities and may anatomically be associated with area V1, whereas the second stage of motion signal integration is thought to occur in area MT and associated areas (MST).

Chapter 7 Summary

7.1 Visual paths of action

William James (1890) was the first to note how the analysis of visual attention may provide important clues about conscious visual awareness:

> Millions of items ... are presented to my senses which never properly enter my experience. Why? Because they are of no *interest* for me. *My experience is what I agree to attend to.* ... Everyone knows what attention is. It is the taking possession by the mind, in clear and vivid form, of one out of what seem several simultaneously possible objects or trains of thought. Focalization, concentration of consciousness are of its essence. It implies withdrawal from some things in order to deal effectively with others (p. 402).

Although the visual system comprises several parallel pathways for the purpose of simultaneously processing different aspects of visual information, the *what* and *how much* of this information that reaches the highest centers of processing in the brain (consciousness) is ultimately determined by (selective) visual attention. Cellular studies of visual attention have confirmed that the mechanism of attentional selection operates either by enhancing cell responses to the object that is being attended to or by attenuating cell responses to the object that is being ignored. These studies have implicated, in particular, the posterior parietal cortex, a region whose involvement in attention to visual form has been documented in earlier clinical studies (Wurtz *et al.*, 1982). The mechanisms that constitute the "expression" of attention, *i.e.*, "the positive difference between information flow at the attended site and the information

flow in its surround", are thought to involve the oculomotor regions of the superior colliculus and the posterior parietal cortex (LaBerge, 1995).

Anterior cortical areas that are purportedly involved in the control of attention are the dorsolateral prefrontal, ventrolateral prefrontal, and anterior cingulate cortices. Furthermore, there are neurons in the dorsolateral and ventrolateral areas that appear to specialize in spatial location and simple image features and, crucially, discharge during delays between a cue and a target. This implies a short-term memory for location and shape attributes that is presumably coupled to a "retrieval mechanisms " that can permit the stored information to activate posterior cortical areas that express attention to the object's shape and location, and to activate anterior and posterior cortical areas that express attention to the execution of actions (*e.g.*, grasping the object).

What we agree to attend to then, the intensity of our attention (concentration), and its duration are regulated mainly from prefrontal cortex that embody voluntary processes, although attentional expression may also be brought about by an intense stimulus or its sudden onset outside our focus of attention (parallel, preattentive attention). In Chapter 2, we set out to determine the cortical specificity of the mechanisms underlying parallel, preattentive dynamic texture segregation. Locally *balanced* counter-motion is thought to elicit a robust response in primate cortical area V1 but not MT (Qian & Andersen, 1994). Attentional requirements can be assessed by requiring subjects to perform a concurrent visual task (Braun, 1994). We applied these techniques to (a) the segregation of regions of orthogonal motion and (b) the detection of motion transparency (Kolb *et al.*, 1995; Kolb *et al.*, 1996).

Moving dots (size 0.01°, life-time $50ms$, velocity $2°/s$, density $10\,\mathrm{deg}^{-2}$) populated 4 adjoining regions (Experiment 1) or separate (Experiments 2-4) regions of the display. In locally balanced counter-motion, pairs of dots remain within 0.5° on opposite trajectories. In locally *unbalanced* counter-motion, dots were up to 16° apart

on opposite trajectories. In *coherent* regions all dot trajectories shared the same orientation, whereas in *incoherent* regions, trajectories of different dot pairs differed in orientation. Subjects identified the region (target) which differed with respect to local balance and/or coherence of motion from the others (4 AFC tasks). Experiment 1 juxtaposed coherent locally balanced counter-motion with vertical and horizontal trajectories, Experiment 2 coherent locally unbalanced counter-motion and locally balanced counter-motion, Experiment 3 incoherent locally unbalanced counter-motion and coherent locally balanced counter-motion, and Experiment 4 coherent and incoherent locally unbalanced counter-motion (target and distractor regions, respectively). To direct visual attention away from moving regions, subjects carried out a visual search among 10 letters presented at or near display center. Each 4AFC task was carried out readily by itself, at presentations times of $100 - 250ms$. In Experiments 2 and 4, 4AFC tasks were performed comparably well with and without the concurrent search task. In Experiment 3, 4AFC performance was at or near chance with the concurrent search task. Locally balanced counter-motion and locally unbalanced counter- motion are thought to stimulate area V1 and areas V1 and MT, respectively. Coherent locally unbalanced counter-motion produces "motion transparency", while incoherent locally unbalanced counter-motion and coherent locally balanced counter-motion do not. Accordingly, Experiment 1 shows that regions of orthogonal motion are segregable even in the absence of a strong response in area MT. Experiment 2 shows that motion transparency can be detected even with attention directed at a concurrent task. Experiments 3 and 4 show that this is not merely a consequence of differential stimulation of area MT.

Taking into account the above *anatomical* limitations of what we can attentively respond to, we further inquired into the *phenomenological* limitations to visual awareness. In the face of James' conjunction theory of attention and awareness we explore the problem of the possibility of visually attending to something that is simply not

seen (James, 1890). In Chapter 3, we described the dramatic dissociation between visual localization and discrimination performance and visual and non-visual awareness of the target in "conflicting", unecological displays (Kolb & Braun, 1995; Braun & Kolb, 1995; Braun & Kolb, 1996). Our two psychophysical displays were fashioned to stimulate area V1 strongly and extrastriate (e.g., area MT) areas poorly. In each display, one quadrant presented a qualitative contrast to the other three, and this "odd" quadrant was consciously perceived in one form of the display (C-form) but not another (NC-form) (100-200ms presentation time).

The first display was composed of paired dots moving on orthogonal trajectories (different directions in odd and other quadrants), either within 0.2° of each pair (NC-form) or separated by several deg (C- form), so that the two forms differentially stimulated units in area MT but not area V1 (Qian & Andersen, 1994). The second display was a dichoptic presentation of arrays of oriented Gabor-elements (different orientations in odd and other quadrants), producing either binocular rivalry (NC-form) or fusion (C-form), so the two forms differentially stimulated binocular but not monocular units. Observers locating the odd quadrant (4AFC tasks), and subsequently rated their confidence in their choice of quadrant (scale of 1 to 10). Performance was comparable (and far above chance) for C- and NC-forms, but performance and confidence were correlated only for C-forms and essentially uncorrelated for NC-forms, implying that performance in NC-forms was not accompanied by visual awareness. The underlying mechanism appeared to be an inhibitory interaction between conflicting visual features. In addition, we attempted to obtain clues to possible neural sites by investigating the spatial range of this interaction. In the first display, target awareness was nil when nearby dots pass each other at 0.05°, but rapidly recovered as this distance increases to 0.15°. In the second display, target awareness was nil when corresponding Gabor elements were presented to left and right eyes at exactly the same location, but recovered rapidly when corresponding elements were displaced

from each other by less than 0.1°. The spatial range of the interactions that restrained visual awareness were comparable to receptive field diameters in striate visual cortex. Thus, the interaction may be related to the "divisive inhibition" suggested by Heeger and Carandini (1994). We surmise that performance may be based on stimulation of area V1 while conscious experience may result from stimulation of extrastriate areas (Crick & Koch, 1995).

Chapter 4 comprises an elaborate demonstration of visual pattern discrimination in the absence of visual awareness (Kolb *et al.*, 1996). Two 40×40 arrays of Gabor elements (orientation $\pm\pi/4$, period 0.25°, $\sigma = 0.125°$, phase $\pm\pi/2$) are presented dichoptically. Fore- and background elements have orthogonal orientation. Foreground elements are arranged to form four letter shapes (size 8×8 elements each) along the horizontal midline. The left and right eye view orthogonal elements at every array location. When left and right eye views are superimposed, the array subjectively appears uniform with no indication of the letter shapes whatsoever (presentation times are too short for one eye to dominate the other).

In Experiment 1 observers discriminate a sequence of 4 identical letters (4AFC) and rate their confidence (scale of 1 to 10). In Experiment 2, the trial is preceded by a normally visible primer letter (50% valid, 50% invalid). In Experiment 3, observers discriminate a sequence of 4 different letters forming a word (4AFC) and rate their confidence. In Experiment 4, observers are visually or auditorily presented with a target word, view a sequence of "conflicting" displays and identify the one that conceals the target word. Letter and word discrimination is performed well above chance without visual awareness (no correlation between confidence and performance) (Experiments 1-3). A valid prime significantly increases performance, and invalid prime reduces it to chance (Experiment 2). Spontaneous identification of a subjectively non-apparent word is also significantly above chance (Experiment 5). Blindsight in normal observers extends to complex patterns. Priming effects are much larger than

in normal vision. Blindsight in normal observers is not limited to forced-choice situations.

In their recent article *Are we aware of neural activity in primary visual cortex?*, Francis Crick and Christof Koch (1995) ponder the notion of "vivid and direct (visual) awareness" regarding eye-of-origin identification:

> The firing of some neurons in V1 depends upon which eye the visual signal is coming through. Neurons higher in the visual hierarchy do not make this distinction, that is, they are typically binocular. Most people are certainly not *vividly and directly aware* of which eye they are seeing with (unless they close or obstruct one eye), although whether they have some *very weak awareness* of the eye of origin is more controversial [...] suggest[ing] that people are not vividly aware of much of the activity in V1 (p. 123).

It seems plausible then to speak of a spectrum of intensities for conscious experience, much like the concentration span in the expression of visual attention, ranging from nil or weak to moderate, in addition to vivid. In Chapter 5, we conclusively demonstrated that certain dichoptic stimulation can unmask eye- of-origin at extremely weak levels of visual awareness. Humans can exploit eye-of-origin information in stereopsis but have difficulty reporting the eye of origin of a visual stimulus. In nonhuman primates there are monocular neurons in V1, but most extrastriate neurons are binocular. We wondered if human observers could access ocularity information in V1 if extrastriate areas were *functionally anaesthetized.* To test this possibility, subjects were asked to report the eye of origin of visual stimuli - some of which are known to suppress MT neurons in macaques (Qian & Andersen, 1994). In all experiments a target stimulus was presented to one eye and a noise stimulus to the other (2AFC tasks). Two types of motion targets were employed: (a) a unidirectional field of dots (MT exciting), (b) a static dot field, or (c) a moving (paired or

unpaired) dot field differing in color from the target dots. Dot density and lifetime were matched to the target. In a preliminary study (Dobbins & Kolb, 1995), four observers, three of them naive, performed at least 300 trials in each condition. All observers performed well above chance when the paired dots (MT-suppressing) target and noise stimulus were labeled by different colors. However, they performed at close to chance levels when color was the sole discriminant for the dots in the two eyes. Three of four observers performed above chance when the paired dots were matched with flicker in the other eye. In addition, they performed better for paired dots than for unidirectional targets. In a further study (Dobbins & Kolb, 1996), four observers, two of them naive, performed at least 500 trials in each condition. In conditions with flicker in one eye, utrocular identification was generally at close to chance levels. In viewing conditions with coherent unbalanced or locally balanced counter-motion in either eye, a combination of the two, or coherent unbalanced or locally-balanced counter-motion with green dots in one eye and red dots in the other eye, three of four observers performed significantly above chance. In addition, performance in cases where differential dichoptic stimulation was enhanced by means of isoluminant color labeling was well above chance for all four observers. The fact that observers in both studies exhibited differential performance across all conditions except those where flicker was employed in one eye (and performance was radically at chance levels) begets two important implications: first, no general artifact of the display could have led to unequivocal utrocular discrimination (the downfall of previous experiments), and second, it is *not* the case that humans may access monocular information "contained" in V1 when higher (binocular) areas are putatively suppressed, but rather that information *becomes accessible* in circumstances where monocular neurons are differentially activated with respect to binocular neurons in V1.

In 1866, the question of whether a person can "distinguish the impression of one eye from those of the other" was first raised by Hermann von Helmholtz, followed by

an account of why humans cannot (normally) distinguish the impressions of the two eyes:

> The image is seen by each eye just as it would be formed on the retina of an imaginary cyclopean eye, as conceived by E. Hering. ... Thus in binocular vision the two retinal images may be supposed to be transferred to the retina of this imaginary eye, where they mutually overlap each other and are then projected correspondingly in space (p. 460).

The lack of discriminating clues due to what Hering termed cyclopean projection appears to also have a functional (ecological) connotation: there is simply no functional need for us to experience the exact nature of a proximal stimulus at our sensory receptors. By analogy, the difference in arrival time of a sound at the two ears is used for auditory localization, there is no reason for us to be aware of one ear receiving an earlier signal. In contrast, the touch sense of the two hand is preserved as sensory experience, because conscious awareness of which hand is being stimulated does carry significant functional value. Are there any circumstances, however, in which a drastic change in behavioral relevance can gauge our awareness to lower-level sensory computations? In Chapter 6, we tackled the problem of how monocular cues contribute to motion transparency, a perception thought to arise from higher-level (binocular) processing. Moving dots (size 0.01°, life-time $50ms$, velocity $2°/s$, density $10\,\mathrm{deg}^{-2}$) populated two monocular regions of equal size. Under binocular fusion left and right eye received 100% overlapping input from the two motion-defined regions.

In Experiment 1 two spatially *uncorrelated* sets of dots with equal and opposite velocities along the vertical axis were superimposed to constitute the binocular image. The strength of the motion-induced transparent percept was independent of the distribution of equal and opposite velocities in either eye. In Experiment 2 two spatially *correlated* sets of dots with equal and opposite velocities along the vertical axis were superimposed to constitute the binocular image. Spatially correlated

dots appeared in pairs at a fixed lateral distance of approximately 0.2° and traveled towards (and past) each other for the duration of their lifetime. Similar displays of spatially uncorrelated dots ("paired dots") viewed by non-human primates are known to suppress neural activity in area MT (Qian & Andersen, 1994). In this case the strength of the motion-induced transparent percept was contingent upon the distribution of equal and opposite velocities in either eye. Subjects judged the intensity of the percept as a function of transparency onset and obtained similarly "strong" results as in Experiment 1 when both eyes received similar input (i.e., monocular equilibrium of equal and opposite motion). However, when both eyes received drastically different inputs (e.g., upward motion in the left eye and downward motion in the right eye) the percept was judged weakest. We excluded the possibility of binocular rivalry supplying this curious asymmetry in Experiment 2 by probing a full range of interocular velocity distributions - from *intraocular* to *interocular* coherence of equal and opposite velocities. In other words, rivalry (if at work at all) should produce comparable results for all such velocity distributions. Correspondingly, the asymmetric results could not be attributed to the "rivalrous" nature of the dichoptic stimulation in the case of intraocular coherence for equable results were obtained in Experiment 1 across all velocity distributions. Furthermore, the proposition that integration and segmentation modeled a coupled, cooperative process would fail to account for the uniform reaction data in Experiment 1. It seems rather that in certain cases of dichoptic motion perception, one eye "learns" to see what the other eye does and appears to compensate for the difference between the monocular images in the global (binocular) percept. In addition, we observed a quasi-linear relationship between the time it takes the adaptive mechanism to fill-in and the total difference between the images.

Bibliography

Adelson, E. H. & Bergen, J. R. (1985). Spatiotemporal enery models for the perception of motion. *Journal of the Optical Society of America A, 2*, 284-299.

Adelson, E. H. & Movshon, J. A. (1982). Phenomenal coherence of moving visual patterns. *Nature, 300*, 523-525.

Adelson, E. H. & Movshon, J. A. (1983). The perception of coherent motion in two-dimensional patterns. In N. I. Badler & J. K. Tsotsos (eds.), *Motion: Representation and Perception.* New York: Elsevier Science Publishing Co., 93-98.

Albright, T. D. (1984). Direction and orientation selectivity of neurons in visual area MT of the macaque. *Journal of Neurophysiology, 52*, 1106-1130.

Allman, J., Miezin, F. & McGuiness, E. (1985a). Direction- and velocity-specific responses from beyond the classical receptive field in the middle temporal visual area (MT). *Perception, 14*, 105- 126.

Allman, J., Miezin, F. & McGuiness, E. (1985b). Stimulus specific responses from beyond the classical receptive field: Neuophysiological mechanisms for local-global comparisons in visual neurons. *Annual Review of Neuroscience, 8*, 407-430.

Andersen, R. A. (1987). The role of the inferior parietal lobule function in spatial perception and visuo- motor integration. In F. Plum, V. B. Mountcastle, and S. R. Geiger (eds.), *Handbook of physiology.* Sec. 1, The nervous system, Vol. IV, higher functions of the brain, Pt. 2, pp. 438-518. Bethesda, MD: American Physiological Society.

Andersen, R. A., Asanuma, C., Essick, G., & Siegel, R. M. (1990). Cortico-cortical

connections of anatomically and physiologically defined subdivisions within the inferior parietal lobule. *Journal of Comparative Neurology, 296*, 65-113.

Andersen, R. A. & Siegel, R. M. (1988). Motion processing in primate cortex. In *Signal and Sense: Local and Global Order in Perceptual Maps*, eds., Edelman, G. Gall, W., & Cowan, W. M. New York: Wiley.

Attneave, F. (1971). The multistability of perception. *Scientific American, 225*, 62-71.

Bacon, W. F. & Egeth, H. E. (1991). Local processes in preattentive feature detection. *Journal of Experimental Psychology, 17*, 77-90, 1991.

Baizer, J. S., Robinson, D. L., & Dow, B. M. (1977). Visual responses of area 18 neurons in awake, behaving monkey. *Journal of Neurophysiology, 40*, 1024-1037.

Barbur, J. L., Ruddock, K. H., & Waterfield, V. A. (1980). Human visual responses in the absence of the geniculo-calcarine projection. *Brain, 103*, 905-928.

Beck, J. (1982). Textural segmentation. In J. Beck (Ed.), *Organization and Representation in Perception*, pp 285-317. Hillsdale, NJ: Lawrence Erlbaum.

Beck, J. (1967). Perceptual grouping produced by line figures. *Perception and Psychophysics, 2*, 491-495.

Beck, J. (1966). Effects of orientation and of shape similarity on perceptual grouping. *Perception and Psychophysics, 1*, 300-302.

Ben-Av, M. B., Sagi, D. & Braun, J. (1992). Visual attention and perceptual grouping. *Perception and Psychophysics, 52*, 277-294.

Bender, M. B. & Krieger, H. P. (1951). Visual function in perimetrically blind fields. *Archives of Neurology and Psychiatry, 65*, 72-79.

Benevento, L. A. & Fallen, J. H. (1975). The ascending projections of the superior colliculus in the rhesus monkey (*Macaca mulatta*). *Journal of Comparative*

Neurology, 160, 339-362.

Bergen, J. & Julesz, B. (1983). Parallel versus serial processing in rapid pattern discrimination. *Nature, 303*, 696-698.

Blake, R. & Cormack, R. H. (1979). On utrocular discrimination. *Perception and Psychophysics, 26*, 53-68.

Blasdell, G. G. & Fitzpatrick, D. (1984). Physiological organization of layer 4 in macaque striate cortex. *Journal of Neuroscience, 46*, 880-895.

Blythe, I. M., Kennard, C., & Ruddock, K. H. (1987). Residual vision in patients with retrogeniculate lesions of the visual pathways. *Brain, 110*, 887-905.

Born, R. T. & Tootel, R. B. H. (1992). Segregation of global and local motion processing in primate middle temporal visual areas. *Nature, 357*, 497-499.

Born, R. T. & Tootel, R. B. H. (1991). Spatial frequency tuning of single units in macaque supragranular striate cortex. *Proceedings of the National Academy of Science, 88*, 7066-7070.

Boussaoud, D., Ungerleider, L. C., & Desimone, R. (1990). Pathway for motion analysis: Cortical connections of the medial superior temporal and fundus of the superior temporal visual areas in the macaque. *Journal of Comparative Neurology, 296*, 462-495.

Braddick, O. (1993). Segmentation versus integration in visual motion processing. *TINS 16, 7*, 263-269.

Braun, J. & Kolb, F. C. (1996). Blindsight in normal observers: Spatial range implicates striate visual cortex. *Investigative Ophtalmology and Visual Science (Supplement), 37*, 1073.

Braun, J. (1995). Contour integration: A computational model based on the formation of "cascades" among short-range interactions. *Neural Computation*, (in

preparation).

Braun, J. & Kolb, F. C. (1995). Blindsight in normal observers. *J. Neuroscience, (Suppl.), 26*, 01378.

Braun, J. (1994). Visual search among items of different salience: removal of visual attention mimics a lesion in extrastriate area V4. *Journal of Neuroscience, 14*, 554-567.

Braun, J. & Julesz, B. (1995). Was William James right about passive, involuntary, and effortless attention? (submitted).

Braun, J. & Sagi, D. (1990). Vision outside the focus of attention. *Perception and Psychophysics, 48*, 45-58.

Bravo, M. J. & Nakayama, K. (1992). The role of attention in different visual-search tasks. *Perception and Psychophysics, 51*, 465-472.

Broadbent, D. E. (1958). *Perception and communication.* London: Pergamon.

Bruce, V. & Green, P. (1986). *Visual perception: physiology, psychology and ecology.* London: Lawrence Erlbaum.

Bruecker, A. & von Bruecke, E. (1902). Zur Frage der Unterscheidbarkeit rechts- und linksaugiger Gesichtseindrücke. *Perceptual Psychophysics, 26*, 53-68.

Bullier, J. & Henry, G. H. (1980). Ordinal position and afferent inputof neurons in monkey striate cortex. *Journal of Comparative Neurology, 193*, 913-935.

Burkhalter, A. & Van Essen, D. C. (1986). Processing of color, form and disparity information in visual areas VP and V2 of ventral extrastriate cortex in the macaque monkey. *Journal of Neuroscience, 6*, 2327-2351.

Campion, J., Latto, R., & Smith, Y. M. (1983). Is blindsight an effect of scattered light, spared cortex, and near-threshold vision? *Behavioral and Brain Sciences, 6*, 432-486.

Cavanagh, P. & Anstis, S. (1991). The contribution of color to motion in normal and color-deficient observers. *Vision Research, 31*, 2109-2148.

Cavanagh, P., Boeglin, J., & Favreau, O. E. (1985). Perception of motion in equiluminous kinematograms. *Perception, 14*, 151-162.

Chang, J. J. & Julesz, B. (1983). Displacement limits for spatial frequency filtered random-dot cinematograms in apparent motion. *Vision Research, 23*, 1379-1385.

Charles, E. R. & Logothetis, N. K. (1989). The responses of middle temporal (MT) neurons to isoluminant stimuli. *Investigative Ophtalmology and Visual Science, 30*, 427.

Chaudhuri, A. (1990). Modulation of the motion aftereffect by selective visual attention. *Nature, 344*, 60-62.

Chelazzi, L. & Desimone, R. (1994). Responses of V4 neurons during visual search. *Society of Neuroscience Abstract, 20*, 1054.

Chelazzi, L., Miller, E. K., Duncan, J. & Desimone, R. (1993). A neural basis for visual search in inferior temporal cortex. *Nature, 363*, 345-347.

Colby, C. L., Gattass, R., Olson, C. R., & Gross, C. G. (1988). Topographic organization of cortical afferents to extrastriate visual area PO in the macaque: A dual tracer study. *Journal of Comparative Neurology, 269*, 392-413.

Corbetta, M., Miezin, F. M., Dobmeyer, S., Shulman, G. L. & Petersen, S. E. (1990). Selective attention modulates neural processing of shape, color, and velocity in humans. *Science, 248*, 1556-1559.

Crick, F. C. & Koch, C. (1995). Are we aware of neural activity in primary visual cortex? *Nature, 375*, 121-123.

Dean, P. (1982). Visual behavior in monkeys with inferotemporal lesions. In D. J. Ingle, M. A. Goodale, & R. J. W. Mansfield (eds.), *Analysis of Visual Behavior.*

Cambirdge, Mass: MIT Press, 587-628.

DeMonasterio, F. M. (1978). Properties of concentrically organized X and Y ganglion cells of macaque retina. *Journal of Neurophysiology, 41*, 1394-1417.

DeMonasterio, F. M. & Gouras, P. (1975). Functional properties of ganglion cells of the rhesus monkey retina. *Journal of Physiology, 251*, 167-195.

Derrington, A. M., Krauskopf, J., & Lennie, P. (1984). Chromatic mechanisms in lateral geniculate nucleus of macaque. *Journal of Physiology, 357*, 241-265.

Derrington, A. M. & Lennie, P. (1984). Spatial and temporal contrast sensitivities of neurones in lateral geniculate nucleus of macaque. *Journal of Physiology, 357*, 219-240.

Desimone, R. (1992). *Neural circuits for visual attention in the primate brain.* In Carpenter, G. & Grossberg, S. (Eds), *Neural networks for vision and image procesing* (pp. 343-364). Cambridge, MA: MIT Press.

Desimone, R. & Duncan, J. (1995). Neural mechanisms of selective visual attention. *Annual Review of Neuroscience* (in press).

Desimone, R. & Schein, S. J. (1987). Visual properties of neurons in area V4 of the macaque: Sensitivity to stimulus form. *Journal of Neurophysiology, 57*, 835-868.

Desimone, R., Schein, S. G., Moran, J. & Ungerleider, L. G. (1985). Contour, color and shape analysis beyond the striate cortex. *Vision research, 25*, 441-452.

Desimone, R. & Ungerleider, L. G. (1986). Multiple visual areas in the caudal superior temporal sulcus of the macaque. *Journal of Comparative Neurology, 248*, 164-189.

DeYoe, E. A. & Van Essen, D. C. (1988). Concurrent processing streams in monkey visual cortex. *Trends in Neurosciences, 11*, 219-226.

DeYoe, E. A. & Van Essen, D. C. (1985). Segregation of efferent connections and receptive field properties in visual area V2 of the macaque. *Nature, 317*, 58-61.

Dick, M., Ullman, S. & Sagi, D. (1991). Short- and long-range processes in structure-from-motion. *Vision Research, 31*, 2025-2028.

Dineen, J. T. & Hendrickson, A. E. (1981). Age-correlated differences in the amount of retinal degeneration after striate cortex lesions in monkeys. *Investigative Ophtalmology and Visual Science, 21*, 749-752.

Dobbins, A. C. & Kolb, F. C. (1995). Eye-of-origin unmasked. *Nature*, (submitted).

Dobbins, A. C. & Kolb, F. C. (1995). MT-suppressing stimulus unmasks eye-of-origin. *Investigative Ophtalmology and Visual Science (Supplement), 36*, 280.

Dobbins, A. C., Jeo, R., & Allman, J.(1994). *Soc. Neurosci. Abstr., 20*, 624.

Dobkins, K. R. & Albright, T. D. (1993). What happens if it changes color when it moves?: I. Psychophysical on the nature of chromatic input to motion detectors. *Vision Research*, (in press).

Dobkins, K. R. & Albright, T. D. (1991). Color facilitates motion correspondence in visual area MT. *Society for Neuroscience Abstracts.*

Dodwell, P. C. & Humphrey, G. K. (1990). A functional theory of the McCollough effect. *Psychology Review, 97*, 78-89.

Douglas, R. J., Koch, C., Mahowald, M., Martin, K. A. C., & Suarez, H. H. (1995). *Science, 269*, 981-985.

Dow, B. M. (1974). Functional classes of cells and their laminar distribution in monkey visual cortex. *Journal of Neurophysiooogy, 37*, 927-946.

Duncan, J., Ward, R., & Shapiro, K. (1994). Direct measurement of attentional dwell time in human vision. *Nature, 369*, 313-315.

Duncan, J. & Humphreys, G. (1992). Beyond the search surface: visual search and attentional engagement. *Journal of Experimental Psychology, 18*, 578-588.

Duncan, J. & Humphreys, G. (1989). Visual search and stimulus similariy. *Psychological Review, 96*, 433-458.

Eby, D. W., Loomis, J. M. & Solomon, E. M. (1989). Perceptual linkage of multiple objects rotating in depth. *Perception, 18*, 427-444.

Enoch, J., Goldman, H., & Sunga, R. (1969). The ability to distinguish which eye was stimulated by light. *Investigative Ophtalmology and Visual Science, 8*, 317-331.

Farah, M. J., Monheit, M. A., & Wallace, M. A. (1991) *Neuropsychologia 29*, 949-958.

Feinberg, T. E., Pasik, T., & Pasik, P. (1978). Extrageniculostriate vision in the monkey. VI. Visually guided accurate reaching behavior. *Brain Research, 152*, 422-428.

Felleman, D. J. & Kaas, J. H. (1984). Receptive-field properties of neurons in middle temporal visual area (MT) of owl monkeys. *Journal of Neurophysiology, 52*, 488-513.

Felleman, D. J. & Van Essen, D. C. (1991). Distributed hierarchical processing in the primate cerebral cortex. *Cerebral Cortex, 1*, 1-47.

Felleman, D. J. & Van Essen, D. C. (1987). Receptive field properties of neurons in area V3 of macaque monkey extrastriate cortex. *Journal of Neurophysiology, 57*, 889-920.

Fitzpatrick, D., Lund, J. S., & Blasdell, G. G. (1985). Intrinsic connections of macaque striate cortex: Afferent and efferent connections of lamina 4C. *Journal of Neuroscience, 5*, 3329-3349.

Fox, R. (1991) in D. Regan (Ed.) *Binocular Vision*, pp 93-110. Boca Raton, FL: CRC Press.

Goldman-Rakic, P. S. (1984a). Modular organization of prefrontal cortex. *TINS, 7*, 419-424.

Goldman-Rakic, P. S. (1984b). The frontal lobes: Uncharted provinces of the brain. *TINS, 7*, 425- 429.

Gouras, P. & Krüger, J. (1979). Responses of cells in foveal visual cortex of the monkey to pure color contrast. *Journal of Neurophysiology, 42*, 850-860.

Graves, R. E. & Jones, B. S. (1992). *Cognitive Neuropsychology, 9*, 487-508.

Green, D. M. & Swets, J. A. (1966). *Signal detection theory and psychophysics.* New York: Wiley.

Greenwald, A. G. (1992). *Am. Psychol., 47*, 766-779.

Gross, C. G. (1973). Inferotemporal cortex and vision. *Progress in Physiological Psychology, 5*, 77- 115.

Gurnsey, R. & Browse, R. A. (1987). Micropattern properties and presentation condition influencing visual texture discrimination. *Perception and Psychophysics, 41*, 239-252.

Hammond, P. (1985). Visual cortical processing: Textural sensitivity and its implications for classical views. In D. Rose & V. G. Dobson (Eds.), *Models of the visual cortex*, pp 326-343. New York: Wiley.

Hammond, P. (1978). Directional tuning of complex cells in area 17 to the feline visual cortex. *Journal of Physiology, 285*, 479-491.

Helmholtz, H. (1866/1962). Handbuch der physiologischen Optik. English. In J. P. C. Southall (Ed.), *Volume 3*, New York: Dover.

Heywood, S. & Ratcliff, G. (1975). Long-term oculomotor consequences of unilateral colliculectomy in man. In G. Lennerstrand & P. Bach-y-Rita (Eds.), *Basic mechanisms of ocular motility and their clinical implications*, pp 561-564. Oxford: Pergamon Press.

Hitchcock, P. F. & Hickey, T. L. (1980). Cell-size changes in the lateral geniculate nuclei of normal and monocularly deprived cats treated with 6-hydroxydopamine and or norepinephrine. *Brain Research, 182*, 176-179.

Horton, J. C. & Hedley-White, E. T. (1984). Cytochrome-oxidase mapping of patches and ocular dominance columns in human visual cortex. *Phil. Trans. R. Soc., 304*, 255-272.

Hubel, D. H. & Livingstone, M. S. (1987). Segregation of form, color, and stereopsis in primate area 18. *Journal of Neuroscience, 7*, 3378-3415.

Hubel, D. H. & Livingstone, M. S. (1985). Complex-unoriented cells in a subregion of primate area 18. *Nature, 315*, 325-327.

Hubel, D. H. & Wiesel, T. N. (1975). Uniformity of monkey striate cortex: A parallel relationship between field size, scatter and magnification factor. *Journal of Comparative Neurology, 158*, 295- 306.

Hubel, D. H. & Wiesel, T. N. (1974). Sequence regularity and geometry of orientation columns in the monkey striate cortex. *Journal of Comparative Neurology, 158*, 267-294.

Hubel, D. H. & Wiesel, T. N. (1972). Laminar and columnar distribution of geniculocortical fibers in macaque monkey. *Journal of Comparative Neurology, 146*, 421-450.

Hubel, D. H. & Wiesel, T. N. (1968). Receptive fields and functional architecture of monkey striate cortex. *Journal of Physiology, 195*, 215-243.

Humphrey, G. K., Goodale, M. A., Corbetta, M., & Aglioti, S. (1995). The McCollough effect reveals orientation discrimination in a case of cortical blindness. *Current Biology, 5*, 545-551.

Humphrey, N. K. & Weiskrantz, L. (1968). Vision in monkeys after removal of the

striate cortex. *Nature, 215*, 595-597.

Hyvärinen, J. (1982). *The Parietal Cortex of Monkey and Man.* Berlin: Springer-Verlag.

Ishai, A. & Sagi, D. (1995). Common mechanisms for visual imagery and perception. *Science, 268*, 1772-1774.

Iwai, E. (1985). Neurophysiological basis of pattern vision in macaque monkeys. *Vision Research, 25*, 425-439.

Jagadeesh, B., Wheat, H. S., & Ferster, D. (1993). Linearity of summation of synaptic potentials underlying direction selectivity in simple cells of the cat visual cortex. *Science, 262*, 1901-1904.

James, W. (1890). *Principles of psychology.* New York: Holt.

Julesz, B. (1984). Toward an axiomatic theory of preattentive vision. In G. M. Edelman, W. E. Gall, & M. Cowan (Eds.), *Dynamic Aspects of Neocortical Function*, pp 585-611. New York: Neurosciences research Foundation.

Julesz, B. (1981). Textons, the elements of texture perception and their interactions. *Nature, 290*, 91-97.

Julesz, B. & Chang, J. J. (1976). Interaction between pools of binocular disparity detectors tuned to different disparities. *Biological Cybernetics, 22*, 107-119.

Kahneman, D. (1973). *Attention and effort.* Englewood Cliffs, NJ: Prentice Hall.

Kaplan, E. & Shapley, R. M. (1982). X and Y cells in the lateral geniculate nucleus of macaque monkeys. *Journal of Physiology, 330*, 125-143.

Karni, A. & Sagi, D. (1991). Where practise makes perfect in texture discrimination: Evidence for primary visual cortex plasticity. *Proc. Natl. Acad. Sci. USA, 88*, 4966-4970.

Karni, A., Ungerleider, L. G., Haxby, J., Jezzard, P., Pannier, J. Cuenod, C. A., Turner, R. & LeBihan, D. (1993). Functional MRI evidence for adult motor cortex plasticity during motor skill learning. *Soc. Neurosc. Abstr., 19*, 1503.

Keating, E. G. (1980). Rudimentary color vision in the monkey after removal of striate and preoccipital cortex. *Brain Research, 179*, 379-384.

Kisvarday, Z. F., Cowey, A., Stoerig, P., & Somogyi, P. (1991). Direct and indirect retinal input into degenerated dorsal lateral geniculate nucleus after striate cortical removal in monkey: implications for residual vision. *Experimental Brain Research, 86*, 271-292.

Knierim, J. J. & Van Essen, J. C. (1992). Neuronal responses to static texture patterns in area V1 of the alert macaque monkey. *Journal of Neuophysiology, 67*, 961-980.

Koch, C. & Ullman, S. (1985). Shifts in selective visual attention: towards the underlying neural circuitry. *Human Neuobiology, 4*, 219-227.

Kolb, F. C., Weber, M., Perona, P., & Braun, J. (1996). Blindsight in normal observers: Pattern discrimination and priming effects. *Investigative Ophtalmology and Visual Science (Supplement), 37*, 1148.

Kolb, F. C. (1995). Speed discrimination during unconscious viewing of apparent motion displays. *Vision Research*, (in preparation).

Kolb, F. C. & Braun, J. (1995). Blindsight in normal observers. *Nature, 377*, 336-338.

Kolb, F. C., Perona, P. & Braun, J. (1995). Perception of motion at different cortical and attentional levels of processing. *Investigative Ophtalmology and Visual Science (Supplement), 36*, 1764.

Kolb, F. C., Weber, M., Braun, J. & Perona, P. (1995). Preattentive segregation of dynamic textures at different levels of cortical processing. *Vision Research*,

(submitted).

Kolb, F. C., Weber, M., Perona, P., & Braun, J. (1995). Blindsight in normal observers and the role of visual awareness in perceptual learning. *Journal of Neuroscience.* (in preparation).

Kolb, F. C., Braun, J. & Perona, P. (1994). Object segmentation and 3-D structure-from-motion. *Investigative Ophtalmology and Visual Science (Supplement). 35*, 99.

Kooi, F. L. & De Valois, K. K. (1992). The role of color in the motion system. *Vision Research, 32*, 657-668.

Kovacs, I. & Julesz, B. (1993). A closed curve is much more than an incomplete one: effect of closure in figure-ground segmentation. *Proc. Natl. Acad. Sci. USA, 90*, 7495-7497.

Kröse, B. & Julesz, B. (1989). The control and speed of shifts of attention. *Cognitive Psychology, 24*, 475-501.

LaBerge, D. (1995). *Attentional Processing.* Cambridge, Mass.: Harvard University Press.

Lamme, V. A. F., Van Dijk, B. W. & Spekreijse, H. (1992). Texture segregation is processed by primary visual cortex in man and monkey. Evidence from VEP experiments. *Vision Research, 32*, 797-807.

Lamme, V. A. F., Van Dijk, B. W. & Spekreijse, H. (1993). Contour from motion processing in primary visual cortex. *Nature, 363*, 541-543.

Lamme, V. A. F., Van Dijk, B. W. & Spekreijse, H. (1994). Organization of contour from motion processing in primate visual cortex. *Vision Research, 34*, 721-735.

Leopold, D. A. & Logothetis, N. K. (1995). Cell-activity reflects monkey's perception during binocular rivalry. *Invest. Ophth. Vis. Sci. Suppl., 36*, 813.

Lepore, F., Cardu, B., Rasmussen, T., & Malmo, R. B. (1975). Rod and cone sensitivity in destriated monkeys. *Brain Research, 93*, 203-221.

Leventhal, A. G., Rodieck, R. W., & Dreher, B. (1981). Retinal ganglion cell classes in the old world monkey: Morphology and central projections. *Science, 213*, 1139-1142.

Livingstone, M. S. & Hubel, D. H. (1984). Anatomy and physiology of a color system in the primate visual cortex. *Journal of Neuroscience, 4*, 309-356.

Logothetis, N. K. & Schall J. D. (1989). Neuronal correlates of subjective visual perception. *Science, 245*, 761-763.

Lund, J. S. & Yoshioka, T. (1991). Local circuit neurons of macaque monkey striate cortex: III. Neurons of laminae 4B, 4A, and 3B. *Journal of Comparative Neurology, 311*, 234-258.

Lund, J. S. (1988). Anatomical organization of macaque monkey striate visual cortex. *Annual Review of Neuroscience, 11*, 253-288.

Lund, J. S. (1987). Local circuit neurons of macaque striate cortex: I. Neurons of laminae 4C and 5A. *Journal of Comparative Neurology, 257*, 60-92.

Lund, J. S. (1973). Organization of neurons in the visual cortex, area 17, of the monkey (*Macaca mulatta*). *Journal of Comparative Neurology, 147*, 455-496.

Lund, J. S. & Boothe, R. G. (1975). Interlaminar connections and pyramidal neuron organization in the visual cortex, area 17, of the macaque monkey. *Journal of Comparative Neurology, 159*, 305-334.

Lynch, J. C. (1980). The functional organization of posterior parietal association cortex. *Behavioral Brain Sciences, 3*, 485-534.

Magnussen, S. & Mathiesen, T. (1989). Detection of moving and stationary gratings in the absence of striate cortex. *Neuropsychologia, 27*, 725-728.

Malach, R. (1994). Cortical columns as devices for maximizing neuronal diversity. *Trends in Neuroscience, 17*, 101-104.

Malach, R., Amir, Y., Harel, M. & Grinvald, A. (1993). Relationship between intrinsic connections and functional architecture revealed by optical imaging and in vivo targeted biocytin injections in primate striate cortex. *Proceedings of the National Academy of Sciences U.S.A., 90*, 10469-10473.

Malik, J. & Perona, P. (1990). Preattentive texture discrimination with early vision mechanisms. *Journal of the Optical Society of America A, 7*, 923-932.

Marcel, A. J. (1983). Consciousness and processing - choosing and testing a null hypothesis. *Cognitive Psychology, 15*, 197-237.

Marr, D. (1982). *Vision.* (San Francisco: Freeman).

Martens, W., Blake, R., Sloane, M., & Cormack, R. (1981). What masks utrocular discrimination. *Perception and Psychophysics, 30*, 521-532.

Maunsell, J. H. R. & Newsome, W. T. (1987). Visual processing in monkey extrastriate cortex. *Annual Review of Neuroscience, 10*, 363-401.

Maunsell, J. H. R. & Van Essen, D. C. (1983). Functional properties of neurons in middle temporal visual area of the macaque monkey: 2. Binocular interactions and sensitivity to binocular disparity. *J. Neurophysiol., 49*, 1148-1167.

McCann, R. S. & Johnston, J. C. (1992). Locus of the single-channel bottleneck in dual-task interference. *Journal of Experimental Psychology, 18*, 471-484.

McCollough, C. (1965). Color adaptation and edge-detectors in the human visual system. *Science, 149*, 1115-1116.

McLeod, P., Driver, J. & Crisp, J. (1988). Visual search for a conjunction of movement and form is parallel. *Nature, 332*, 154-155.

Meeres, S. L. & Graves, R. E. (1990). Localization of unseen visual-stimuli by humans with normal vision. *Neuropsychologia, 28*, 1231-1237.

Merikle, P. M. (1992). Consciousness is a subjective state. *Am. Psychol., 47*, 792-795.

Michael, C. R. (1985). Laminar segregation of color cells in the monkey cortex. *Vision Research, 25*, 415-423.

Michael, C. R. (1978). Color vision mechanisms in monkey striate cortex: simple cells with dual opponent-color receptive fields. *Journal of Neurophysiology, 41*, 1233-1241.

Milhailovic, L. T., Cupic, D., & Dekleva, N. (1973). Changes in the number of neurons and glial cells in the lateral geniculate nucleus of the monkey during retrograde cell degeneration. *Journal of Comparative Neurology, 142*, 223-230.

Mishkin, M., Ungerleider, L. G., & Macko, K. A. (1983). Object vision and spatial vision: Two cortical pathways. *Trends in Neuroscience, 6*, 414-417.

Mishkin, M. (1982). A memory system in the monkey. *Philosophical Transactions of the Royal Society of London, Series B, 298*, 85-95.

Mohler, C. W. & Wurtz, R. H. (1977). Role of striate cortex and superior colliculus in visual guidance of saccadic eye movements in monkeys. *Journal of Neurophysiology, 40*, 74-94.

Moran, J. & Desimone, R. (1985). Selective attention gates visual processing in the extrastriate cortex. *Science, 229*, 782-784.

Motter, B. C. (1993). Focal attention produces spatially selective processing in visual cortical areas V1, V2, and V4 in the presence of competing stimuli. *Journal of Neurophysiology, 70*, 909-919.

Motter, B. C. (1994). Neural correlates of attentive selection for color or luminance in extrastriate area V4. *Journal of Neuroscience, 14*, 2178-2189.

Movshon, J. A., Adelson, E. H., Gizzi, M. S., & Newsome, W. T. (1990). The analysis of moving visual patterns. In C. Chagas, R. Gattass, and C. G. Gross (eds.), *Pattern Recognition Mechanisms.* Rome: Vatican Press, 117-151.

Movshon, J. A. & Newsome, W. T. (1984). Functional characteristics of striate cortical neurons projecting to MT in the macaque. *Society for Neuroscience Abstracts, 10*, 933.

Mozer, M. C. (1991). *The perception of multiple objects.* Cambridge, Mass.: Bradford/MIT Press.

Nakayama, K. (1985). Biological image motion processing: A review. *Vision Research, 25*, 625- 660.

Nakayama, K. & Mackeben, M. (1989). Sustained and transient components of focal visual attention. *Vision Research, 29*, 1631-1647.

Nakayama, K. & Shimojo, S. (1990). Real world occlusion constraints and binocular rivalry. *Vision Research, 30*, 1811-1825.

Nakayama, K. & Silverman, G. H. (1986). Serial and parallel processing of visual feature conjunctions. *Nature, 320*, 264-265.

Neisser, U. (1967). *Cognitive psychology.* New York, NY: Appleton Century Crofts.

Nelson, J. I. & Frost, B. J. (1978). Orientation-selective inhibition from beyond the classic visual receptive field. *Brain Research, 139*, 359-365.

Newsome, W. T., Britten, K. H., & Movshon, W. T. (1989). Neural correlates of a perceptual decision. *Nature, 341*, 52.

Newsome, W. T. & Pare, E. B. (1986). A selective impairment of motion perception following lesions of the middle temporal area (MT). *Journal of Neuroscience, 8*, 2201-2211.

Newsome, W. T., Wurtz, R. H., Dürsteler, M. R., & Mikami, A. (1985). Deficits in visual motion perception following ibotenic acid lesion of the middle temporal visual area of the macaque monkey. *Journal of Neuroscience, 5*, 825-840.

Nothdurft, H. C. (1991). Texture segmentation and pop-out from orientation contrast. *Vision Research, 31*, 1073-1078.

Nothdurft, H. C. & Li, C. Y. (1985). Texture discrimination: Representation of orientation and luminance differences in cells of the cat striate cortex. *Vision Research, 25*, 99-113.

Nowlan, S. J. & Sejnowski, T. J. (1994). Filter selection model for motion segmentation and velocity integration. *J. Opt. Soc. Am. A, 11*, 3177-3200.

Olson, R. & Attneave, F. (1970). What variables produce similarity grouping? *American Journal of Psychology, 83*, 1-21.

Ono, H. & Barbeito, R. (1985). Utrocular discrimination is not sufficient for utrocular identification. *Vision Research, 25*, 289-299.

Pashler, H. (1991). Shifting visual attention and selecting motor responses: distinct attentional mechanisms. *Journal of Experimental Psychology, 17*, 1023-1040.

Pashler, H. (1993). Doing two things at the same time. *American Scientist, 81*, 48-55.

Pasik, P. & Pasik, T. (1982). Visual functions in monkeys after total removal of visual cerebral cortex. In W. D. Neff (Ed.), *Contributions to sensory Physiology, Vol. 7*, pp 147-200. New York: Academic Press.

Perenin, M. T. & Jeannerod, M. (1983). Are extrageniculostriate pathways nonfunctional in man? *Behavioral and Brain Sciences, 6*, 458-459.

Perenin, M. T. (1978). Visual function within the hemianopic field following early cerebral hemidecortication in man. II. Pattern discrimination. *Neuropsychologia,*

16, 697-708.

Perenin, M. T. & Jeannerod, M. (1978). Visual function within the hemianopic field following early cerebral hemidecortication in man. I. Spatial localisation. *Neuropsychologia, 16*, 1-13.

Perry, V. H., Oehler, R., & Cowey, A. (1984). Retinal ganglion cells that project to the dorsal lateral geniculate nucleus in the macaque monkey. *Neuroscience, 12*, 1101-1123.

Perry, V, H. & Cowey, A. (1981). The morphological correlates of x- and y-like retinal ganglion cells in the retina of monkeys. *Experimental Brain Research, 43*, 226-228.

Petersik, J. T., Hicks, K. I., & Pantle, A. J. (1980). Apparent movement of successively generated subjective figures. *Perception, 7*, 371-383.

Pickersgill, M. J. (1961). On knowing with which eye one is seeing. *Quarterly Journal of Experimental Psychology, 13*, 168-172.

Poggio, T., Fahle, M. & Edelman, S. (1992). Fast perceptual learning in visual hyperacuity. *Science. 256*, 1018-1021.

Poggio, G. F., Motter, B. C., Squatrito, S., & Trotter, Y. (1985). Responses of neurons in visual cortex (V1 and V2) of the alert macaque to dynamic random-dot stereograms. *Vision Research, 25*, 397- 406.

Poggio, G. F. (1984). Processing of stereoscopic information in primate visual cortex. In G. M. Edelman, W. E. Gall, & W. M. Cowan (eds.), *Dynamic Aspects of Neocortical Function.* New York: Wiley, 613-636.

Poggio, G. F. & Fischer, B. (1977). Binocular interactions and depth sensitivity in striate and prestriate cortex of behaving rhesus monkey. *Journal of Neurophysiology, 40*, 1392-1405.

Pöppel, E., Held, R. & Frost, D. (1973). *Nature, 243*, 295-296.

Porac, C. & Coren, S. (1986). Sighting dominance and utrocular discrimination. *Perception and Psychophysics, 39*, 449-451.

Press, W. A., Knierim, J. J. & Van Essen, D. C. (1994). Neuronal correlates of attention to texture patterns in macaque striate cortex. *Society of Neuroscience Abstract, 20*, 838.

Ptito, A., Lassonde, M., Lepore, F., & Ptito, M. (1987). Visual discrimination in hemispherectomized patients. *Neuropsychologia, 25*, 869-879.

Qian, N. & Andersen, R. A. (1994). Transparent motion perception as detection of unbalanced motion signals: 2. Physiology. *Journal of Neuroscience, 14*, 7367-7380.

Qian, N., Andersen, R. A. & Adelson, E. H. (1994a). Transparent motion perception as detection of unbalanced motion signals: 1. Psychophysics. *Journal of Neuroscience, 14*, 7357-7366.

Qian, N., Andersen, R. A. & Adelson, E. H. (1994b). Transparent motion perception as detection of unbalanced motion signals: 3. Modeling. *Journal of Neuroscience, 14*, 7381-7392.

Ramachandran, V. S. & Cobb, S. (1995). Visual attention modulates metacontrast masking. *Nature, 373*, 66- 68.

Reynolds, J., Chelazzi, L. Luck, S. & Desimone, R. (1994). Sensory interactions and effects of selective spatial attention in macaque area V2. *Society of Neuroscience Abstract, 20*, 1054.

Richards, W. (1973). Visual processing in scotomata. *Experimental Brain Research, 17*, 333-347.

Robinson, D. L. & Petersen, S. E. (1984). Posterior parietal cortex of the awake monkey: Visual responses and their modulation by behavior. In F. Reinoso-Suarez & C. Ajmone-Marsan (Eds.), *Cortical integration*, pp 279-290. New York: Raven press.

Rockland, K. S. & Pandya, D. N. (1981). Laminar origins and terminations of cortical connections of the occipital lobe in the rhesus monkey. *Brain Research, 179*, 3-20.

Rodman, H. R., Gross, C. G. & Albright, T. D. (1989). Afferent basis of visual response properties in area MT of the macaque. I. Effects of striate cortex removal. *J. Neuroscience, 9*, 2033-2050.

Rodman, H. R., Gross, C. G. & Albright, T. D. (1990). Afferent basis of visual response properties in area MT of the macaque. II. Effects of superior colliculus removal. *J. Neuroscience, 10*, 1154- 1164.

Rubenstein, B. S. & Sagi, D. (1990). Spatial variability as a limiting factor in texture-discrimination tasks: Implications for performance asymmetries. *Journal of the Optical Society of America A, 7*, 1632-1642.

Sagi, D. (1990). Detection of an orientation singularity in gabor texture: Effect of signal density and spatial frequency. *Vision Research, 30*, 1377-1388.

Sagi, D. & Julesz, B. (1987). Short-range limitation on detection of feature differences. *Spatial Vision, 1*, 39-49.

Saito, H., Tanaka, K., Isono, H., Yasuda, M., & Mikami, A. (1989). Directionally selective responses of cells in the middle temporal area (MT) of the macaque monkey to the movement of equiluminous opponent color stimuli. *Experimental Brain Research, 75*, 1-14.

Salzman, D. C., Britten, K. H., & Newsome, W. T. (1990). Cortical microstimulation influences preceptual judgments of motion direction. *Nature, 346*, 174-177.

Sato, T. (1988). Direction discrimination and pattern segregation with isoluminant chromatic random-dot cinematograms. *Investigative Ophtalmology and Visual Science (Suppl.), 29*, 449.

Schacter, D. L. (1992). Implicit knowledge - new perspectives on unconscious processing. *Proc. Nat. Acad. Sci. USA, 89*, 11113-11117.

Scheider, W. & Shiffrin, R. M. (1977). Controlled and automatic human information processing: I. detection, search, and attention. *Psychological Review, 84*, 1-66.

Schiller, P. H. & Lee, K. (1991). The role of primate extrastriate area V4 in vision. *Science, 251*, 1251-1253.

Schiller, P. H. & Malpeli, J. G. (1978). Functional specificity of lateral geniculate nucleus laminae of the rhesus monkey. *Journal of Neurophysiology, 41*, 788-797.

Shapley, R., Kaplan, E., & Soodak, R. (1981). Spatial summation and contrast sensitivity of X and Y cells in the lateral geniculate nucleus of the macaque. *Nature, 292*, 543-545.

Shapley, R. & Perry, V. H. (1986). Cat and monkey retinal ganglion cells and their visual functional roles. *Trends in Neuroscience, 9*, 229-235.

Sidis, B. *The Psychology of Suggestion* (Appleton, New York, 1898).

Smith, S. (1945). Utrocular or "which eye" discrimination. *Journal of Experimental Psychology, 35*, 1-15.

Snowden, R. J., Treue, S. & Andersen, R. A. (1992). The response of neurons in area V1 and area MT of the alert rhesus monkey to moving random dot patterns. *Experimental Brain Research, 88*, 389- 400.

Spatz, W. B. (1977). Topographically organized reciprocal connections between area 17 and MT (visual area of superior temporal sulcus) in the marmoset *Callithrix jacchus. Experimental Brain research, 27*, 559-572.

Sperling, G. & Melchner, M. J. (1978). The atttention operating characteristic: some examples from visual search. *Science, 202*, 315-318.

Stoerig, P. & Cowey, A. in *Prog. in Brain Res.* Vol. 95 (eds Hicks, T. P., Molotchnikoff, S. & Ono, T.) 445-459 (Elsevier Science Publisher, 1993).

Stoerig, P. & Cowey, A. (1991). Increment threshold spectral sensitivity in visual field defects. *Brain, 116*, 1487-1512.

Stoerig, P. & Cowey, A. (1989). Spectral sensitivity in blindsight. *Nature, 342*, 916-918.

Stoerig, P. (1987). Chromaticity and achromativity. Evidence for a functional segregation in visual field defects. *Brain, 110*, 869-886.

Stoerig, P., Hübner, M., & Pöppel, E. (1985). Signal detection analysis of residual vision in a field defect due to a post-geniculate lesion. *Neuropsychology, 23*, 589-599.

Stoner, G. R. & Albright, T. D. (1993). Image segmentation cues in motion processing: implications for modularity in vision. *J. Cognitive Neuroscience, 5*, 129-149.

Thorell, L. G., De Valois, R. L., & Albrecht, D. G. (1984). Spatial mapping of monkey V1 cells with pure color and luminance stimuli. *Vision Research, 24*, 751-769.

Treisman, A. (1985). Preattentive processing in vision. *Computer Vision and Image Processing, 31*, 156-177.

Treisman, A. (1988). Features and objects: The 14th Bartlett Memoral Lecture. *Quarterly Journal of Experimental Psychology A, 40*, 201-237.

Treisman, A. (1991). Search, similarity, and integration of features between and within dimensions. *Journal of Experimental Psychology, 17*, 652-676.

Treisman, A. (1993). *The perception of features and objects.* In Baddeley, A. & Weiskrantz, L. (Eds), *Attention: Selection, awareness, and control* (pp. 1-35).

Oxford: Clarendon Press.

Treisman, A. & Gelade, G. (1980). A feature integration theory of attention. *Cognitive Psychology, 12*, 97-136.

Treisman, A. & Gormican, S. (1988). Feature analysis in early vision: evidence from search assymetries. *Psychology Review, 12*, 97-136.

Treisman, A. & Souther, J. (1985). Search asymmetry: A diagnostic for preattentive processing of separable features. *Journal of Experimental Psychology, 114*, 285-310.

Ungerleider, L. G. & Desimone, R. (1986). Cortical connections of visual area MT in macaque. *Journal of Comparative Neurology, 22*, 190-222.

Ungerleider, L. G. & Mishkin, M. (1982). *Two cortical visual systems.* In Ingle, D. J., Goodale, M. A. & Manfield, R. J. (Eds), *Analysis of visual behavior* (pp. 549-580). Cambridge, MA: MIT Press.

Van Essen, D. C. & Gallant, J. L. (1994). Neural mechanisms of form and motion processing in the primate visual system. *Neuron, 13*, 1-10.

Van Santen, J. P. H. & Sperling, G. (1984). Elaborated Reichart detectors. *Journal of the Optical Society of America A, 2*, 300-321.

Van Trees, H. L. (1968). *Detection, Estimation, and Modulation Theory: Part 1.* John Wiley and Sons.

Wang, H. T., Mathur, B., & Koch, C. (1989). Computing optical flow in the primate visual system. *Neural Computation, 1*, 92-103.

Watson, A. B. & Ahumada, A. J. (1986). Model of visual-motion sensing. *Journal of the Optical Society of America A, 2*, 322-341.

Weiskrantz, L. (1986). *Blindsight. A case study and implications.* Oxford: Oxford University Press.

Weiskrantz, L., Warrington, E. K., Sanders, M. D. & Marshall, J. (1974). *Brain, 97*, 709-728.

Weller, R. E., Kaas, J. H., & Wetzel, A. N. (1979). Evidence for the loss of x-cells of the retina after long-term ablation of visual cortex in monkeys. *Brain Research, 160*, 134-138.

Weller, R. E. & Kaas, J. H. (1989). Parameters affecting the loss of ganglion cells of the retina following abaltion of striate cortex in primates. *Visual Neuroscience, 3*, 327-349.

Westheimer, G. (1981). In D. Ottoson (Ed.). *Progress in Sensory Physiology: Vol I*, pp 2-30, Berlin: Springer Verlag.

Wurtz, R. H. & Albano, J. E. (1980). Visual-motor function of the primate superior colliculus. *Ann. Rev. Neurosci., 3*, 189-226.

Wurtz, R. H. & Goldberg, M. E., & Robinson, D. L. (1982). Brain mechanisms of visual attention. *Scientific American., 246*, 124-135.

Yang, Y. & Blake, R. (1994). Broad tuning for spatial frequency of neural mechanisms underlying visual perception of coherent motion. *Nature, 371*, 793-796.

Yukie, M. & Iwai, E. (1981). Direct projection from the dorsal lateral geniculate nucleus to the prestriate cortex in macaque monkeys. *Journal of Comparative Neurology, 201*, 81-97.

Zeki, S. M. (1978). Uniformity and diversity of structure and function in rhesus monkey prestriate visual cortex. *Journal of Physiology, 277*, 273-290.

Zeki, S. M. (1969). Representation of central visual fields in prestriate cortex of monkey. *Brain Research, 14*, 271-291.

Zeki, S. M. & Shipp, S. (1988). The functional logic of cortical connections. *Nature, 335*, 311-317.

Zihl, J. (1980). Blindsight: Improvement of visually guided eye movements by systematic practice in patients with cerebral blindness. *Neuropsychologia, 18*, 71-77.

Zihl, J. & von Cramon, D. (1979). The contribution of the "second" visual system to directed visual attention in man. *Brain, 102*, 835-856.

Zihl, J., von Cramon, D., & Mai, N. (1983). Selective disturbance of movement vision after bilateral brain damage. *Brain, 106*, 313-340.

Zohary, E., Celebrini, S., Britten, K. H., & Newsome, W. T. (1994). Neuronal plasticity that underlies improvement in perceptual performance. *Science, 263*, 1289-1292.